NUMERICAL INVESTIGATION OF SOLVENT AND THERMAL HYBRID PROCESSES FOR THIN HEAVY OIL RESERVOIRS

A Thesis

Submitted to the Faculty of Graduate Studies and Research

In Partial Fulfillment of the Requirements

for the Degree of

Master of Applied Science

in

Petroleum Systems Engineering

University of Regina

by

Zuojing Zhu

Regina, Saskatchewan

December, 2012

UNIVERSITY OF REGINA

FACULTY OF GRADUATE STUDIES AND RESEARCH

SUPERVISORY AND EXAMINING COMMITTEE

Zuojing Zhu, candidate for the degree of Master of Applied Science in Petroleum Systems Engineering**,** has presented a thesis titled, ***Numerical Investigation of Solvent and Thermal Hybrid Processes for Thin Heavy Oil Reservoirs,*** in an oral examination held on December 5, 2012. The following committee members have found the thesis acceptable in form and content, and that the candidate demonstrated satisfactory knowledge of the subject material.

External Examiner:	Dr. Tsun Wai Kelvin Ng, Environmental Systems Engineering
Co-Supervisor:	Dr. Fanhua Zeng, Petroleum Systems Engineering
Co-Supervisor:	Dr. Gang Zhao, Petroleum Systems Engineering
Committee Member:	Dr. Farshid Torabi, Petroleum Systems Engineering
Committee Member:	Dr. Paul Laforge, Electronic Systems Engineering
Chair of Defense:	Dr. Christopher Oriet, Department of Psychology

ABSTRACT

Western Canada has the second largest oil resources in the world. Over 90% is heavy oil and bitumen. Vapour Extraction (VAPEX), similar to Steam Assisted Gravity Drainage (SAGD) but using solvent to reduce the oil viscosity, has been proposed to produce heavy oil reservoirs in an environmentally sustainable way. However, while this process might work well for thicker reservoirs, such as those in Alberta, it will likely not meet economic thresholds for thinner reservoirs, such as those in Saskatchewan. The low flow rate in the pure VAPEX process is mainly due to three reasons: low mass transfer rate compared to thermal transfer rate, poor communication efficiency between the injector and the producer because of the reservoir heterogeneity and long distance between the injector and the producer, and poor horizontal well conformity.

In this thesis, two categories of thermal and solvent hybrid processes are investigated to enhance the oil recovery for thin heavy oil reservoirs: electrical resistive heating with solvent injection and steam with solvent co-injection in both SAGD and Cyclic Steam Stimulation (CSS). Both categories are numerically investigated by using CMG's STARS.

Electrical resistive heating with solvent injection (ERH-S), a novel process, is presented and investigated to enhance the communication efficiency between the injector and the producer. This process can also improve the horizontal well conformity. The electrical heating is the most suitable to be coupled with the solvent process since the electrical heating (1) generates uniform heating results along the horizontal wellbore; (2) increases apparent permeability along the wellbore; (3) is

not affected by the reservoir heterogeneity, such as thief zones and shale; (4) reduces water cut; and (5) reduces the formation damage caused by asphaltene precipitation. Through the numerical simulations and analysis, ERH-S shows three features that contribute to the enhanced oil flow: (1) the heat from the electrode establishes good communication between the injector and the producer by viscosity reduction; (2) the in-situ generated heat through ERH along with the horizontal wellbore is not susceptible to reservoir heterogeneity, and, thus, the horizontal well conformity can be improved; (3) the solvent can reduce the viscosity of the heavy oil in unheated zones where the ERH cannot reach, and it can also assist viscosity reduction of heavy oil in the heated zone. The simulation results show that this hybrid process can improve the oil rate 2 to 5 times over VAPEX.

SAGD and CSS are two successfully applied enhanced heavy oil/bitumen production techniques. When these two techniques are applied in thin heavy oil reservoirs, due to the significant heat loss, the Steam-Oil Ratio (SOR) is too high to make these techniques economical. Simulations for steam with solvent co-injection, SAGD with solvent, and CSS with solvent show that under similar temperature and pressure between solvent dew points and operating conditions, the solvent injection can show better Cumulative Steam-Oil Ratio (CSOR).

This study indicates that the hybrid processes using thermal and solvent have great potential to recover Western Canada's thin heavy oil/bitumen reservoirs. It is recommended that laboratory investigation should be conducted in future.

ACKNOWLEDGEMENTS

First and foremost, I would like to express my sincere gratitude to my supervisor, Dr. Fanhua (Bill) Zeng, and co-supervisor, Dr. Gary Zhao, for their continuous guidance, patience, and support in making this study and thesis possible.

I gratefully acknowledge the Petroleum Technology Research Centre (PTRC) for financial support of the research project entitled "Hybrid process of electrical resistive heating with solvent injection" awarded to Dr. Fanhua (Bill) Zeng.

I appreciate the theoretical discussions and guidance from Dr. Paul Laforge. I would also like to thank Computer Modeling Group (CMG) for their kind technical support.

I am also thankful to my family for their encouragement at all times and unconditional support, even when I am thousands of miles away. Mom, Dad – this thesis is because of you.

I would like to extend my gratitude to Dr. Fanhua (Bill) Zeng's research group for their encouragement, inspiration, and friendship during my studies at the University of Regina.

DEDICATION

To my dear mother, Cui'e, Zhou and father, Zhenkui, Zhu, for always believing in me and encouraging me to realize my dream.

TABLE OF CONTENTS

LIST OF TABLES

LIST OF FIGURES

CHAPTER 1

INTRODUCTION

1.1 Background

The vast oil sand deposits in Canada, Venezuela, and Russia are estimated to have 2,100 billion barrels of oil in place. Nearly half of these oil sand resources, or about 980 billion barrels, are located in Alberta, Canada. Most of the heavy oils have extremely high viscosity, ranging from 2,000 to more than 1,000,000 mPa.s at standard conditions. As well, the pay zones of these heavy oil reservoirs are often very thin (<10 m). The deposits are usually underlain and overlain by beds of water-sands and shales, and they all rest on a limestone basement rock. Some deposits are stacked, physically segregated from one another by heavy, impermeable shale strata. Therefore, these reservoirs are characterized by conditions that are not generally economically conducive to thermal enhanced heavy oil recovery processes.

Generally, there are two popular ways to reduce the viscosity of heavy oil: (1) thermal-related methods and (2) solvent dissolution/dilution into heavy oil. For the first type, it is common and effective to inject steam into the reservoir. Representative processes of thermal recovery include Steam Assisted Gravity Drainage (SAGD) and Cyclic Steam Stimulation (CSS), which are commercially applied on a large scale in heavy oil reservoirs. Electrical resistive heating (ERH) for heavy oil production is also a thermal process in which electricity is introduced into the near wellbore region of a well. The ERH process is a continuous process without injecting foreign fluids into the reservoir. The most popular solvent injection process

applied in laboratories or field tests, currently, is the process of vapour extraction (VAPEX). However, both categories have their own limitations.

1.2 Problem Statement and Research Objective

In order to better understand this process, other hybrid processes, such as steam assisted gravity drainage (SAGD) with solvent injection (SAGD-S) and cyclic steam stimulation (CSS) with solvent injection (CSS-S) were simulated and investigated. Simple efficiency comparisons in each hybrid process were also conducted.

Vapour extraction (VAPEX) is considered to be an alternative method to thermal EOR processes and has delivered very encouraging lab experiment results in the last two decades. However, based on the current technology and theoretical models, the pilot tests cannot achieve the expected results as in the lab experiments.

As to the traditional thermal processes related to steam injection, such as SAGD and CSS, more and more negative attention is arising with reference to climate change and high water usage. Moreover, high heat loss to overburden and underburden in thin heavy oil reservoirs makes steam injection processes more uneconomical.

Considering the limitations of thermal processes and solvent injection processes, a thermal hybrid process, in which a small amount solvent is introduced into the reservoir with a heat medium, is created potential alternative. The hybrid process combines two mechanisms for viscosity reduction: heat and solvent dilution. SAGD with solvent injection and CSS with solvent injection have been tested and successfully applied in oil fields. However, both processes still need higher steam

volume and higher temperature, which consume too much water and emits much carbon dioxide.

Also, during the electrical resistive heating process, the temperature is does not necessarily need to be as high as steam injection to reduce the viscosity to a very low level, which can save more energy. On the other hand, using electrical heating achieved the temperatures reached using steam is not energy efficient. Adding solvents with electrical heating could mobilize more bitumen at a lower temperature. The question, then, is how much energy should be used to heat the reservoir and what kind of solvent should be injected into the reservoir, and, also, how do the two mechanisms combine to reduce the viscosity? In order to better understand the process of electrical and solvent injection and solve these questions from the technical perspective, simulations were run.

This study proposes a novel thermal hybrid process and analyzes the performance of this hybrid process with numerical simulation. This hybrid process provides new insight into the heavy oil EOR techniques. The effects of operating conditions (such as electrode placement, voltage, and well placement) and reservoir properties (such as water saturation and formation heterogeneity) on the performance of the hybrid process were thoroughly investigated through a series of numerical simulations.

1.3 Thesis organization

There are five chapters in this thesis. Chapter 1 provides an introduction to the hybrid processes together with the problem statement, research objectives, and methodology of this study. Chapter 2 is a comprehensive review of the previous

studies on hybrid processes. Chapter 3 presents the numerical investigation of the hybrid process of electrical resistive heating with solvent injection (ERH-S) by using CMG's STARS and sensitivity analysis. Chapter 4 simulates and analyzes the other two hybrid processes, SAGD/SAGD-S and CSS/CSS-S from the perspective of process description and results analysis. Chapter 5 provides conclusions and recommendations for future work.

CHAPTER 2

LITERATURE REVIEW

The vast oil sand deposits in Canada, Venezuela, and Russia are estimated to have 2,100 billion barrels of oil in place. Nearly half of these oil sand resources, or about 980 billion barrels, are located in Alberta, Canada, in which 12% of the Alberta deposit lies at a depth of 75 m and less with an average seam thickness of 32 m and 88% lies at a depth of 75 m to 750 m with an average seam thickness of somewhat below 20 m. The deposits are usually undelainr and overlain by beds of water-sands and shales and all rest on a limestone basement rock. Some deposits are stacked, physically segregated from one another by heavy, impermeable shale strata. (Mossop, 1980; Strom et al., 1980);.

Two major types of techniques, miscible and thermal, have been applied for enhancing heavy oil production. The VAPEX process is representative of miscible production. For thermal processes, SAGD and CSS are the most popular, with different application conditions. Also, electrical heating, an alternative method to thermal steam injection, is attracting more and more attention in the industry.

2.1 VAPEX

In VAPEX, a mixed solvent vapour is injected into the reservoir via a horizontal injection well and reduces the viscosity of heavy oil, after which the diluted, low viscosity oil is produced by gravity drainage into the lower horizontal wells. The solvent in VAPEX performs the same function as the steam in a SAGD process. For the well pattern, similar to the well pattern of SAGD, a horizontal

producer is drilled right below the injector. The vapour solvent chamber is formed around and above the injector and grows with time as more oil is produced. Under the influence of gravity, the diluted oil flows within the diffusion layer and to the producer. A schematic of the mechanism of VAPEX is presented in Figure 2-1.

Thermal recovery methods are recognized as the most effective for heavy oil and bitumen. However, the large heat requirement can make them inefficient and uneconomic in many reservoirs, particularly those with thin pay zones, low porosity, high water saturation, low rock thermal conductivity, and those with aquifers (Butler and Jiang, 1997).

Experimental studies have shown that extraction of heavy oil and bitumen using VAPEX is a technically viable alternative to thermal recovery methods (Das and Butler, 1995); (Das, 1998).

Meanwhile, due to its in-situ upgrading, lower environmental pollution, and lower capital costs, etc., VAPEX is superior to steam processes.

VAPEX, although an evolution of SAGD, is a non-thermal process. VAPEX could be operated at reservoir temperature with no heat loss in the reservoir. Generally, VAPEX delivers lower lower production rates than thermal processes for the same reservoir with the same well configuration, largely because molecular diffusion rather than thermal conduction controls its rates and this is relatively slow.

In VAPEX processes, the solvent is injected into the reservoir at or near the vapour pressure in order to keep the solvent vapourized in the reservoir. The injected solvent is dissolved into oil by diffusion to form an oil-solvent mixture whose viscosity depends on the concentrations of the solvents in the mixtures. So,

maintaining the vaporization of injected solvent is critical to reducing the amount of the solvent required to fill the reservoir space vacated by produced oil. This condition limits the selection of solvents to light hydrocarbons, which have high vapour pressures. Pure solvents usually have vapour pressures lower than the reservoir pressure, and this would tend to make their application in VAPEX impractical. The use of mixed solvent, however, could overcome this problem. During the process, oil swelling by dissolved solvent and de-asphalting at suitable conditions are also helpful to enhance the oil rate and improve the quality of products.

In 1974, Allen tried the 'huff and puff' experimental process in which propane or ethane was injected in cycles to extract the Athabasca bitumen in a packed model. In 1976, Allen also conducted an experiment with injection of a liquid solvent with a non-condensable gas at reservoir pressure and temperature (Das and Butler, 1998). Butler and Mokrys (1989) carried out experiments in a Hele-Shaw cell to confirm that such a system is a direct analog of the SAGD process. From their experimental results, dissolution of solvent caused a significant viscosity reduction. They also observed that the drainage height decreased with time. Their experimental results confirmed the theoretical relationship between the drainage rate and the square root of cell permeability. With the fixed permeability, the drainage rate is a linear function of square root of bitumen height.

Butler and Mokrys (1991) improved their early experiment on VAPEX with simultaneous injection of solvent and hot water. This process made a connection between VAPEX and SAGD. The results suggested that intermediate heating

occurred in the range of 40-70^{o}C. This would be economically more attractive in comparison to conventional SAGD or VAPEX alone.

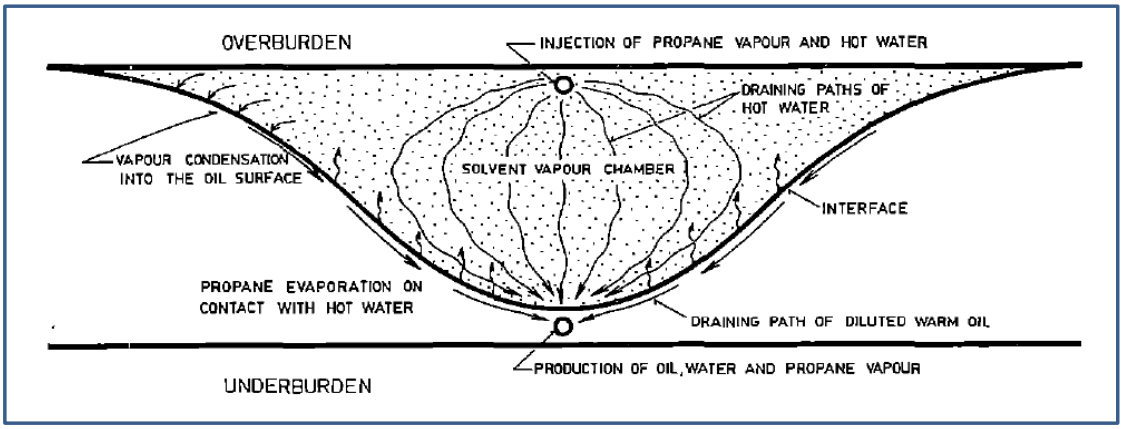

Figure 2-1 Mechanism of VAPEX (Butler and Jiang, 1997)

In spite of its apparent potential results based on the laboratory results, it is difficult to predict the field scale behavior because of the incomplete understanding of some important aspects, such as mass transfer across the gas-liquid interface. The majority of analytical models used currently are based on the assumption of diffusion into a stagnant liquid layer with constant molecular diffusivity and are inclined to under-estimate the rate of solvent dissolution. Therefore, low drainage rates and high solvent/oil ratio were not promising enough for an economically viable project because of the control of molecular diffusion.

Lab experiments have shown that the oil production rates in physical model tests using reservoir sand can be several times higher than the rate predicted by the simple diffusion model (Das, 1998). Possible reasons for that difference are discussed below:

The molecular diffusivity increases with solvent concentration (due to decreased oil viscosity) and increases in the gas/oil interfacial area due to the presence of a saturation transition zone at the interface. Enhanced mass transfer is due to convective dispersion in porous media.

(Redford and Hanna, 1981) described a process that involves the simultaneous injection of steam, gas, and hydrocarbon solvent into the sand formation to recover heavy oil. It was observed that the recovery exhibited the beneficial effects of both the gas and solvent as the concentration of the gas in the steam-solvent injection stream was initially increased. The gas tested included carbon dioxide, oxygen, and ethane. The preferred concentration was 0.02 to 0.2 SCF gas/lb steam injected. The preferred solvent was naphtha with a concentration

less than 5 volume % of steam injected. The combination of vapour extraction with steam or other thermal media is increasingly attracting attention.

2.2 Thermal hybrid processes

Conventional thermal recovery processes, such as steam flooding, CSS, and SAGD, inject one fluid to improve oil properties to make it flow easier. Therefore, there are complications of generating, transporting (while avoiding excessive heat losses), and disposing of the injected fluid. Also, these in-situ thermal methods are energy intensive and require large quantities of fresh water. Electrical resistive heating (ERH) does not require a heat transporting fluid, which can be particularly beneficial with deep reservoirs or reservoirs with thin pay-zones where conventional thermal methods are not cost-effective due to excessive heat loss. Since the heat is generated within the formation, this method is slightly affected by the depth and heterogeneity of the reservoir and is hardly influenced by permeability variations within the formation.

VAPEX is analogous to the SAGD process where the steam is replaced with gaseous hydrocarbon. The hydrocarbon vapour rises from the upper horizontal well, creating a chamber, then diffuses to the heavy oil surface and dissolves into the bulk oil in a miscible process. However, potential disadvantages are the high cost of the solvent and the loss of the solvent that remains in the vapor chamber. Also, the process of VAPEX is likely to be slow with a long period before there is sufficient penetration of the vapor into the oil over a large enough area.

Combined technologies in the form of hybrid processes of thermal with solvents can offer the potential of higher oil rates and recoveries but with less energy and water consumption than single processes such as SAGD and CSS.

Interest in hybrid process technologies is growing. Recent investigations (Nasr et al.,2003; Deng, 2005; King et al.,2005; Simangunsong and Mamora, 2006; Ardali et al., 2011) have considered combining steam and solvent injection processes. These processes combine the benefits of steam and solvents in the recovery of heavy oil and bitumen and lead to accelerated oil production rate, higher oil recovery, and lower energy to oil ratio. Gupta and Wan (2003) found the solvent-aided process actually has a lower oil production rate at the early stage but can efficiently reduce the oil production decline rate (Wan et al., 2004). Zhao (2007) proposed a steam alternating solvent process, which involves injecting steam and solvent alternately, and the basic well configurations are the same as those in the SAGD process. Numerical simulation suggested that the oil production rate of a steam assisted solvent process could be higher than that of a SAGD process, while the energy input was 18% less than that of SAGD. Cristofari et al. (2006) studied the effects of solvent injection on in-situ combustion and found that solvent extraction of light and medium components from the oil phase followed by air injection might realize significant synergies by combining the benefits of both technologies.

2.3 SAGD and SAGD-S

2.3.1 SAGD

The application of SAGD is becoming increasingly important in Canada because of the vast reserves accessible under this successful production method. Dr. Roger Butler initially introduced the concept of Steam Assisted Gravity Drainage (SAGD) as a promising and effective innovation in heavy oil production. It is characterized by introducing steam into a reservoir via a higher horizontal injection well and producing heated oil using an horizontal production well situated under the horizontal injection well. The SAGD process starts from the circulation of steam from injector to producer so that the bitumen between the producer and injector is heated enough to flow to the lower producer. Steam circulation stops when there is good communication between the injector and producer. After that, steam is continually injected via the horizontal injection well and a steam chamber is formed and developes upwards from the injector, in which the temperature is essentially that of the injected steam. The steam flows towards the perimeter of the steam chamber and condenses. The heat from the steam is mainly transferred by thermal conduction into the surrounding reservoir, partly by thermal convection. The steam condensate and heated oil flow to the horizontal production well by gravity. As the heated oil is produced, the steam chamber grows both horizontally and vertically (Butler, 1994). There are two types of flow existing in the SAGD process. One is ceiling drainage in which bitumen is pulled away from the front immediately after mobilization and the other is slope drainage in which bitumen mobility is controlled by conduction heating from the steam zone. Typically, the length of SAGD wells is between 500

and 1,000 meters, the inter-well distance of the two parallel wells is between 3 to 10 meters, and inter-well spacing is between 90 and 120 meters. Figure 2-2 illustrates the SAGD mechanism.

The economics of the SAGD process are controlled by the costs of steam generation and water treatment and recycling. Generally, the cumulative injected steam (in cold water equivalent) to the produced oil ratio (CSOR) is used to measure the thermal efficiency of the SAGD process. Gates and Chakrabarty (2005) used STARS to optimize the CSOR by altering the steam injection pressure and concluded that the CSOR can be reduced significantly by operating SAGD with a profile of steam injection pressure throughout the life of the process over that of constant injection pressure. Gates and Chakrabarty pointed out that the steam injection pressure should be relatively high before the chamber contacts the overburden and lower afterwards to reduce heat loss to the overburden. Edmunds and Chhina (2001) suggested that CSOR is a reasonable surrogate for an economic objective function and that it is a monotonic function of operating pressure. They concluded that the economics of a SAGD project are more sensitive to the steam/oil ratio than to the oil production rate because of the fluctuating gas price, which can decide the cost of steam generation. They also mentioned that the economic optimum operating pressure for SAGD seems to be as low as 400 kPa for typical McMurray reservoirs. Low pressure is favoured because it leads to low temperature and, hence, low steam consumption. Based on the numerical simulation analysis, Egermann proposed a method to obtain and maintain an optimized development of the steam chamber throughout the production life of the well pair. After applying the proposal to Mobil's Celtic SAGD pilot, roughly 100% incremental oil production could

be achieved by adjusting the steam injection rate to the potential of the reservoir and monitoring the production rate to keep the steam chamber as large as possible but far enough away from the production well to prevent steam breakthrough (Egermann et al., 2001). For an economical SAGD project, the minimum nominal reservoir requirements would involve reservoir properties such as thickness, permeability, oil saturation, and so on. Currently, there are some important parameters influencing a successful SAGD project (McCormack, 2001):

- pay thickness >12 m of continuous, high quality pay (10wt% oil)
- permeability >3.0 Darcy
- no bottom water
- no top gas/water
- competent cap rock
- reservoir operating pressure >1,000 kPa
- minimal adverse fluid/rock interactions

Along with minimum nominal reservoir parameters, operating variables including preheating, injector/producer spacing, injection pressure, steam injection rate, and sub-cool temperature are of the utmost importance to a SAGD project. A very basic method, numerical simulation, was applied for the determination of the operating variables. Numerical simulations have been conducted to optimize the SAGD operating parameters by classical methods and provide technical support for new project applications.

2.3.2 SAGD-S

Aiming at improving oil rates, improving CSOR, reducing energy, and minimizing water disposal requirements, Alberta Research Council (ARC) developed a novel approach for combining hydrocarbon solvents with steam for injection into a reservoir as a method of recovering heavy oil from viscous reservoirs. This method was patented and successfully tested in the field as Expanding Solvent-SAGD (ES-SAGD). Figure 2-3 presents the concept of ES-SAGD. The hydrocarbon solvents are soluble in bitumen at reservoir conditions, which allows a greater reduction in viscosity compared to traditional SAGD. Due to the lower bitumen viscosity, the ES-SAGD process allows greater oil production rates than SAGD. The goal of the ES-SAGD process is to increase the oil production and limit the energy and water usage (Nasr et al., 2003).

The hydrocarbon solvent is most effective when it is in a gaseous state at the point of injection but condenses at the steam chamber walls and dissolves into the heated bitumen. With the pressure drawdown, lighter components of solvent vapourize creating a solution-gas drive mechanism. It is ideal for the solvent to have a similar vapourization temperature as the steam at a given pressure. Overall, it has been found that the ES-SAGD method allows for accelerated production and increased ultimate recovery of the field in comparison to the SAGD method. In addition, ES-SAGD has the potential to reduce the SOR, decrease the operating pressure, improve mobility ratio of displacing and displaced fluid, reduce interfacial tension, decrease water losses, decrease the required steam temperature, and reduce the bitumen viscosity. ES-SAGD, if implemented effectively, would vastly improve

the overall profitability of an oil sands project, and then the cost of the solvent is the only issue with ES-SAGD. It has been found that a solvent recovery rate of over 70% is typical for most ES-SAGD projects. In order to increase the recovery of solvent, cross flow, solvent sequencing, and pressure reduction can be utilized (Orr, 2009).

Gupta and Gittins in 2009 presented a proposal involving solvent injection until the steam chamber has reached its maximum height. However, Matt and John in 2009 argued that solvent should be used as soon as the circulation phase is complete. The argument arose mostly because of the unclear analogy generally between heat and mass transfer in the reservoir. It is believed that in the steam chamber, steam contributes latent heat via condensation while solvent diffuses into the bitumen (Orr, 2009).

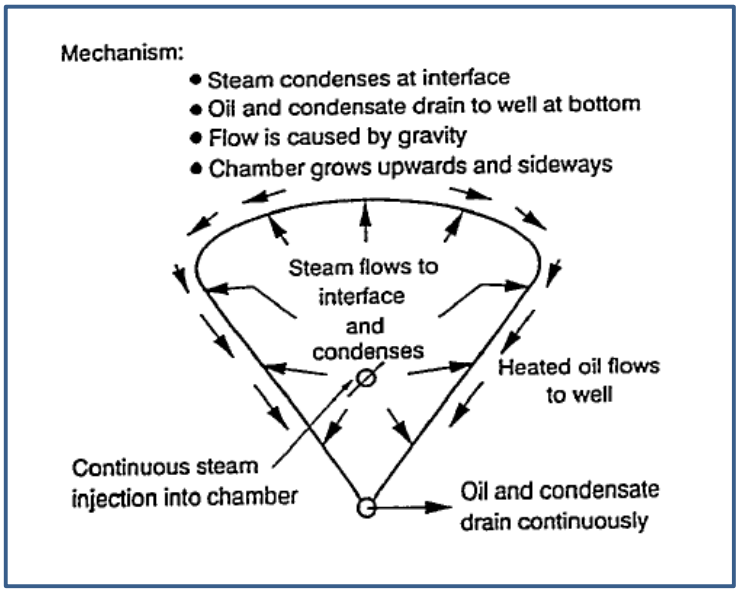

Figure 2-2 Conceptual diagram of the steam assisted gravity drainage process (Courtesy R.M Butler)

2.4 Cyclic steam stimulation (CSS)

The cyclic steam stimulation (CSS) process was originally discovered by Shell in 1957 during the testing of a steam drive in the Mene Grande field in Venezuela (Farouq Ali, 1982). This cycle is composed of three separate phases, namely:

- Injection phase
- Soak period
- Production phase

Figure 2-4 shows the concept of the vertical CSS process.

In this process, a single well (vertical or horizontal) is used both as an injector and producer. Cycles are repeated when rates are too low or in some cases, steam to oil ratio (SOR) too high to be economical. Usually, three or four cycles are used but as many as 24 cycles have been reported, such as Canadian Natural Resources Limited (CNRL) and Imperial Oil Limited (IOL) in the Promise area of Alberta. Cyclic steam stimulation is often used as a precursor to steam flooding. The advantages of cyclic steam stimulation are:

- quicker response time
- higher oil-steam ratios
- does not require communication between wells

The CSS recovery process involves a variety of recovery mechanisms, including formation re-compaction, solution gas drive, fluid expansion, condensates sensible heat, and gravity drainage. Not all mechanisms happen in one cycle of CSS. They change their roles with the cycles. As CSS adopts multiple mechanisms to

recover bitumen, it is more tolerant than other thermal recovery methods to variations in different reservoirs.

2.4.1 Injection Phase

The injection period usually lasts for several months depending on the injection rate and the volume of steam to be injected. Generally, injection pressure is dependent on reservoir pressure and depth and is usually kept below the formation fracture pressure to avoid fracturing the reservoir rock (low pressure cyclic steam stimulation (LPCSS)). Reservoir depths in thermal stimulation are usually less than 1000 meters, and a fracture gradient of 1 psi/ft (22620 kg/m^2s^2) of depth is often assumed (Bagci et al., 2008). However, in some cases, injectivity can only be initiated by fracturing of the reservoir rock, in which case, higher pressure is needed (higher pressure cyclic steam stimulation (HPCSS)). An example of this is the Cold Lake oil sand in Alberta (Beattie et al., 1991).

High-pressure injection into a tar-sand reservoir causes fracturing and widespread pore volume (PV) changes (deformation) in the formation. The deformation involves both dilation and subsequent re-compaction.

Dilation

Two observations show that significant dilation of the reservoir happens during the steam injection period in the first cycle. First, surface benchmark arrays at Cold Lake have measured surface uplifts as high as 45 cm during steam injection in the first cycle, far larger than can be attributed to thermal expansion or tensile fracturing of the formation. Second, steam injectivity at Cold Lake is greater than might be expected from native reservoir properties. Surface heave and high observed

injectivity can be explained by two mechanisms that increases porosity. First, oil sands demonstrate nonlinear compressibility behaviour. In addition, shear failure can be included in the formation at sufficiently low effective stresses in the presence of anisotropic stresses. Shear failure caused by increasing pore pressure leads to dilation of the pore system.

As steam is injected into a relatively incompressible reservoir, pore pressure increases and effective stress decreases. At pore pressures corresponding to low effective stresses, the formation compressibility increases by about an order of magnitude and shear failure might also occur. Both these phenomena cause dilation, with rapid increase in porosity and permeability. This greatly increases the steam injectivity, and injector pressures increase slowly thereafter.

The dilation is reflected by uplift of the ground surface above the injection location. Also, dilation is not reversible.

Re-compaction

Surface heave at Cold Lake is cyclical, increasing during injection and decreasing during production. However, some of the heave is permanent. Some areas could have 15 cm uplift remain unchanged for several years, although injection and production have continued during that time. Hence, while partial reversal of the dilation have occurred, re-compaction to the original porosity is not occurring. Generally, re-compaction cannot begin immediately when the pressure begins to decline following dilation. During HPCSS, after steaming stops, the bottomhole pressure (BHP) is sufficiently high that the well can flow without pumping, which is called flow back. After flow-back ends at a BHP of around original reservoir

pressure, the pump is seated for production. CMG STARS cannot simulate so great a change in pressure difference with a relatively small fluid production until an initial period of elastic behaviour with little re-compaction to support the pressure is assumed (Beattie et al., 1991). Beattie et al. (1991) pointed out that there are two phases for re-compaction: an initial elastic period when no recovery of dilation occurs and porosity changes only as a result of original compressibility and a re-compaction period with an enhanced compressibility that allows recovery of some of the dilation that occurred during injection.

Permeability Changes

With dilation occurring, an increase in the absolute permeability of the reservoir will accompany the porosity increase. A model was built by Beattie and Boberg (1991) that is currently applied in CMG STARS:

$$k_{xyz} = k_{0xyz} exp\left[\frac{KMUL_{xyz}(\Phi - \Phi_0)}{1 - \Phi_0}\right]$$

where k and Φ are permeability and porosity, respectively and k_0 and Φ_0 are original permeability and porosity, respectively. KMUL is a user-defined multiplier.

2.4.2 Soak Period

After the injection of the required slug of steam, the well is shut-in and allowed to 'soak' for a period of three or four weeks. This is done to promote the partial condensation of steam, which heats the reservoir rock and fluids, and also to achieve an even distribution of the injected heat (Farouq Ali, 1982).

2.4.3 Production Period

During a typical CSS cycle, 10% of the calendar days are for steam injection, 10% are for soak, and 80% are for production operations (Scott, 2002). Strategies to manage orderly steaming and production operations for commercial developments have been developed. Unlike SAGD, where the sensible heat of any condensate injected has no value in the recovery process, the heat from injected condensate does enhance recovery in the CSS process. The key performance indicator for a CSS cycle, similar to the SAGD process, is the Oil-Steam Ratio (OSR) between the steam volume injected and the bitumen volume produced in a cycle.

Bottom water and/or top gas zones always present challenges for CSS development in terms of controlling the communication with bottom water or top gas zones. Imperial Oil Limited (IOL) reported about 30-40% lower recovery factors in areas with a gas cap from its M&P Trunk pads. IOL also reported that with bottom water, a significant stand-off distance is required from the water oil contact to the perforation interval (Jiang et al., 2009). Commercial operations now occur in net sands as thin as 10 m with bitumen saturations as low as 6 weight per cent and permeability as low as 1 Darcy. In terms of depth, because the CSS process requires the reservoir to be fractured to enable access to the reservoir, dependent on the extent to which steam is contained with the bitumen-bearing zone, the presence of shales and clays have little impact on the CSS process, and deeper reservoirs are more favourable for application of CSS (Batycky et al., 1997).

Currently, the oil recovery in most of the CSS projects is in the range of 25~35% of OOIP. Various processes have been tested in the field to improve the

ultimate oil recovery for CSS. Those processes include air injection, solvent injection, and also combined drive with gravity drainage. Infill wells have also been tested in existing CSS operations.

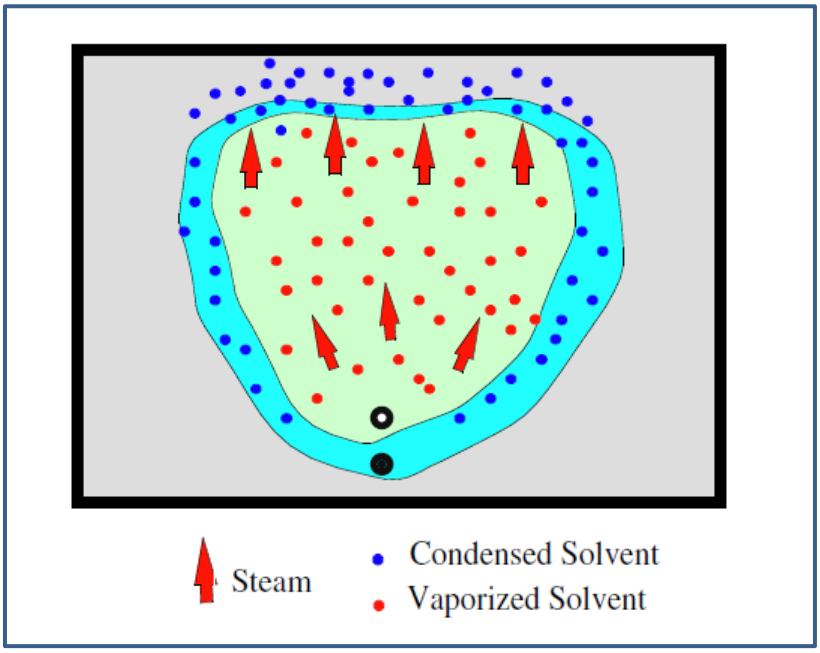

Figure 2-3 ES-SAGD conceptual diagram (Courtesy ARC)

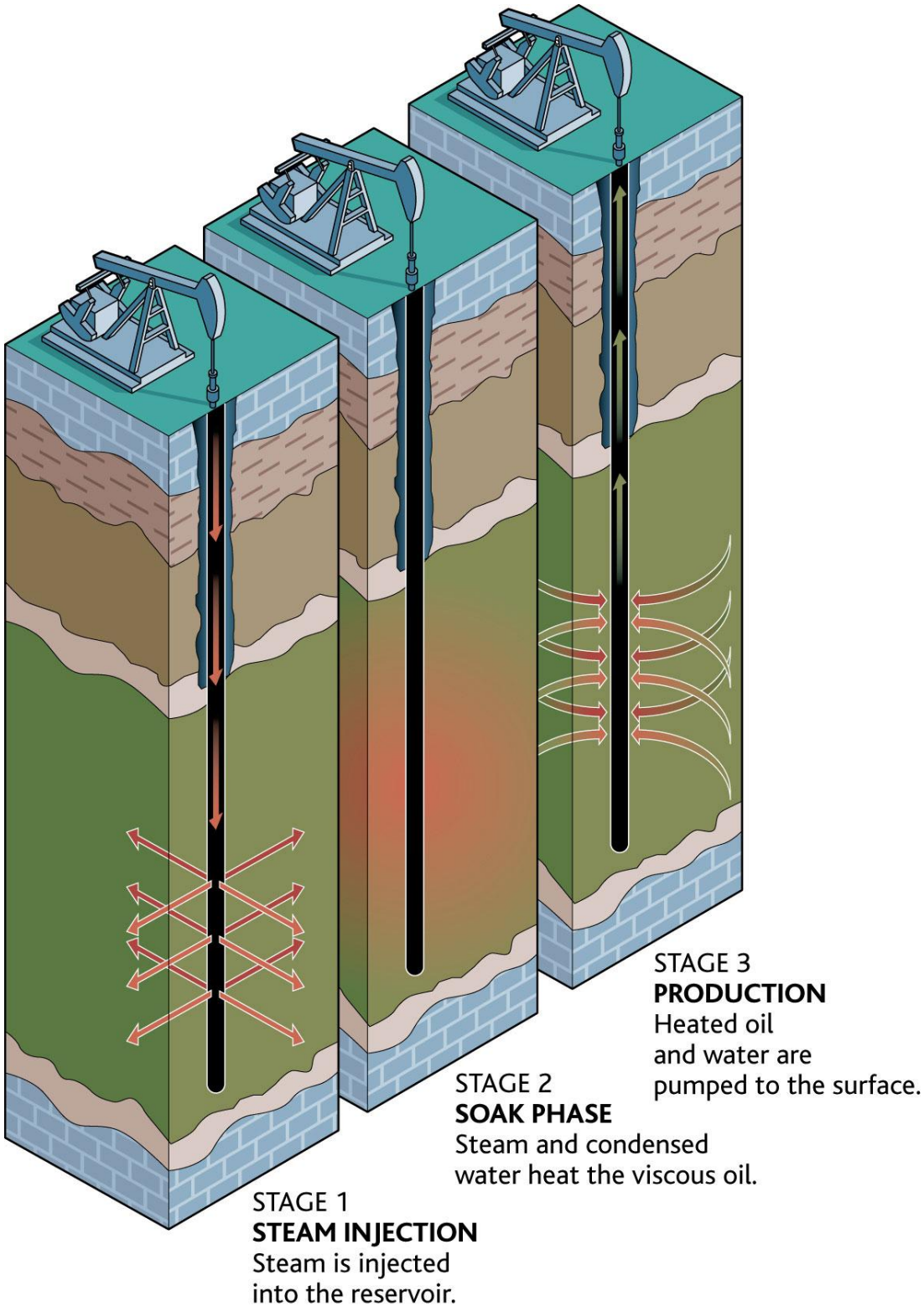

Figure 2-4 the concept of vertical CSS process (Canadian National Resources Limited)

2.5 Cyclic Solvent Injection (CSI)

Cyclic solvent injection (CSI) is considered to be the most promising post CHOPS follow-up process. In CSI, a solvent mixture (light hydrocarbon) is injected and allowed to soak into the reservoir before production. CSI could be a good option for some thin reservoirs that are not economic with thermal production methods. Figure 2-5 shows the schematic process of CSI. CSI is believed to be a potential method after CHOPS because of the high permeability zone and existence of wormholes.

Lim et al. (1995) investigated cyclic stimulation with supercritical ethane through a single horizontal injector/producer well located at the base of reservoir with Cold Lake oil reservoir conditions. The hot ethane was injected with the pressure above the ethane supercritical pressure. Supercritical ethane enhanced the cyclic solvent gas process by improving the early production rate. As well, there was an increase of recovery of solvent in the blowdown at the end of the experiment.

Ivory et al. (2009) conducted CSI experiments consisting of primary production followed by six (28%C3H8-72%CO2) injection cycles. Oil recovery after primary production and six solvent cycles was 50%. Also, Ivory et al. developed a numerical model of the CSI process that included the non-equilibrium rate equations describing the delay in solvent reaching its equilibrium concentration as it dissolves or exsolves in the oil in response to changes in the pressure and/or gas-phase composition

Laboratory-scale numerical simulation of CSI has been investigated at Alberta Innovates-Technology Futures (AITF) for a long time, and the work is

focused on using the previous learning to improve field-scale simulation for CSI as well as other solvent processes, with an aim of ultimately facilitating the development of improved production.

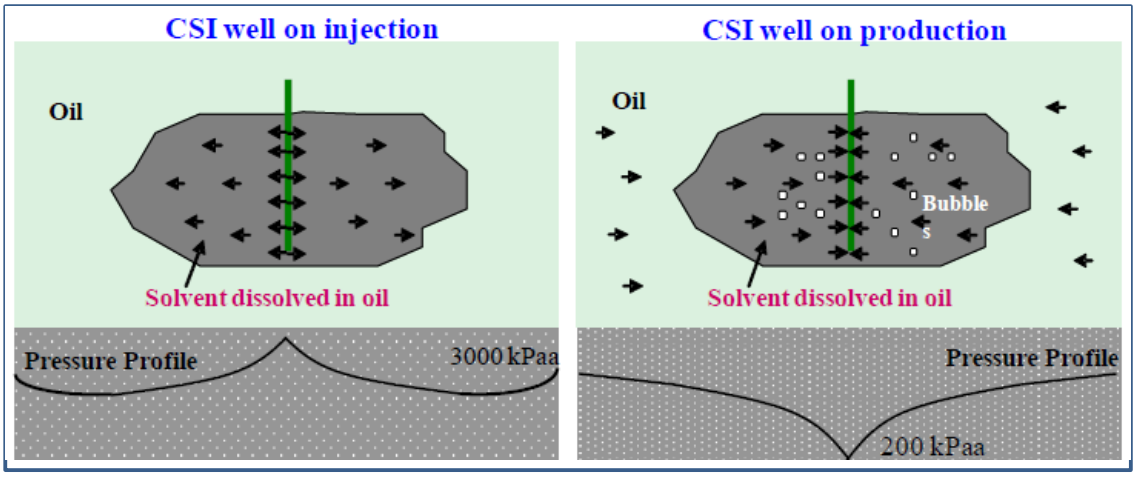

Figure 2-5 Schematic process of CSI (Chang and Ivory, 2012)

2.6 CSS with Solvent (CSS-S)

The concept of using a light hydrocarbon as a steam additive is not new, as evidenced by several patents granted in the late 1970s and early 1980s (Leaute, 2002b). The use of CO_2 and solvents with CSS using vertical wells has been demonstrated (Stone and Ivory, 1987) to cause increased oil recovery as a result primarily of synergistic effects of steam and solvent in reducing oil viscosity.

Various methods have been proposed to use hydrocarbon solvent in combination with steam to increase the oil recovery in a wide range of reservoir conditions and well configurations. LASER-CSS (liquid addition to steam for enhancing recovery process), which is from Imperil Oil Limited, cited and referenced most of methods.

Due to the fact that low molecular weight solvent moves quickly through the formation and is produced with vapour phase, low molecular weight hydrocarbon could hardly improve steam-flood oil recovery (Richardson et al., 1997). This bypassing of light hydrocarbons might have been particularly severe in a California steam-flood with continuous venting of pattern producers surrounding an injector. Richardson instead proposed the use of heavier hydrocarbons with boiling points that are higher than water to counteract inter-well bypassing of solvent.

In the LASER, solvent is co-injected with steam in a CSS process in which solvent was around 6% volume (Leaute, 2002a). The concept of the LASER process is presented in Figure 2-6. Application of the LASER process is intended to use the late CSS cycles, in which the gravity drainage is believed to dominate the recovery mechanism instead of formation re-compaction, solution gas drive, and steam

flashing. Imperial Oil tested this process at its Cold Lake operations where C5+ was injected into 8 vertical CSS wells (Leaute and Carey, 2005). The purpose of the pilot was to determine the reduction in CSOR and solvent recovery. In that process, the recovered solvent composition was close to that of the injected solvent. The overall performance of this pilot was very encouraging; 10 m^3 of incremental bitumen produced for every 1 m^3 of diluents lost to the reservoir.

Horizontal wells improve oil recovery as compared to vertical CSS wells since they increase contact with the reservoir and more effectively utilize gravity drainage.

Co-injection of solvent (C_6H_{14}, condense), injection of solvents before or after steam-injection in the same cycle, and alternate CSS and cyclic solvent injection cycles were strategically simulated on a horizontal CSS well pattern (Chang et al., 2009). From the strategy of co-injection of steam and solvent, the calendar day oil ratio (CDOR) increased significantly with increase in C_6H_{14} concentration in the injected steam up to a 5 mole % C_6H_{14} concentration in steam. Above 5% C_6H_{14} concentration, there was a marginal increase in oil production with the increase in C_6H_{14} concentration, which was also demonstrated by Leaute et al. (1997).

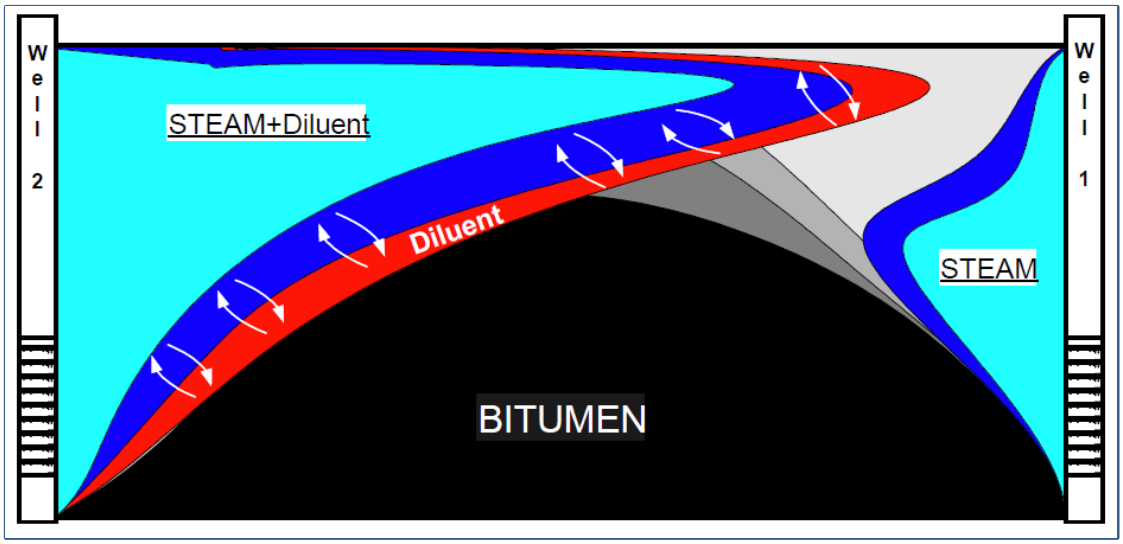

Figure 2-6 LASER process concept (in-situ) (Leaute, 2002b)

2.7 Electrical Resistive Heating with Solvent (ERH-S)

Different electrical heating (EH) methods for heavy oil production have been proposed in the past fifty years. In general, there have three types of electrical heating: microwave heating (frequency range > 300 MHz), resistive heating, and inductive heating. Koolman et al. (2008) compared different electrical heating methods in terms of reservoir effectiveness, technical feasibility and estimation of CAPEX in order to approach an economical application. (1) Microwave heating basically benefits from natural reservoir water content and is based on the friction of water dipoles at their resonant frequency. Analysis has suggested that if the reservoir water content is 10%, then a microwave heating effect can be expected up to a distance of 1 meter from the source; further heat propagation would reply on thermal conduction only. Therefore, microwave stimulation gives only a small effectiveness, but it requires a huge installation commitment. In the case of resistive heating, either the well pipes or the reservoir itself can serve as a resistor where the electrical energy dissipates (Koolman et al., 2008).

(2) Well pipe resistors do not provide adequate effectiveness because the heat propagation works only with thermal conduction from the resistively heated tubing into the reservoir. A disadvantage for resistive reservoir heating is that electrodes must be used. The current flows along the path of least resistance, leading to huge current densities on these paths where the conductivity is good. Hot spots at the point of electrodes with high current densities might be generated, leading to coking and, therefore, loss of electrode-to-reservoir contact, which may not be reversible. (3) Inductive heating offers a much better scenario. Eddy currents are

generated in the reservoir, and no contact between the reservoir and inductor is needed. Heating is only generated in zones with conductivity – and higher conductivity is given where bituminous oil sands containing water reside. The heat is generated in the very place where it is needed. However, inductive heating is hard to install, especially for large-scale applications. Based on the heating area in the reservoir, resistive heating was investigated in this thesis research along with co-injection with solvent into the reservoir because electrical resistive heating can heat a much wider reservoir with some certain initial water saturation than the other two electrical heating methods do.

Electrical resistive heating (ERH) for heavy oil reservoirs is also widely known in the petroleum industry. Conventional thermal recovery processes such as steam injection, steam soak, and in-situ combustion inject one fluid to change oil properties to make it flow easier. Therefore, there are complications of generating, transporting (while avoiding excessive heat losses), and disposing of the injected fluid. ERH does not require a heat transporting fluid, which can be particularly beneficial in deep reservoirs and thin pay-zones where conventional methods are not cost-effective due to excessive heat loss through the adjacent formations. In-situ electrical heating could be a potentially viable heavy oil/ bitumen production technology for reservoirs that are not accessible for SAGD and CSS processes, such as low initial injectivity reservoirs, steam override, and thinner reservoirs.

The ERH process relies to a certain degree on conductivity in the reservoir to carry electrical current between the electrodes and convert it into heat by resistance to its passage. In homogeneous reservoirs, the conductive medium may be

the connate water; in heterogeneous and stratifies pay zones, it could be extensive shale streaks or sands intervals of high water saturation. The current flow in the formation is primarily via ionic conduction through the water-saturated portion of the interconnected pore spaces throughout the reservoir. Electrical energy is converted into heat energy through associated Ohmic losses in the formation or joule effect. Then, Electrical Resistive Heating can provide quick and even heating and be independent of the reservoir permeability or heterogeneity. The overall effect of the heat generation is to reduce the pressure drop near the wellbore by decreasing oil viscosity and improving oil mobility. The current travels from the surface power conditioning unit and through the delivery system to the electrode assembly and is forced through the reservoir matrix, returning to the power conditioning unit by way of a ground return system. Figure 2-7 and Figure 2-8 present the schematics of single vertical and horizontal formation-resistive heating configurations, respectively.

The most successful application so far for electrical resistive heating is remediation technique, which has been demonstrated as a rapid and effective method for the removal of volatile and semi-volatile chlorinated and petroleum hydrocarbons for contaminated soil (Vermeulen and McGee, 2000).

Pizarro et al. (1990) presented low-frequency electrical heating data from a field test performed at Rio Panan oil field in Brazil. The field was shallow, targeting a single oil-bearing formation of small thickness with a rather high viscosity of 2500 cp, characteristics that made this reservoir an appropriate choice for electrical heating as opposed to steam injection. Primary production was increased from 1.2

bbls/day to 13 bbls/day after 70 days of applying 30 kW power across the producing wells, which were 328 ft apart (Pizarro and Trevisan, 1990).

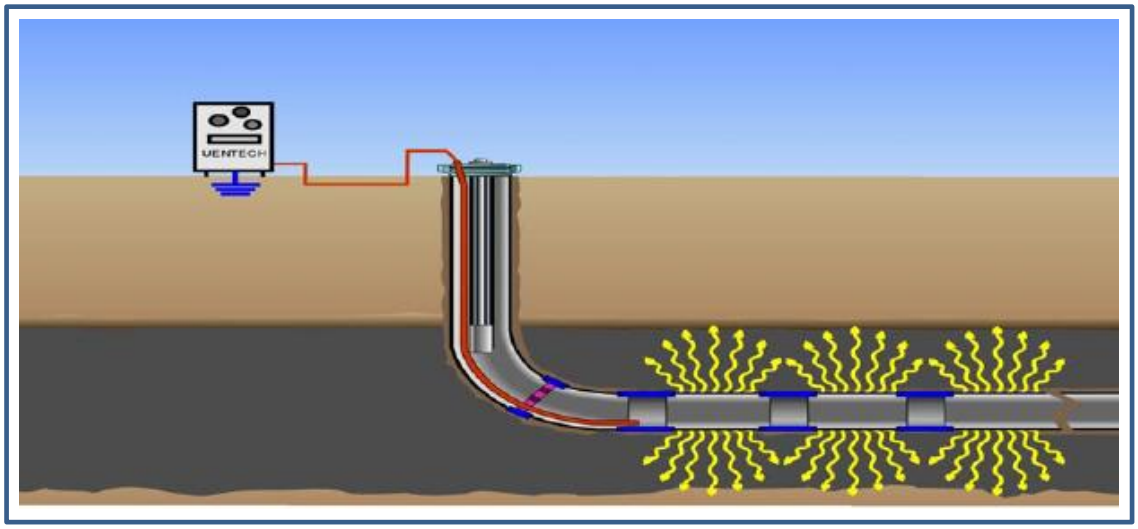

Figure 2-7 Formation-resistive heating system in a horizontal well (Sierra et al., 2001)

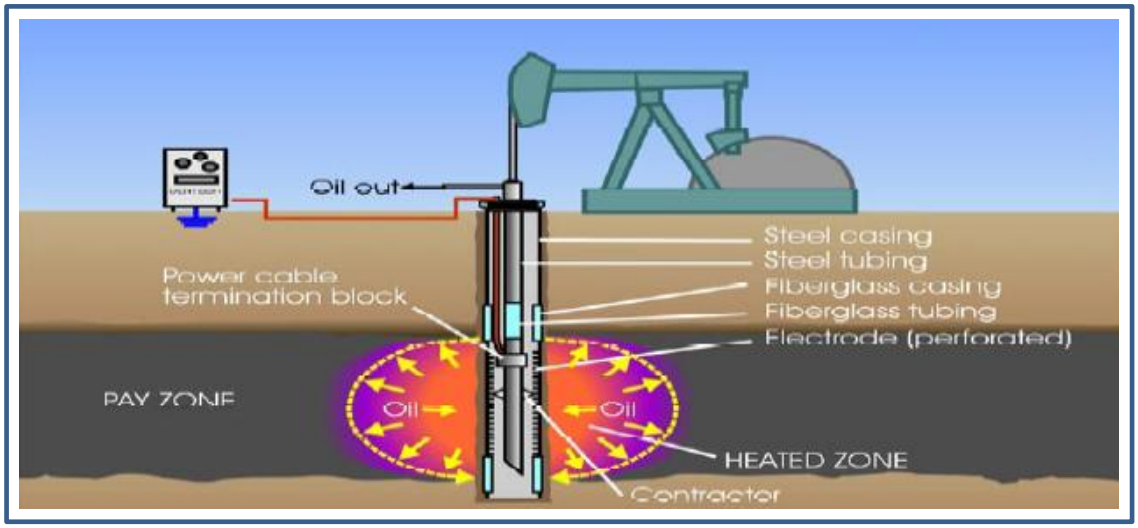

Figure 2-8 Formation-resistive heating system in a vertical well (Sierra et al., 2001)

Rice presented analysis of a single oil production well in the Schoonebeek reservoir in the Netherlands. The reservoir sands are 31 m thick with porosity of 0.3 and permeability in the range 200-4000 md, the oil has an in-situ viscosity of 160 mPa.s and is waxy with a cloud point very close to the reservoir temperature of 40^{o}C. The reservoir pressure of about 7000 kPa is supported by a strong edge aquifer. Primary production was increased from 13 m^{3}/day to 30 m^{3}/day with the surface power of 60 kW and the bottomhole temperature in the range 54-60^{o}C. The well productivity index increases by a factor in the range 1.5 to 4 (Rice et al., 1992).

Uentech International Corp. and its previous associated companies have developed several offshoots of low frequency heating systems. One is a tubing heating system where the metal tubing is energized in a controlled manner by electric power. Another is a block reservoir heating system in a multi-well pattern configuration that is analogous to steam cycling in a production/injection pattern. Both are in experimental stages and have not yet been carried out in field tests (Sierra et al., 2001).

Pizarro developed a numerical model designed to stimulate EOR by in-situ electric heating. With an implicit treatment and the simultaneous solution of the equations, the simulator was validated against basic analytical solutions and a field-test case. They concluded that standard cases involving the resistive method can be handled by pure radial models, and the wellbore damage was gradually removed with the application of resistive heating (Pizarro and Trevisan, 1990).

Wang presented a model to optimize electrical processes by vapourizing water in-situ. In their studies, they used CMG to perform a series of preliminary

simulations of electrical resistive heating in the Athabasca oil sands. The simulation results showed that the incremental bitumen recovery is significant when the formation water is heated to the point of vapourization. The smaller the electrode spacing, the higher the water injection rate, and the electrical heating rate can improve bitumen production during electrical resistive heating processes (Wang et al., 2008).

However, there are some disadvantages for electrical resistive heat, which are listed below (Sierra et al., 2001):

A. The largest problem is the requirement for a carrier of the electrical current. The electrical resistive heating is, therefore, limited.

B. The thermal conductivity of a porous medium changes with the temperature change, as will the electrical conductivity (connate water electrical conductivity). Consequently, the energy transferred from electricity will fluctuate.

C. It is difficult to keep a balance of suitable conductivity and yet have sufficient resistivity to prevent a dead short circuit that could be caused by brine-saturated thick sand intervals.

Thus, it might be desirable to inject water into the reservoir from time to time to maintain a path for the electrical current. This process consists of converting electrical power into heat by utilization of flood water itself as a resistance heating element in the region of the water-injection well. Furthermore, the water injected could probably pick up the heat and transmit it farther into the formation by the convective process.

Yuan patented the wet electrical heating process for VAPEX/SAGD start up. In the process, low frequency AC electrical power is used to heat the reservoir between the injection and production wells during the start-up period. 'Wet electric' means to inject brine solution around the wells to create electrolyte zones. This allows Ohmic heating of the targeted zone between the wells to be achieved much more uniformly and faster. WEH could shorten the SAGD initialization process. WEH also provides the potential for the well pair to be drilled further apart. No detailed VAPEX test was reported with this type of electrical heating (Yuan et al., 2004).

A list of candidate reservoirs suitable for resistive heating systems is given below (Sierra et al., 2001):

- Heavy oil reservoirs where steam cannot be used due to various reasons such as depth of the reservoir, poor injectivity for steam, or infrastructures for steam are not justifiable.
- Reservoirs in which modest amounts of heat will produce significant change in production.
- Reservoirs with overlain permafrost or having high permeability streaks or fractures.
- Limestone heavy oil reservoirs.

Other typically desired properties for the candidates are:

- API gravity in 10-20 Degree range.
- Pay thickness of 2 meters or larger.
- Primary unstimulated oil production of 30 bopd/well or more.

- Formation resistivity of 30 ohm-meters or more.
- Oil viscosity of 100 cp or higher.

CMG's STARS simulator already includes this process. CMG's STARS also is capable of modeling solvent injection processes by using solubility equilibrium values (K values) to calculate the concentration fraction of solvent in each fluid phase and model electrical resistive heating based on Heibert theory (1986). Therefore, the hybrid process of resistive electrical heating and solvent injection can be directly modeled with CMG's STARS simulator.

2.8 Summary

From the literature review, the advantages and disadvantages for three thermal hybrid processes can be summarized as shown in Table 2-1:

Table 2-1 Advantages and disadvantages for each process

	SAGD	CSS	VAPEX	ERH
Advantages	Generally higher recovery; Better justified SOR at higher recovery factor.	More robust and tolerate to heterogeneities; Better SOR initially.	No steam need; No CO_2 emission.	Less water required and CO_2 emission; Intensive energy input and controlled temperature increase; Without limitation in reservoir selection.
Disadvantages	Requires higher vertical to horizontal permeability ratio; Limitation in thickness of the reservoir; Too much water usage and CO_2 emission.	Lower recovery factor; Not applicable in areas with thick bottom water or top gas; Too much water usage and CO_2 emission	Low oil rate; Heterogeneity impact.	Need current carrier; Big impact from fluctuated conductivity.

CHAPTER 3

NUMERICAL INVESTIGATION OF SOLVENT AND ERH HYBRID PROCESS

3.1 Model description

Reservoir resistive electrical heating is already widely known in the petroleum industry. CMG's STARS simulator already includes this process. CMG's STARS is also capable of modeling solvent injection processes (Zeng et al., 2008) by using solubility equilibrium values (K values) to calculate the concentration fraction of solvent in each fluid phase.

A series of simulations was completed to evaluate the performance of a hybrid resistive electrical heating process coupled with solvent injection in a symmetry model. Due to the symmetry of the well pattern used, only half of the model needed to be simulated. The dimensions of the standard model are 30m×30m ×10m. The grid size used in the simulation is 1m×3m×0.5m for the model. The total grid number is 30*10*20=6000. The basic parameters of the simulation model are shown in Table 3-1.

The viscosity and density of the dead oil used in this simulation at 27^{o}C and 400 kPa are 6217.86 mPa.s and 979.92 kg/m^{3}, respectively. The water-oil and gas-liquid relative permeability data are shown in Figure 3-1 and Figure 3-2. The solvent used in the simulation is C1+NC_4. The viscosity and densities at different NC_4 concentrations are modeled with CMG's WINPROP. The viscosity decreases with

the temperature increase, and the trend is shown in Figure 3-3. The relationship between oil-phase viscosity and temperature is computed according to CMG:

$$\ln(\mu_o) = \sum_{i=1}^{n_c} f_i \ln(\mu_i)$$

where μ_i is the component viscosity and n_c is the number of components in the oil-phase.

The K value correlation is used. The coefficient of the correlation is included in Table 3-1.

In CMG's STARS, solubility is defined by the K-values of the components. As a function of p and T, the K-value can be calculated by the following correlation:

$$\mathrm{K} = \left(\frac{\mathrm{KV1}}{\mathrm{p}}\right) * \mathrm{EXP}(\mathrm{KV4}/(\mathrm{T} - \mathrm{KV5})$$

where T is temperature in K and p is gas phase pressure in kPa. KV1, KV4, and KV5 correspond to the units of p and T.

In the basic hybrid process model, the ground voltage is set as 0 V and the injector/producer is set as the electrode, which has a high voltage. The ground and electrode form a circuit that makes the current flow from the electrode to the ground and causes the energy consumption to heat the reservoir. Thermal and electrical properties of the basic model are in Table 3-2.

Table 3-1 Basic Parameters

Parameters	Value
Reservoir Dimension	30 m×30 m×10 m
Permeability	5000 md(in Base Case)
Porosity	0.35
Initial water saturation	30%
Oil Viscosity @ 27 ^{o}C and 400 kPa	6217.86 cp
KV1 (k value correlation)	2.309e+06 kPa
KV4 (k value correlation)	-2727.4
KV5 (k value correlation)	-2727.4
Dispersion coefficients in oil phase	0.000864 m2/day
Dispersion coefficients in gas phase	0.002 m2/day
Production pressure	490 kPa
Injection pressure	400~490 kPa (Changing with position)
Top injection pressure	490 kPa
Relative permeability curve	Figure 3-1, Figure 3-2
Standard Voltage	110~250 V (Changing in different simulations)

Figure 3-1 Water-oil relative permeability data

Figure 3-2 Gas-liquid relative permeability curves

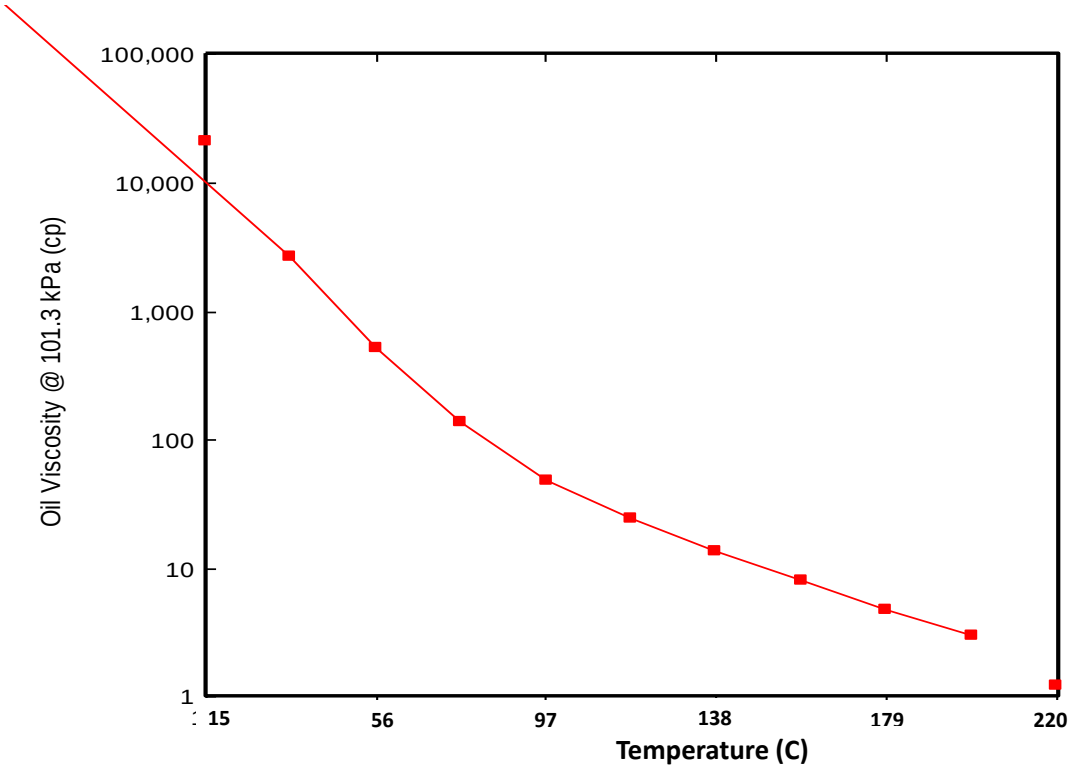

Figure 3-3 Viscosity vs. Temperature

Table 3-2 Thermal and Electrical Properties of the Basic Model

Property	Volumetric Heat Capacity	Thermal Conductivity
Overburden	2.35E+06 J/(m3.^{o}C)	1.728E+05 J/(m*day* ^{o}C)
Underburden	2.35E+06 J/(m3. ^{o}C)	1.728E+05 J/(m*day* ^{o}C)
Rock	2.35E+06 J/(m3. ^{o}C)	6.6E+05 J/(m*day* ^{o}C)
water		5.34E+04 J/(m*day* ^{o}C)
Oil Phase		1.15E+04 J/(m*day* ^{o}C)
Gas Phase		140 J/(m*day* ^{o}C)
Rock Compressibility	7E-6 1/kPa	

3.2 Sensitivity analysis

This section discusses a sensitivity analysis that was done to evaluate the future performance of the Electrical Heating (EH) process. As mentioned previously, the water content plays an important role during EH. With the temperature increasing, the water around the electrode could be vapourized due to the overheating of the electrode area resulting in the cut-off of the electrical circuit and process termination. However, under the reservoir conditions, because the pressure is relatively high, the water vapourization temperature increases correspondingly. The vapourization temperatures of different pressures in this model are shown in Table 3-3.

When the water vapourizes into steam around the electrode, the conductivity of the electrical current stops. On the other hand, the steam could form a chamber that assists in reducing the oil viscosity as well. Simulations with temperatures higher than the vapourization temperature were reported by Wang et al. (2008), so all the simulations in thesis were completed at temperatures under the water vapourization temperature.

Table 3-3 Pressure vs. Water Vaporization Temperature (www.engineeringtoolbox.com)

Reservoir Pressure (kPa)	Water Vaporization Temperature (^{o}C)
400	143.61
410	144.5
420	145.38
430	146.23
440	147.08
450	147.9
460	148.72
470	149.51
480	150.3
490	151.07
500	151.83
600	158.83
700	164.95
800	1170.41
900	175.35
1000	179.88

3.2.1 The Electrode Choice

The hybrid process of Electrical Heating with Solvent Injection Process has two mechanisms for reducing the viscosity of heavy oil: viscosity reduction with temperature increase and viscosity reduction with solvent injection.

In this scenario, the bottom-hole pressures of the producer and injector are kept constant at 490 kPa and 465 kPa, separately. (b)

Figure 3-4 shows the cumulative oil as a function of time for these eight cases, which involve four Injector-as-Electrode cases (Cases 1, 2, 3, 4) and four Producer-as-Electrode cases (Cases 5, 6, 7, 8) in 110 V, 170 V, 220 V, and 240 V. The worst cumulative oil production was obtained under the lowest voltage and Producer-as-Electrode case (110 V), and the best cumulative oil production was obtained with the highest voltage and Injector-as-Electrode case (240 V). From comparison of the curves, under the same voltage, the Injector-as-Electrode cases show higher cumulative oil productions than the Producer-as-Electrode cases in 3000 days. From the trail simulations, after 3000 days simulation, the curve shapes will not change any more. As a consequence, the simulation time in my research is chosen as 3000 days. **Error! Reference source not found.** and Figure 3-5 show the comparison of oil recoveries under different voltages when the producer and injector act as electrodes separately.

However, when the producer acts as an electrode, the cumulative oil productions of the Producer-as-Electrode cases at the same voltage are higher than those of the Injector-as-Electrode cases in the first 1400 days. The most likely reason for these results is because of the heat loss to the underburden when the

electrode is placed along with producer because the gap between the electrode/producer and underburden is much shorter than that between the electrode/injector and underburden.

Table 3-4 compares the temperature, NC_4 oil mole fraction, and oil viscosity in the location of the Producer (30,1,20) and Injector (30,1,14) in Case 4 and Case 8, separately. Figure 3-6 shows the local properties with the producer position changing with time.

In this scenario, the water plays a very important role. During the high voltage heating process, the temperature increases quickly and highly, and, consequently, more water will become less dense and easy to produce.

Figure 3-7 shows comparisons of water saturation, electrical potential, electrical conductivity, and cumulative energy input in different voltage values. From Figure 3-7 (a), because the temperature is low , the water saturation and electrical conductivity keep almost constant; consequently, the cumulative energy keeps increasing until the last day. Figure 3-7 (b) shows a much matched trend in water saturation, electrical conductivity, and electrical potential. With the water saturation decreasing, the electrical conductivity and potential decrease as well. Comparing Figure 3-7 (c) and Figure 3-7 (d), the electrical current stops due to the water saturation decreasing to zero. Although the temperature increase of 240 V is higher than that of the 220 V case, water saturation can keep a slow decrease in 240 V, which can maintain electrical conductivity.

Figure 3-8 shows the viscosity changing with time. Also, the relationship between viscosity, temperature, and NC_4 distribution is shown. When the

temperature is high, the NC_4 fraction is low. From Figure 3-8, there is an optimal temperature for the NC_4 fraction maximum. The temperature is around 40~45^{o}C.

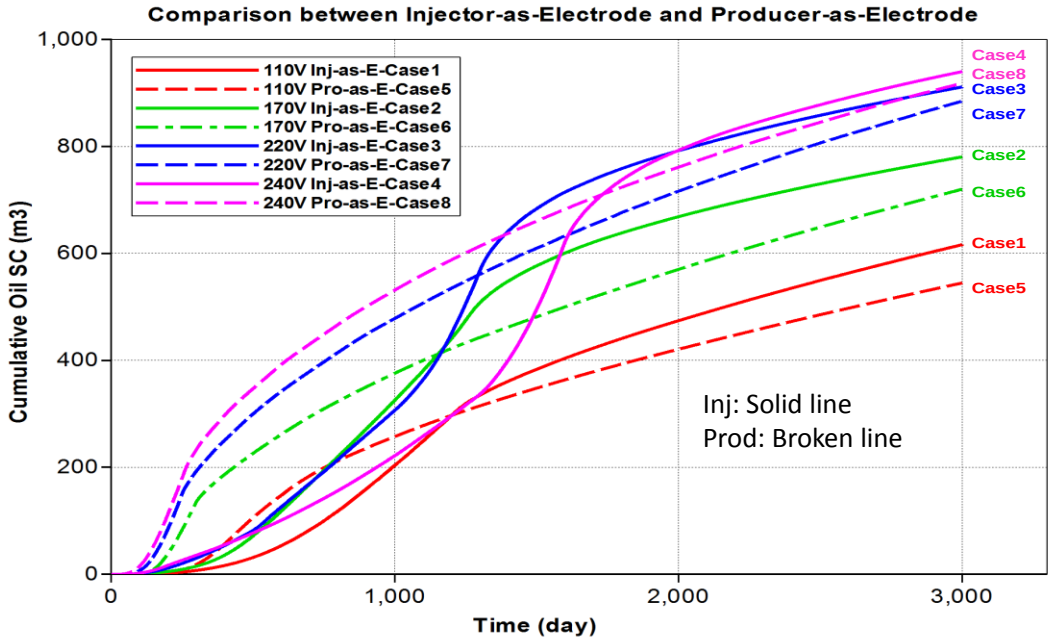

(a)

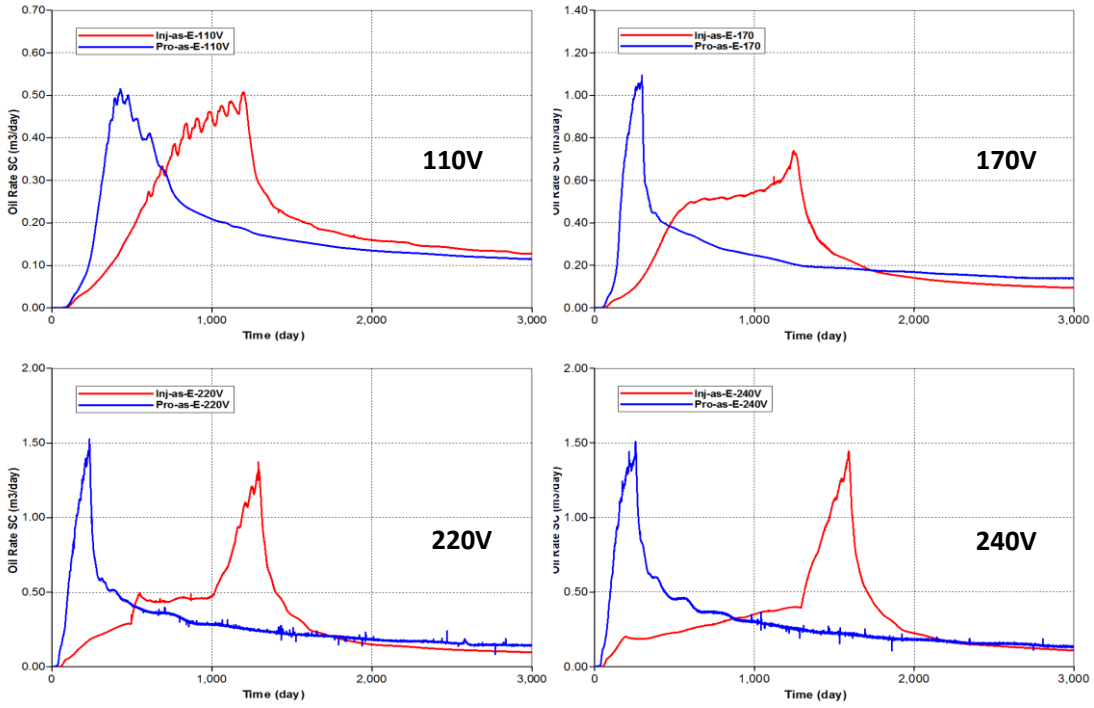

(b)

Figure 3-4 Effect of electrode position (a) Cumulative oil production and (b) oil rate at different Voltage

Figure 3-5 Oil Recovery Comparison between Electrode within Injector and Electrode within Producer

Table 3-4 Comparison of parameters in Case 4 and Case 8

Location	Electrode Position	Temperature (^oC)	NC_4 (oil mole fraction)	Oil Viscosity (cp)
30,1,20 (Producer)	Injector-as-Electrode	63	0.0499	191.9
	Producer-as-Electrode	80.4	0.2071	15.8555
30,1,14 (Injector)	Injector-as-Electrode	145.3	0.005654	10.8424
	Producer-as-Electrode	87.7	0.2699	6.6938

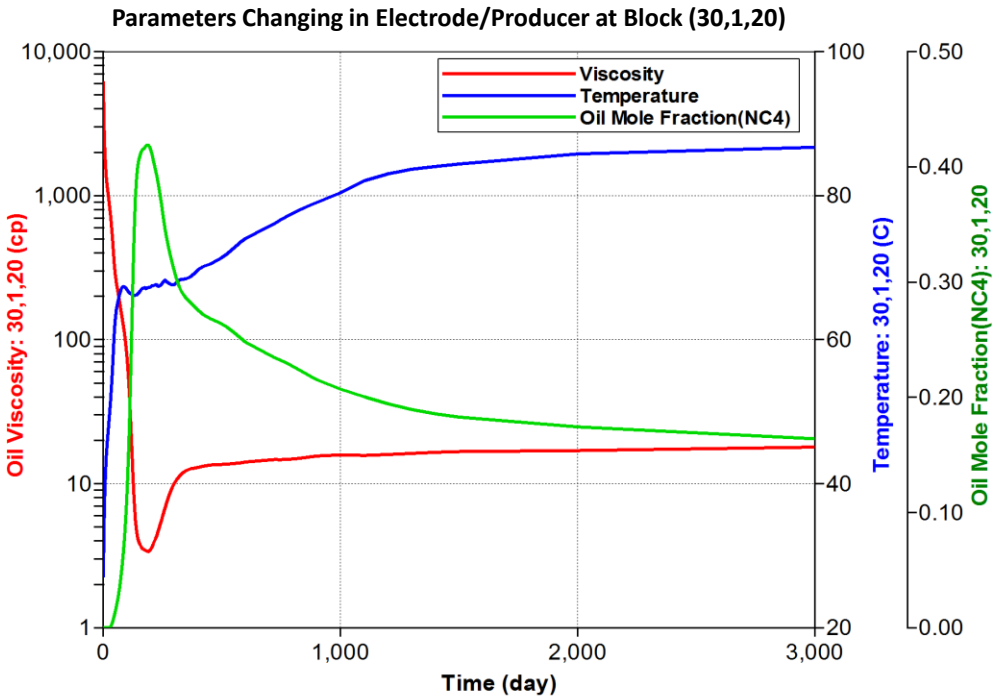

(a)

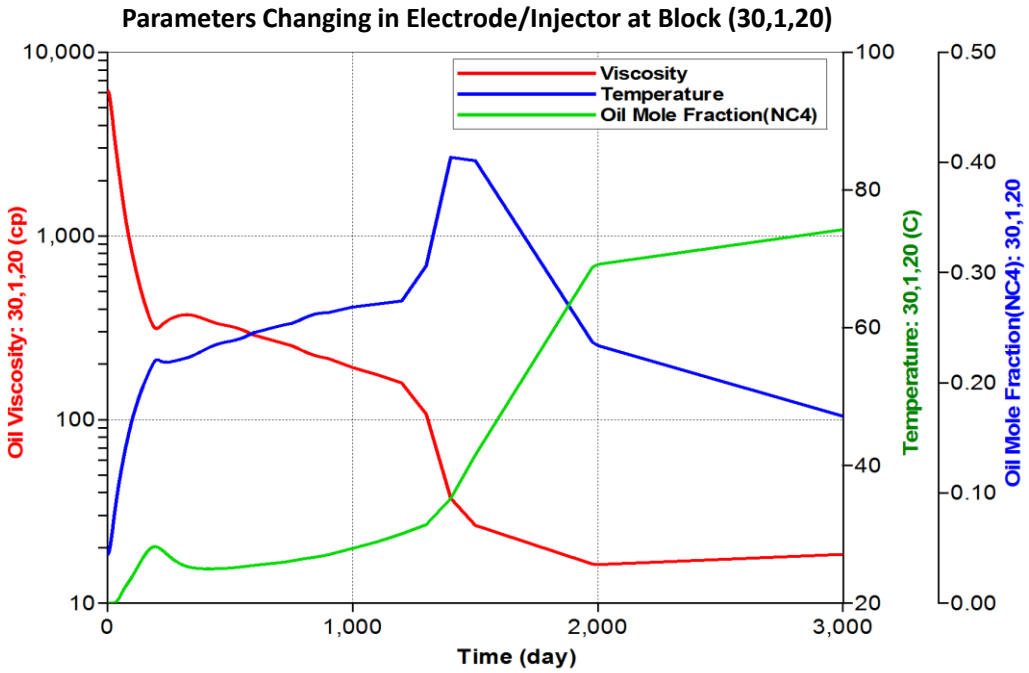

(b)

Figure 3-6 Viscosity, NC_4 fraction, and Temperature change with time at block (30,1,20) (a) producer as electrode; (b) injector as producer

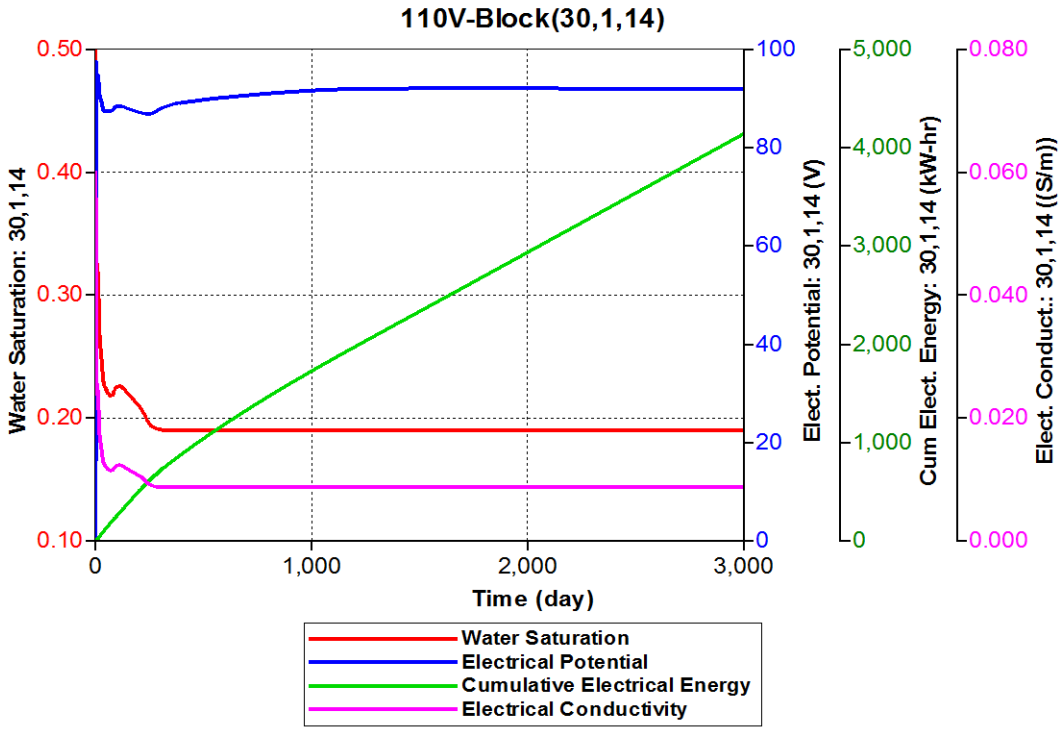
110V-Block(30,1,14)
Water Saturation: 30,1,14
Elect. Potential: 30,1,14 (V)
Cum Elect. Energy: 30,1,14 (kW-hr)
Elect. Conduct.: 30,1,14 ((S/m))
Time (day)
Water Saturation
Electrical Potential
Cumulative Electrical Energy
Electrical Conductivity

(a)

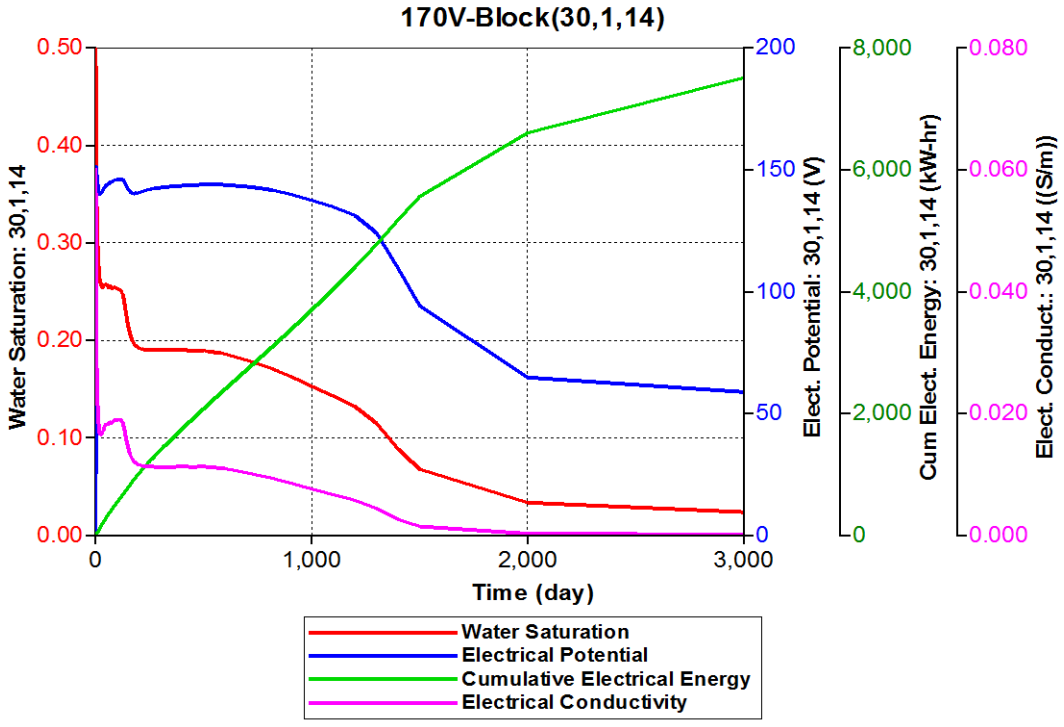
170V-Block(30,1,14)
Water Saturation: 30,1,14
Elect. Potential: 30,1,14 (V)
Cum Elect. Energy: 30,1,14 (kW-hr)
Elect. Conduct.: 30,1,14 ((S/m))
Time (day)
Water Saturation
Electrical Potential
Cumulative Electrical Energy
Electrical Conductivity

(b)

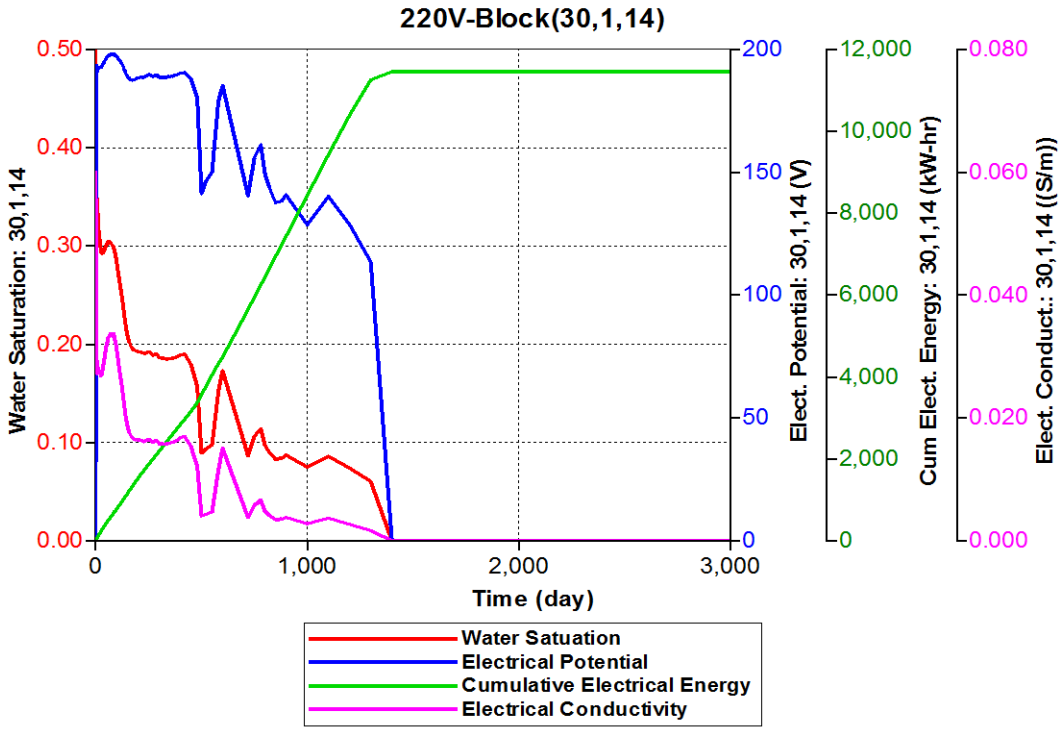

(c)

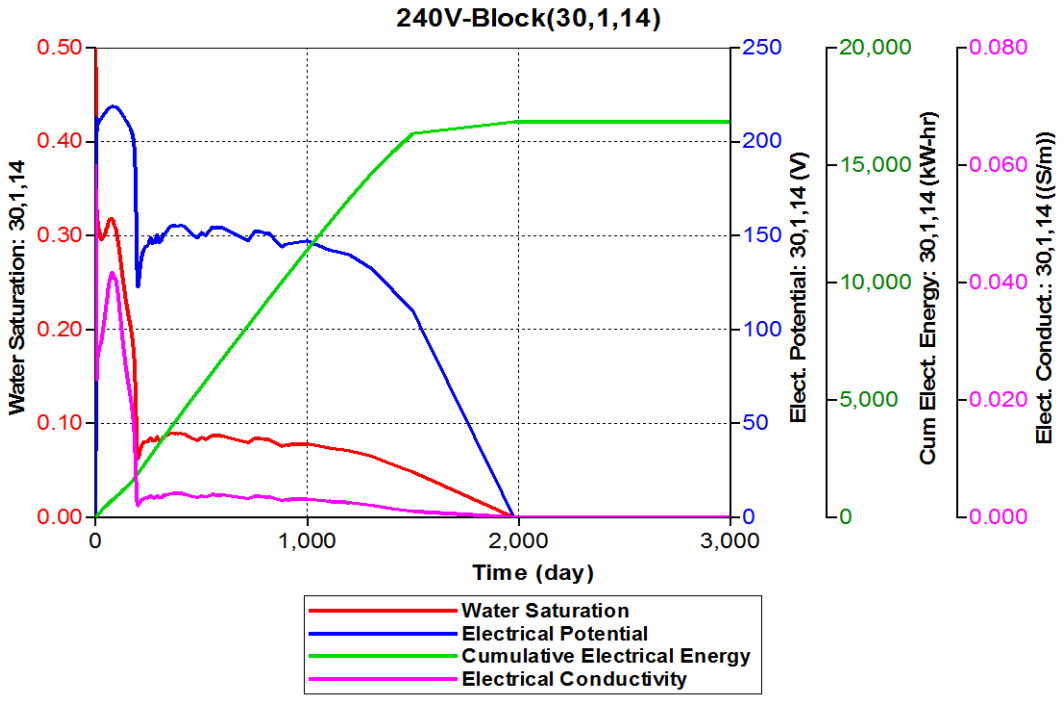

(d)

Figure 3-7 Electrical properties changing in electrode location

(a) 110 V; (b) 170 V; (c) 220 V; (d) 240 V

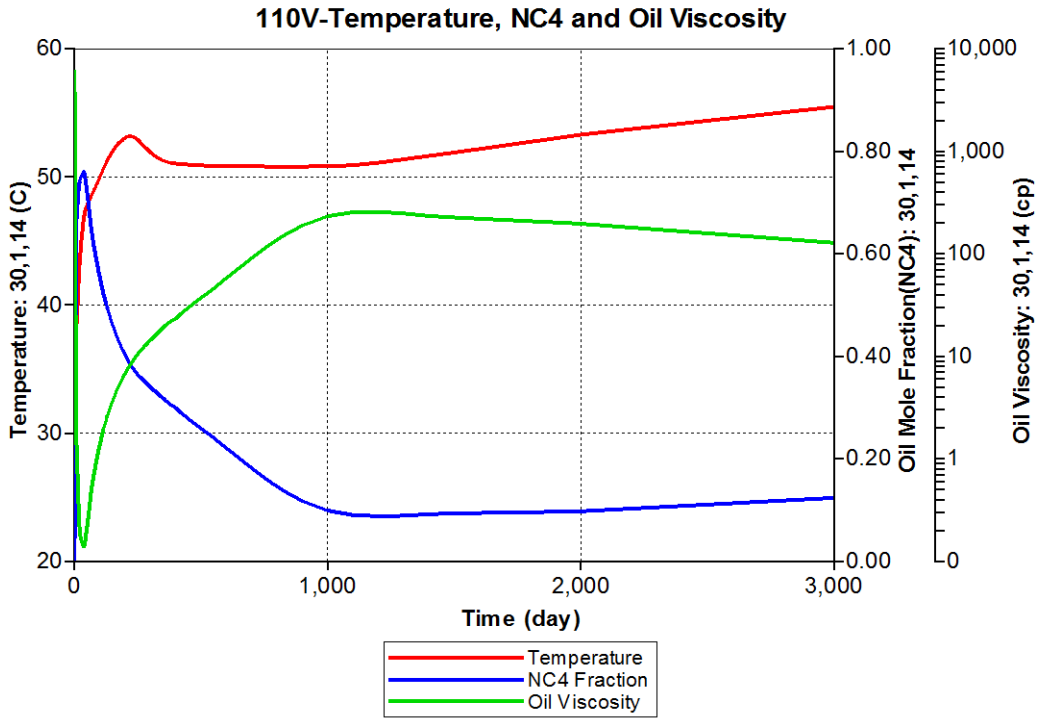
110V-Temperature, NC4 and Oil Viscosity
Temperature: 30,1,14 (C)
Oil Mole Fraction(NC4): 30,1,14
Oil Viscosity: 30,1,14 (cp)
Time (day)
Temperature
NC4 Fraction
Oil Viscosity

(a)

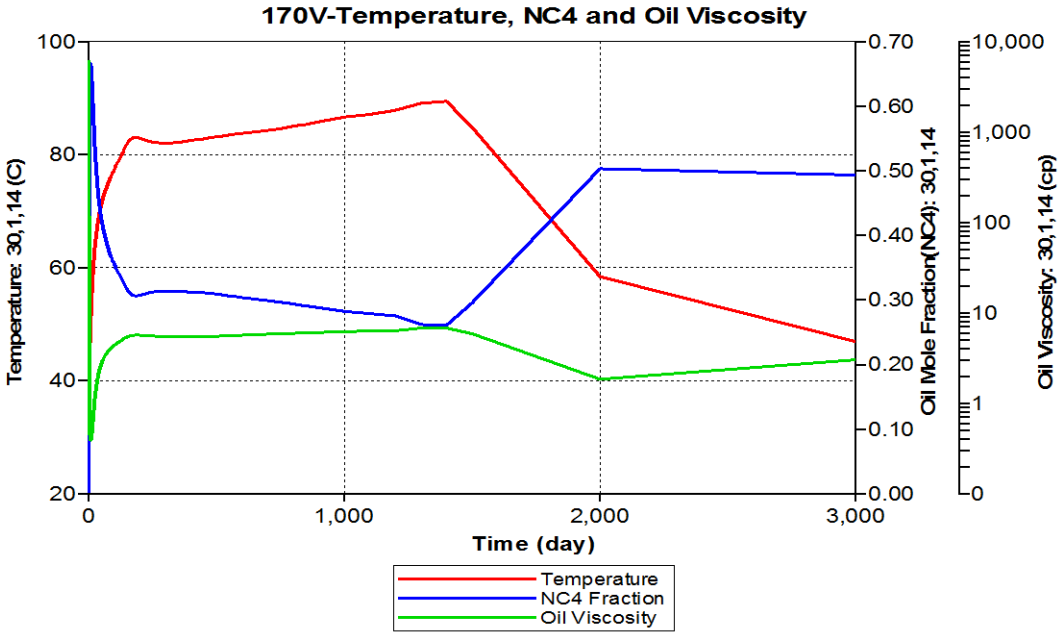
170V-Temperature, NC4 and Oil Viscosity
Temperature: 30,1,14 (C)
Oil Mole Fraction(NC4): 30,1,14
Oil Viscosity: 30,1,14 (cp)
Time (day)
Temperature
NC4 Fraction
Oil Viscosity

(b)

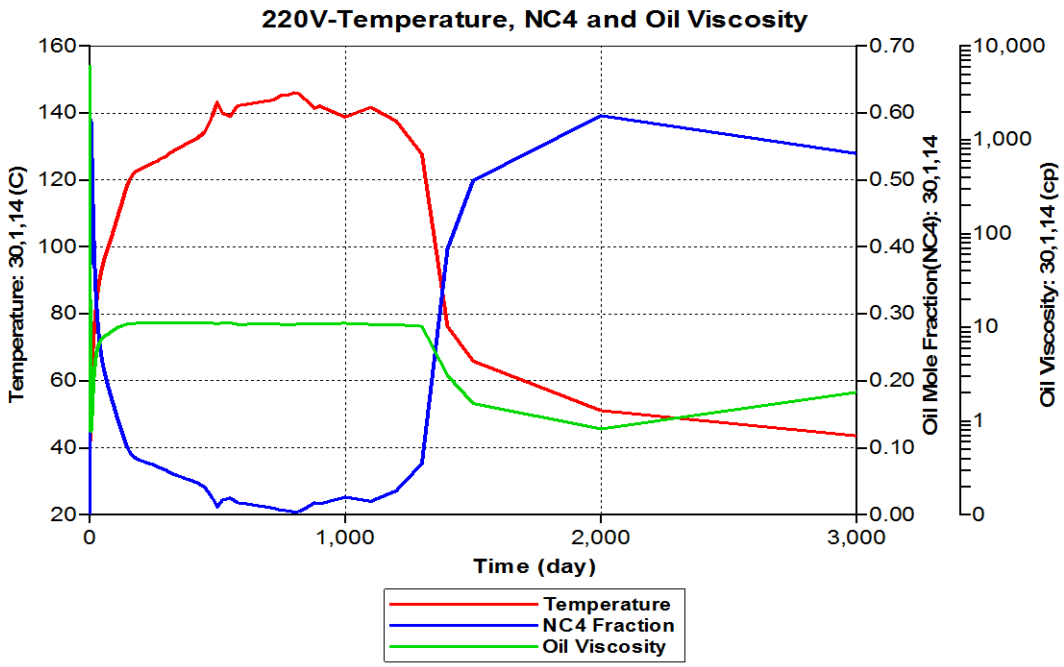

(c)

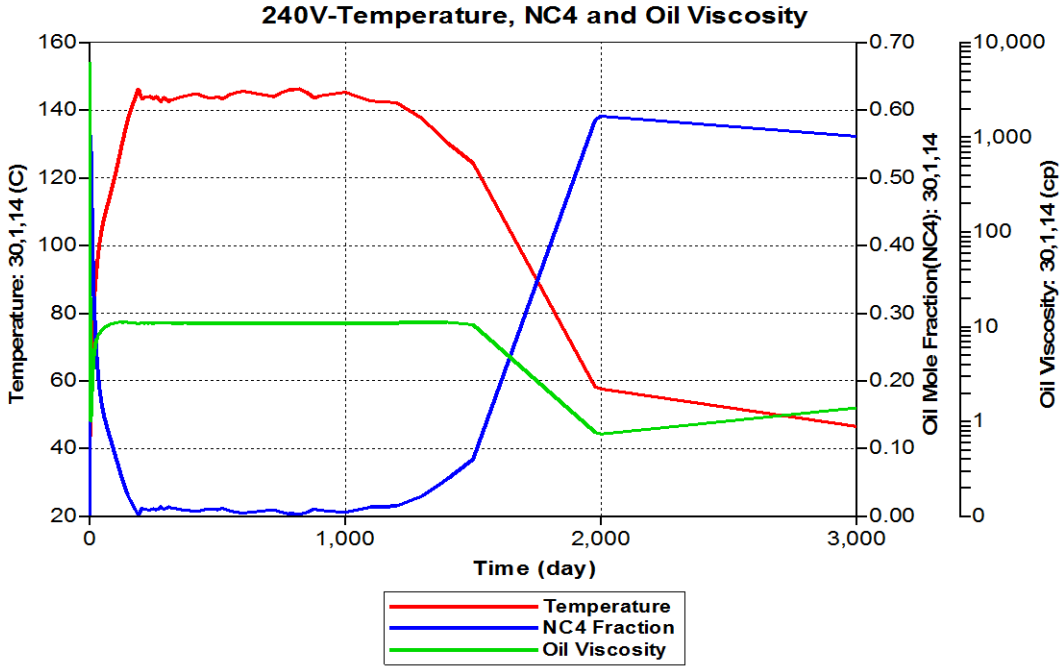

(d)

Figure 3-8 Comparison of viscosity, temperature, and NC_4 in

(a)110 V (b)170 V (c)220 V (d)270 V

3.2.2 Hybrid Process vs. VAPEX

In order to evaluate this hybrid process, we compared the hybrid process with solvent injection alone. In this scenario, two permeability values with the hybrid process and VAPEX (solvent injection alone) are compared. Figure 3-9 presents a very clear difference between the hybrid process and non-EH process in both permeability values. For the high permeability value, the cumulative oil recovered with the hybrid process is around 3.5 (=897.5m^3/259.4m^3) times higher than that of the VAPEX process. The counterpart of the 1000 md value, this number reaches up to 7.38 (=158.3m^3/21.4m^3), which is higher than that from higher permeability reservoir. From this scenario comparison, the positive results illustrate that this hybrid process can effectively enhance the oil recovery and more efficient in low permeability reservoir than high permeability reservoir.

Figure 3-10 gives the change in the specific block (producer) location properties with time. From Figure 3-10 (a), the observation is that there are three stages in the hybrid process: 1. heating dominating the viscosity reduction, 2. heating and solvent dissolution playing a combined role for viscosity reduction; 3. solvent dissolution taking the dominating role in viscosity reduction. Understanding this process will help to optimize the hybrid process technically and economically.

In the hybrid process, because the temperature accelerates the solvent dissolution, the oil saturation distribution in the hybrid process is different from the VAPEX process. Comparing the oil saturation between the hybrid process and VAPEX process, as shown in Figure 3-11 and Figure 3-13, the cumulative oil results are easily explained. Under the hybrid process, the solvent dissolution penetrates

further because of the temperature increase; however, in the solvent injection part of the process, the solvent forms a chamber that is the same as the VAPEX solvent chamber. Consequently, the viscosity distribution forms as the NC_4 dissolution chamber, which is shown in Figure 3-15.

Figure 3-12 and Figure 3-14 show the oil viscosity and saturation changing with NC_4 distribution dissolution in a specific block of the hybrid process and VAPEX process, respectively. Block(24,1,14) is located above injector and the Block(28,1,6) is in the middle of producer and injector.

The hybrid process of electrical resistive heating and solvent injection shows a better oil recovery performance than solvent injection alone. In the hybrid process, there are three stages. First, mainly the electrical resistive heating increase reduces the viscosity. Second, the electrical resistive heating, accompanied with NC_4 dissolution, lessens the viscosity together. In the last stage, when the electrical resistive heating terminates, the NC_4 dissolution plays a leading role in reducing the oil viscosity. From the Figure 3-10 (a), the 3 stages can be seen clearly.

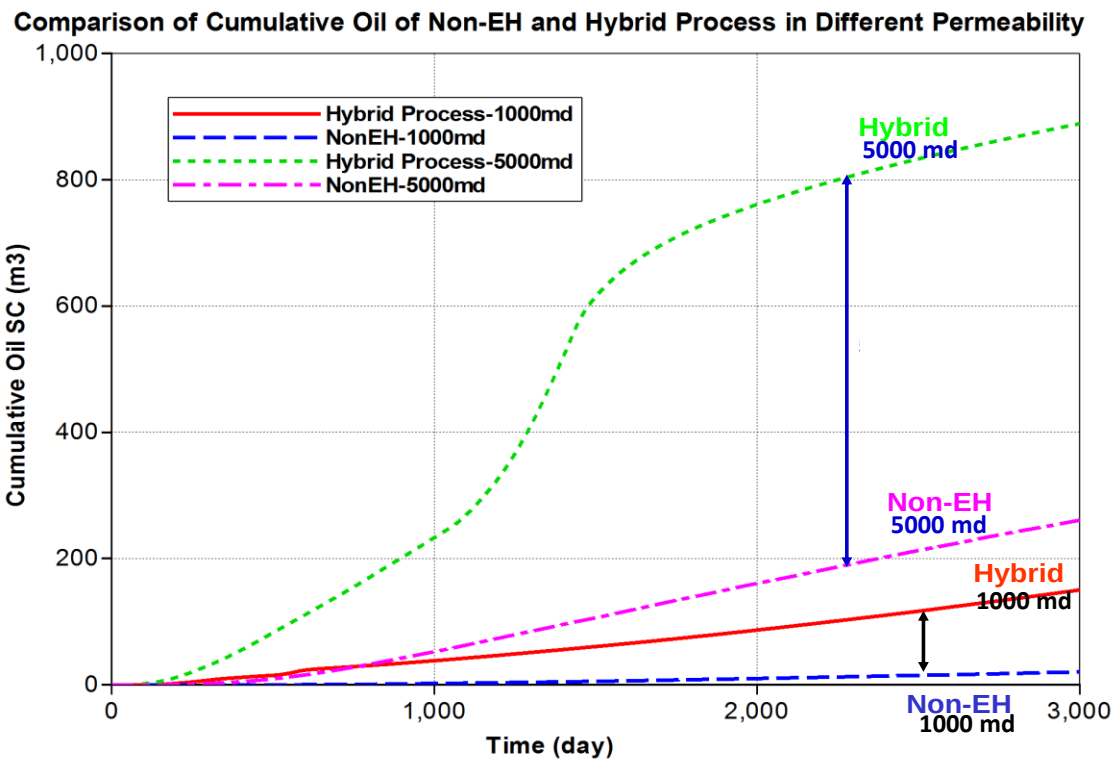

Figure 3-9 Comparison of cumulative oil of hybrid process and VAPEX (Non-EH) process with different permeabilities

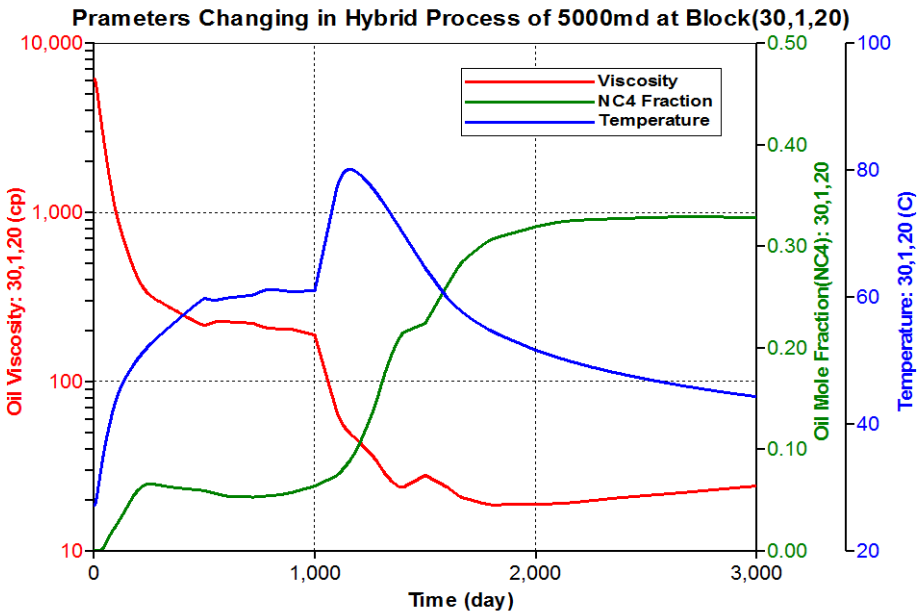

(a)

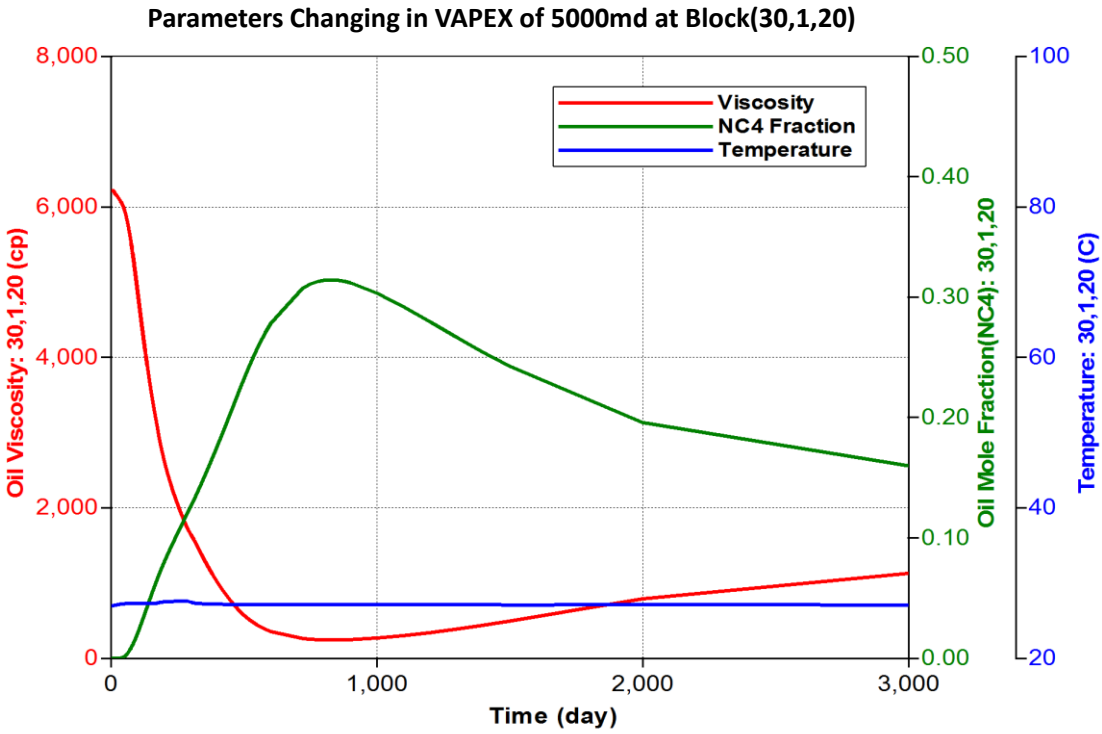

(b)

Figure 3-10 Parameters changing at block (30,1,20) in 5000 md (a) hybrid process; (b) VAPEX (non-EH)

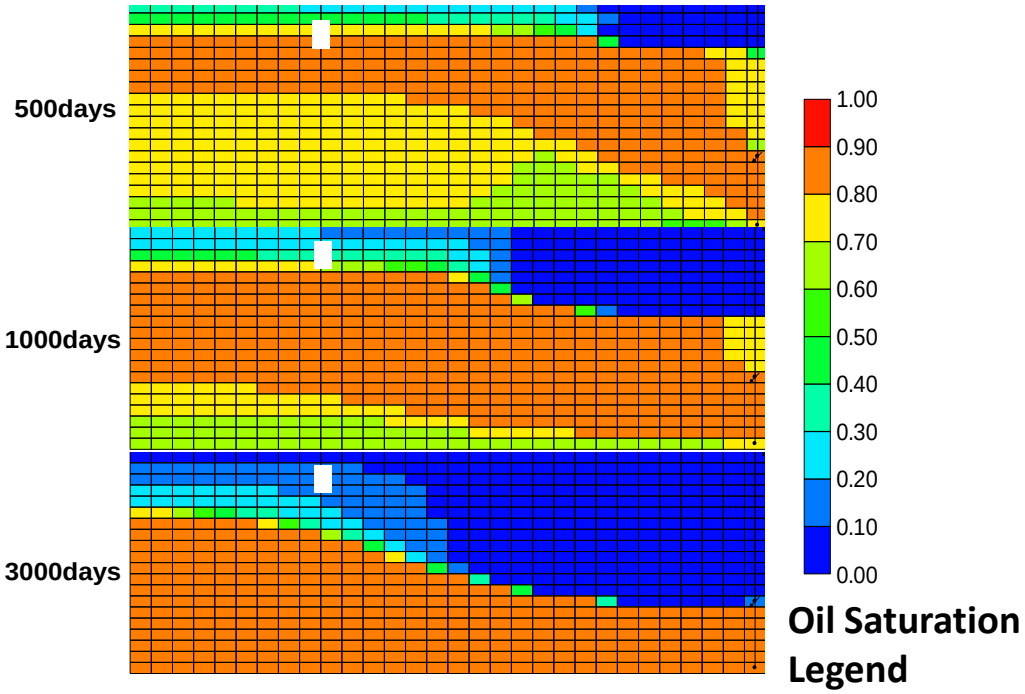

Figure 3-11 Oil saturation distribution trend in hybrid process

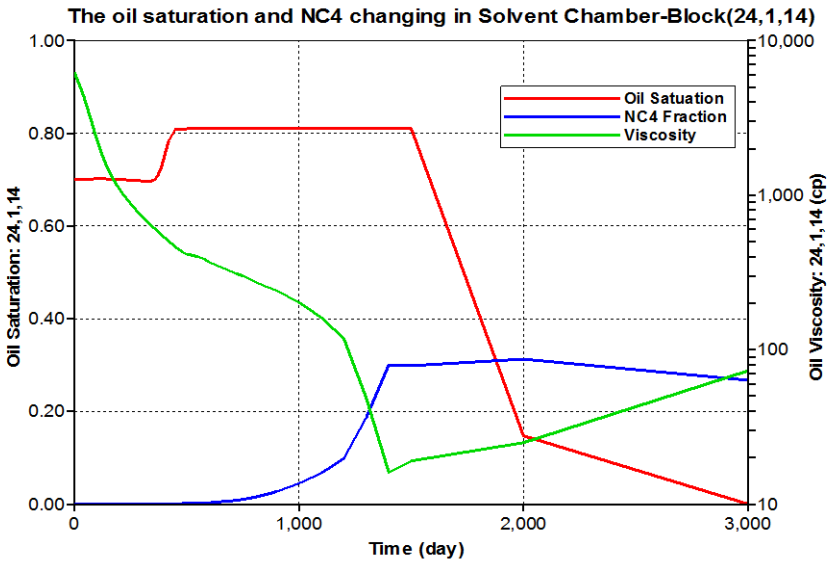

Figure 3-12 Oil saturation changing in the specific block of influenced chamber at block (24,1,14) in hybrid process

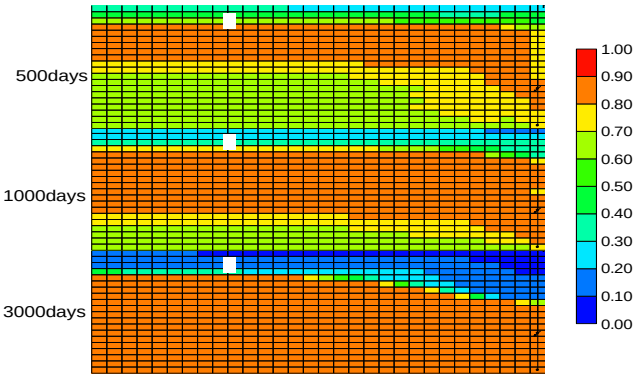

Figure 3-13 Oil saturation distribution trend in VAPEX process

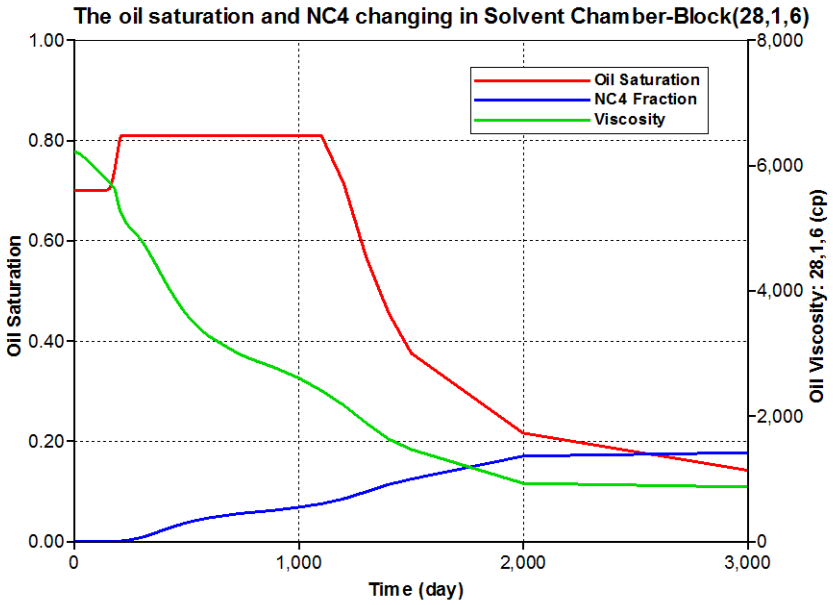

Figure 3-14 Oil saturation changing in the specific block of influenced chamber at block (28, 1, 6) in VAPEX

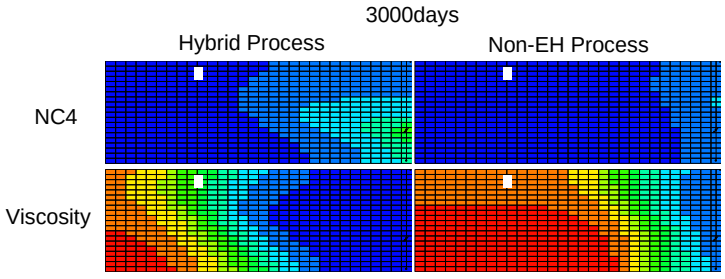

Figure 3-15 Comparison of NC_4 and viscosity distribution in hybrid process and VAPEX process at 3000 days

3.2.3 Well Location

These scenario simulations were performed placing the producer in the lowest layer and setting the distance between injector and producer as 2 m, 3 m, 4 m, and 5 m. The different well locations are shown in Figure 3-15. The producer is at a constant bottom-hole pressure of 490 kPa. From the previous case results, the electrode and injector are located together. In order to evaluate the performance under a reasonable pattern, two series of simulations were conducted.

Series 1: the optimal solvent ratio of C1 to NC_4 is decided by CMG's WINPROP in different injector locations which have different layer pressures.

Series 2: the solvent ratio of C1 to NC_4 is kept the same in different well positions.

The solvent ratios in this scenario are shown in the Table 3-5.

As shown in Figure 3-17, when the distance between the injector and producer is 3 meters, the cumulative oil is best in all 4 cases at 3000 days simulation. However, the case with closer distance (2 m) presents a very rapid oil rate in the first 500 days. On the contrary, when the solvent ratio is kept the same in all the cases from Figure 3-19, the case with 3 m distance has the worst cumulative oil. In reality, the solvent ratio is related to the injection pressure. Higher solvent ratio C1 to NC_4 will be costly.

From Figure 3-18, the 3 m case has the largest oil saturation area of all four cases after 3000 days, which agrees with the Figure 3-17. The reasons behind this result are: (1) when the well distance is 2 meters, the oil with high temperature is produced quickly and cause the steam chamber is smaller than that of 3 meter case;

(2) when the well distance is 4 meters, the heated area above the injector is smaller than that of 3 meters case. Figure 3-19 shows a perfect match to Figure 3-20 in which the 5 m case has the largest area of all four cases. In all 9 cases in this scenario, the best case is the 3 m case, which has the highest cumulative oil. Figure 3-21 explains Figure 3-17 very well in the first 1500 days when the 3 m case has a quick oil rate increase. In Figure 3-22, the 3 m case has the largest oil viscosity distribution area.

Following the same procedure, different voltage (110 V) scenarios in the four well locations (2 m, 3 m, 4 m, and 5 m) with the optimal solvent ratio was simulated. Figure 3-23 shows the cumulative oil recovery. In the 110 v voltage scenario, the 3 m case still has the best cumulative oil production of all four well cases (2 m, 3 m, 4 m, and 5 m). The 2 m case has the fastest oil rate at the beginning of production with gravity drainage in a smaller distance between the injector and the producer.

Figure 3-24 presents a very good explanation for Figure 3-23. The 3 m case shows the better oil viscosity distribution in the simulation.

Figure 3-25 shows the comparison of viscosity, temperature, NC_4 fraction, and oil saturation distribution of the producer location (30,1,20) with the different injector positions under the optimal solvent ratio.

Figure 3-26 shows the comparison of viscosity, temperature, NC_4 fraction, and oil saturation distribution of the injector location (30,1,14) with the different injector positions under the optimal solvent ratio. From Figure 3-25, the temperature is under 40^oC in the producer location, and the viscosity reduction in this location is

caused by the NC_4 fraction. The NC_4 distribution changes with the temperature, which is proven in the first section.

In Figure 3-26, the temperature is increased to over 50^oC, and the NC_4 decreases with the temperature increase. In this location, the viscosity of this location is changed by combining the temperature increase and NC_4 dissolution.

Also, simulations with the same solvent ratio at 110 V were completed. The cumulative oil production comparison is shown in Figure 3-27, which agrees with Figure 3-19, no matter how much voltage is used.

Figure 3-28 and Figure 3-29 explain Figure 3-27 very well from the oil saturation and oil viscosity point of view. The trends of saturation and viscosity lines are similar.

This section demonstrates that there is an optimal distance between the injector and producer when the solvent is kept as the optimal ratio, which is calculated by the dewpoint under the injection pressure. In this section, the best distance is 3 meters as the heat can increase to its highest point and the solvent can penetrate up and horizontally.

However, when the injection pressure is higher than the local reservoir pressure and the solvent ratio is calculated by the injection pressure, then the bigger the distance, the better the cumulative oil production. When the injector is closer to the producer, the heat caused by electricity energy will be easily produced with fluid and the solvent as well. At the same time, the higher the injector, the larger the affected zone that the solvent can penetrate because the pressure difference between the injection pressure and local pressure is bigger when the injector is higher.

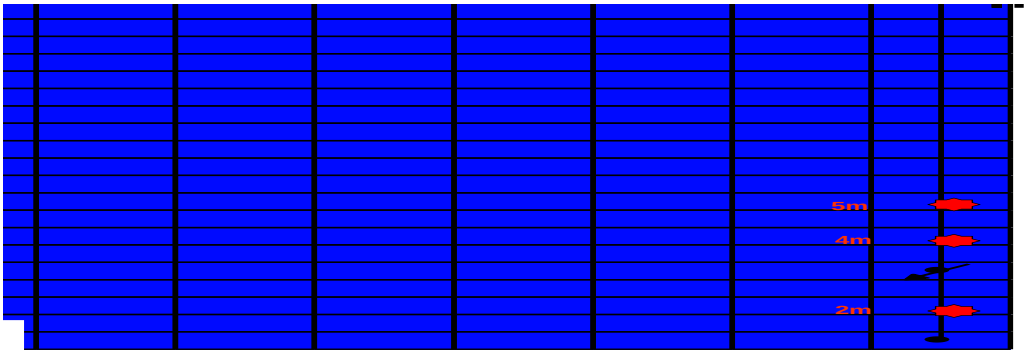

Figure 3-16 Well location

Table 3-5 Solvent Ratio in different injector location

Injector Location (distance from Producer)	Optimal Solvent Ratio			Same Solvent Ratio (22:78)		
	Pressure (kPa)	C1 (%)	NC_4 (%)	Pressure (kPa)	C1 (%)	NC_4 (%)
2m	475	20	80	485	22	78
3m	465	18	82	485	22	78
4m	455	17	83	485	22	78
5m	445	16	84	485	22	78

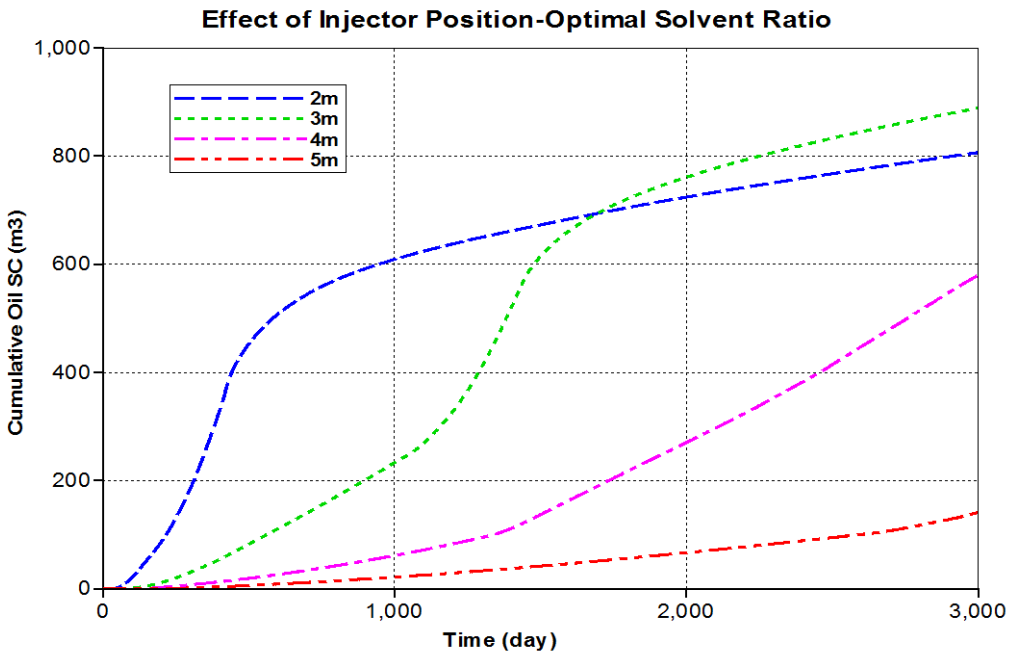

Figure 3-17 Effect of well location on optimal solvent ratio in corresponding location pressure

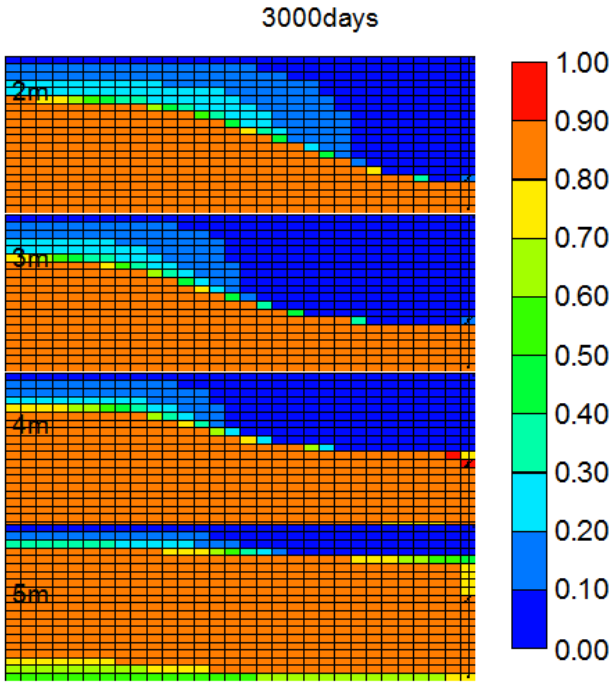

Figure 3-18 oil saturation in different well spacing cases

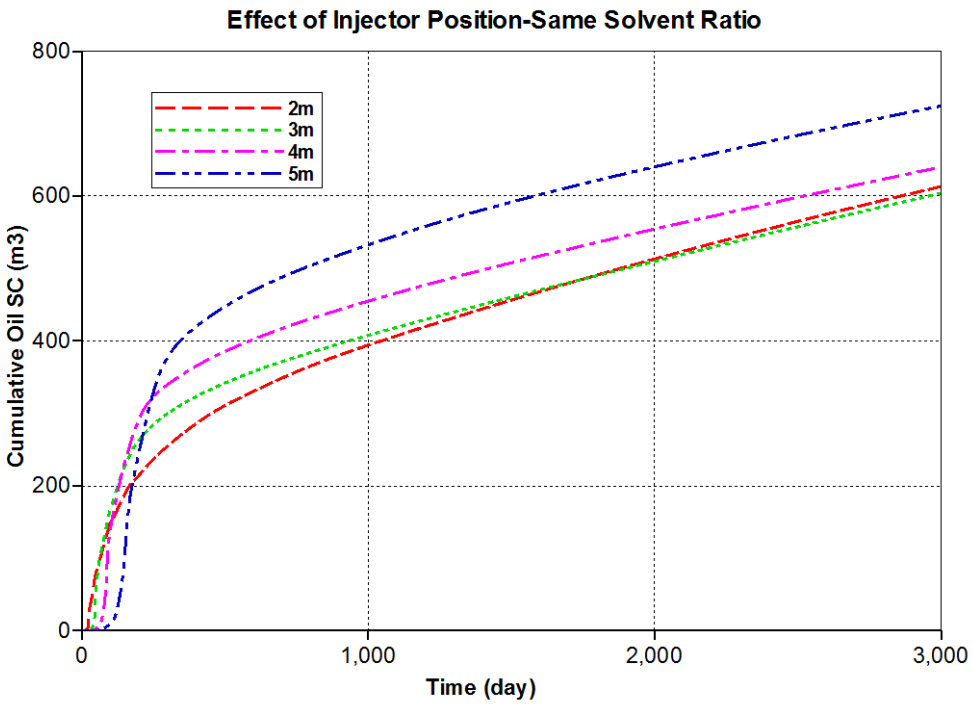

Figure 3-19 Effect of well position with same solvent ratio at same injection pressure

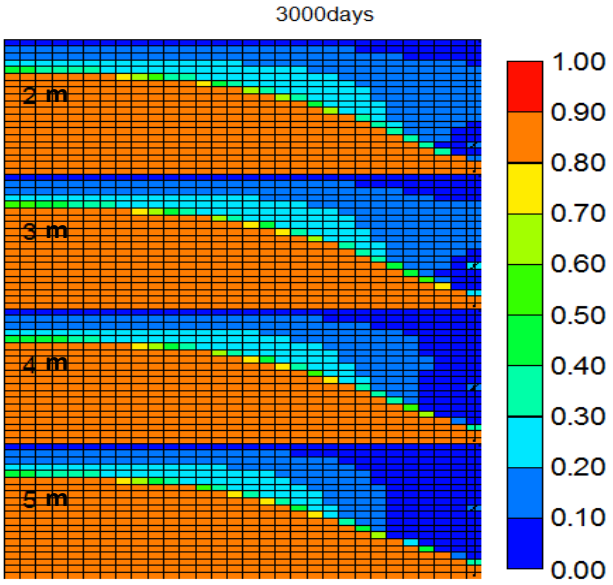

Figure 3-20 Comparison of oil saturation in different well locations (2 m, 3 m, 4 m, 5 m) at 3000 days (same solvent ratio)

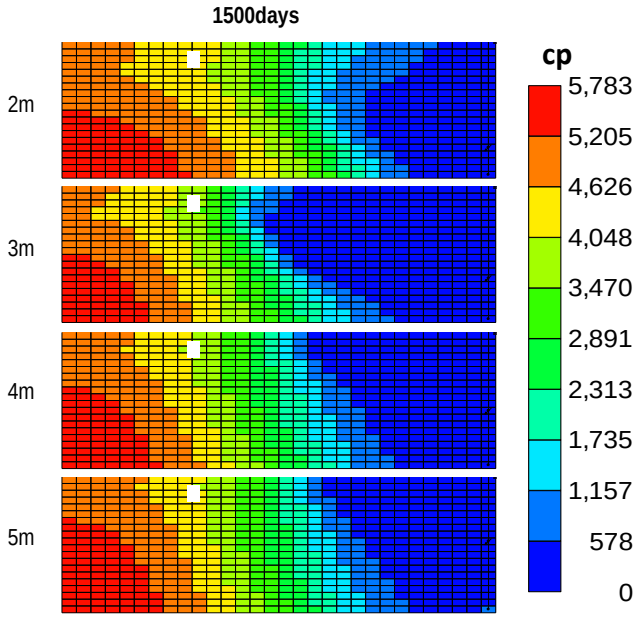

Figure 3-21 Oil viscosity distribution comparison in different injector positions at 1500 days

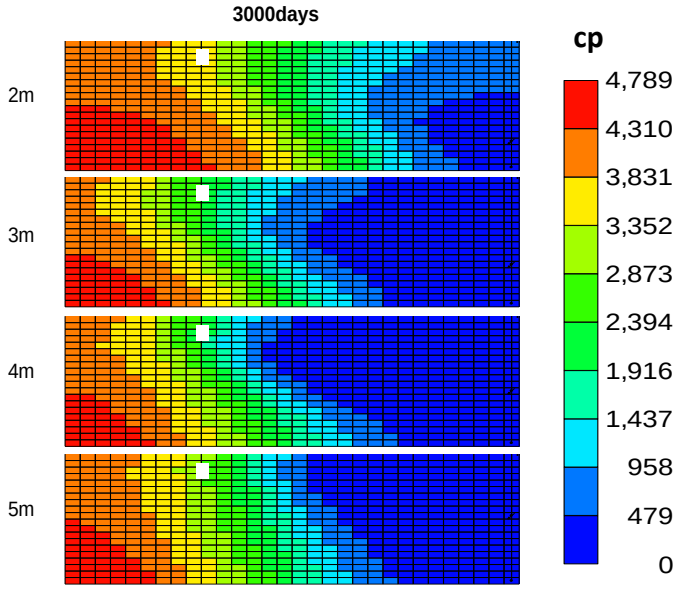

Figure 3-22 Oil viscosity distribution comparison in different injector positions at 3000 days

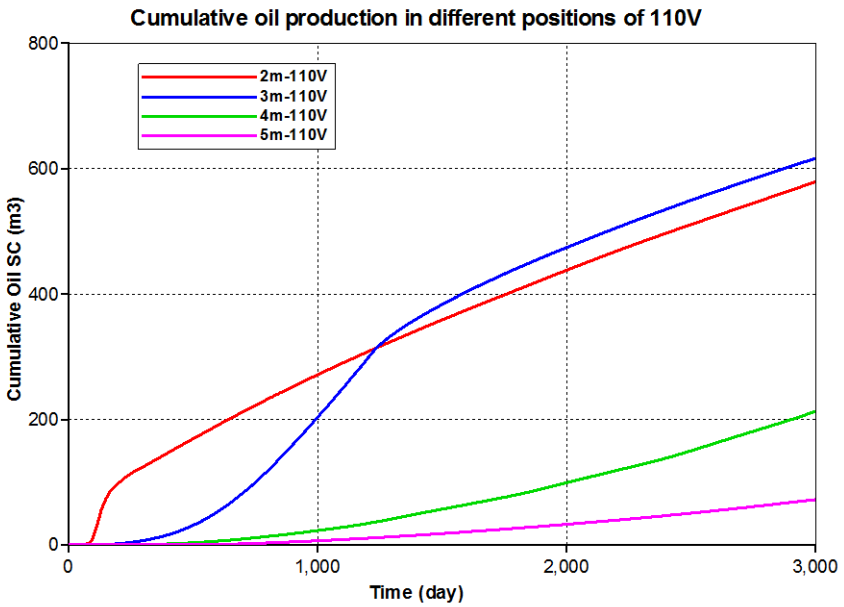

Figure 3-23 Comparison of cumulative oil production in different injector positions at 110 V

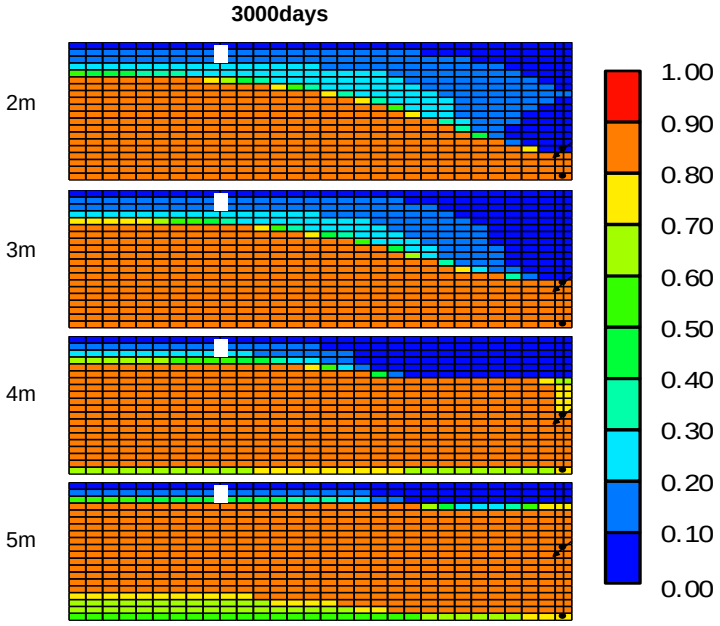

Figure 3-24 Oil saturation distribution at different injector positions at 110 V at 3000 days

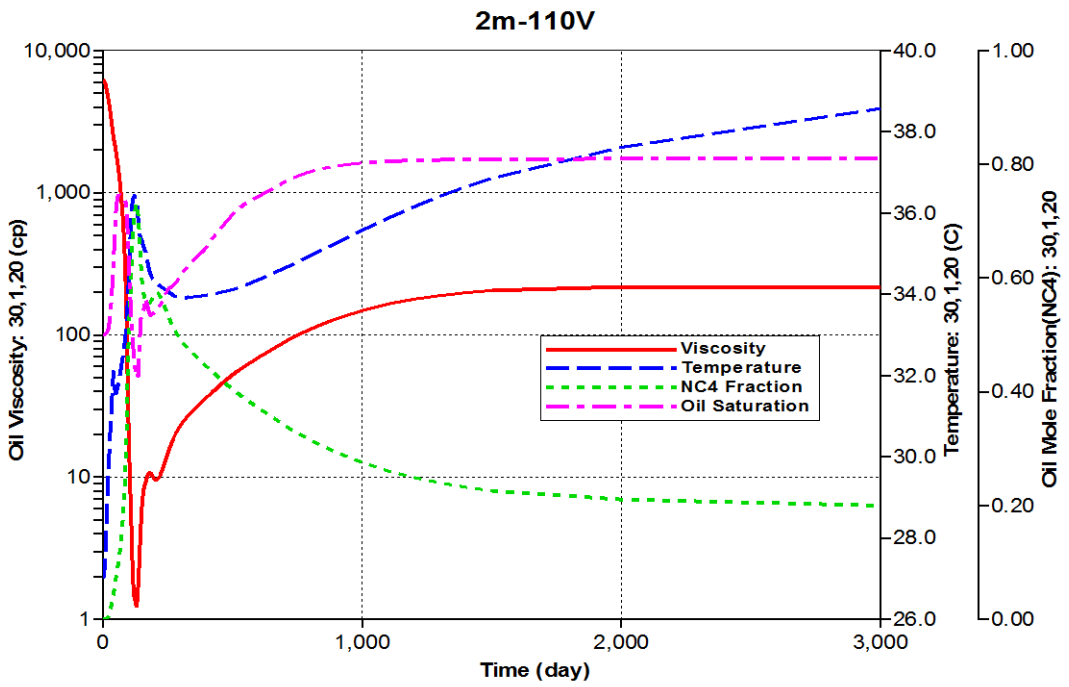
2m-110V
Oil Viscosity: 30,1,20 (cp)
Temperature: 30,1,20 (C)
Oil Mole Fraction(NC4): 30,1,20
Time (day)
Viscosity
Temperature
NC4 Fraction
Oil Saturation
10,000
1,000
100
10
1
40.0
38.0
36.0
34.0
32.0
30.0
28.0
26.0
1.00
0.80
0.60
0.40
0.20
0.00
0
1,000
2,000
3,000

(a)

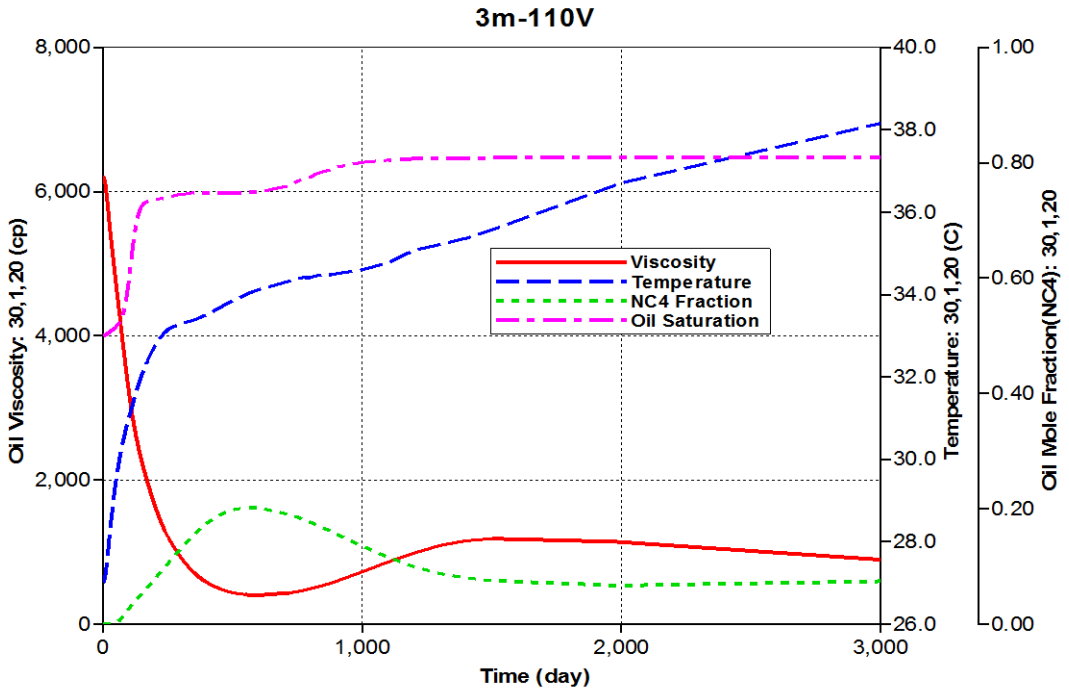
3m-110V
Oil Viscosity: 30,1,20 (cp)
Temperature: 30,1,20 (C)
Oil Mole Fraction(NC4): 30,1,20
Time (day)
Viscosity
Temperature
NC4 Fraction
Oil Saturation
8,000
6,000
4,000
2,000
0
40.0
38.0
36.0
34.0
32.0
30.0
28.0
26.0
1.00
0.80
0.60
0.40
0.20
0.00
0
1,000
2,000
3,000

(b)

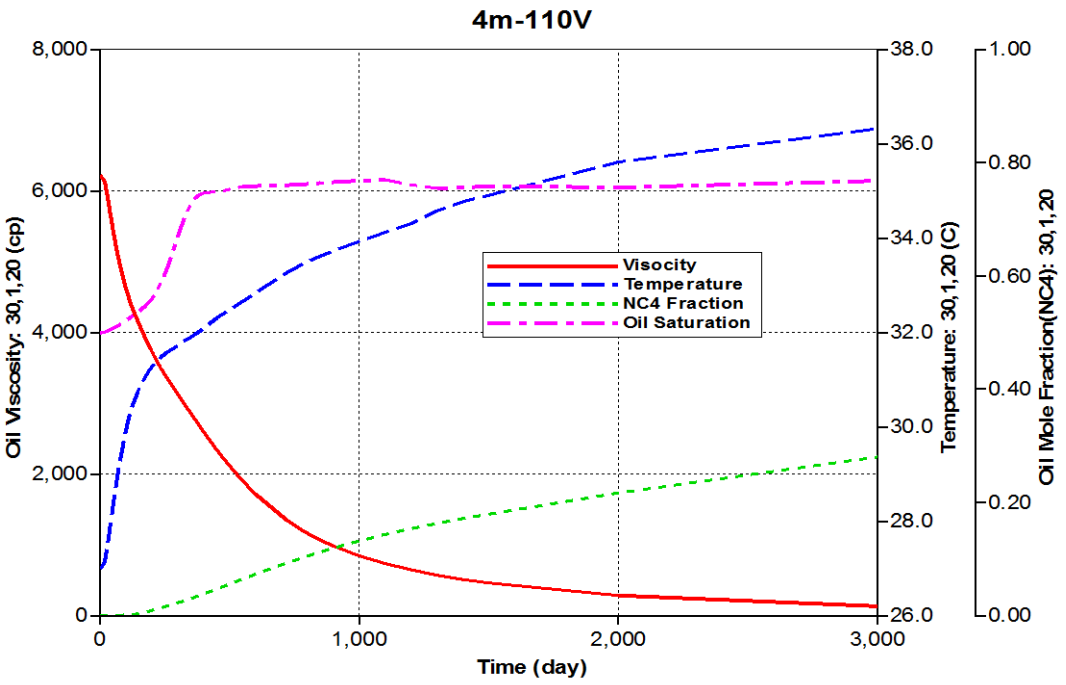
4m-110V
Oil Viscosity: 30,1,20 (cp)
Temperature: 30,1,20 (C)
Oil Mole Fraction(NC4): 30,1,20
Time (day)
Visocity
Temperature
NC4 Fraction
Oil Saturation
8,000
6,000
4,000
2,000
0
38.0
36.0
34.0
32.0
30.0
28.0
26.0
1.00
0.80
0.60
0.40
0.20
0.00
0
1,000
2,000
3,000

(c)

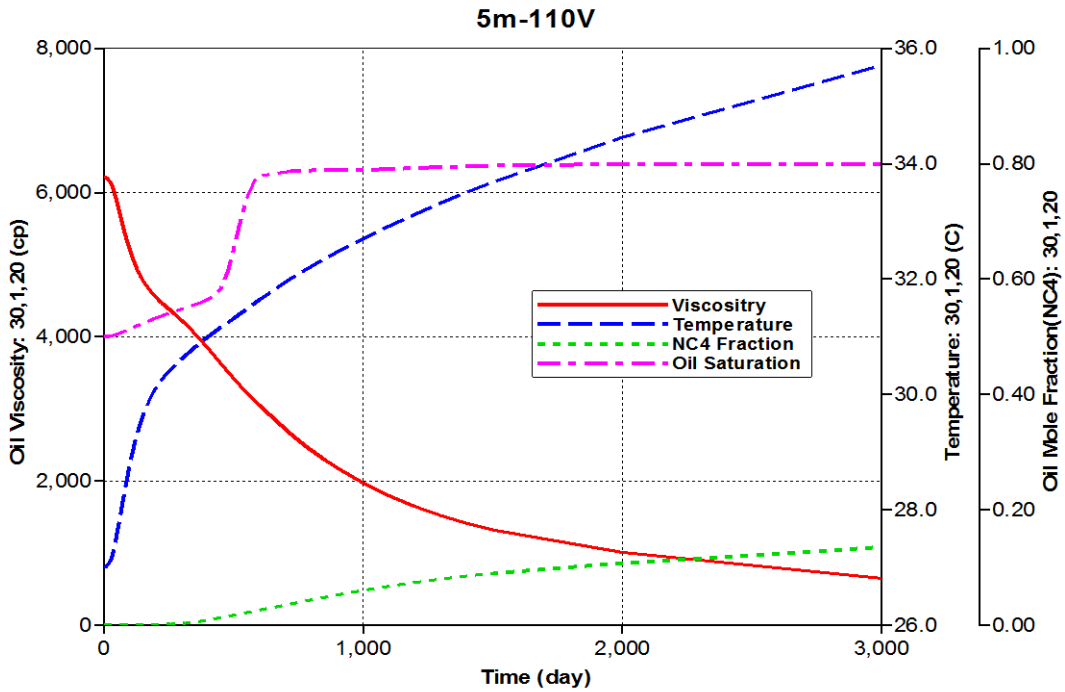
5m-110V
Oil Viscosity: 30,1,20 (cp)
Temperature: 30,1,20 (C)
Oil Mole Fraction(NC4): 30,1,20
Time (day)
Viscositry
Temperature
NC4 Fraction
Oil Saturation
8,000
6,000
4,000
2,000
0
36.0
34.0
32.0
30.0
28.0
26.0
1.00
0.80
0.60
0.40
0.20
0.00
0
1,000
2,000
3,000

(d)

Figure 3-25 Viscosity change with time at producer position (a) 2 m; (b) 3 m; (c) 4 m; (d) 5 m

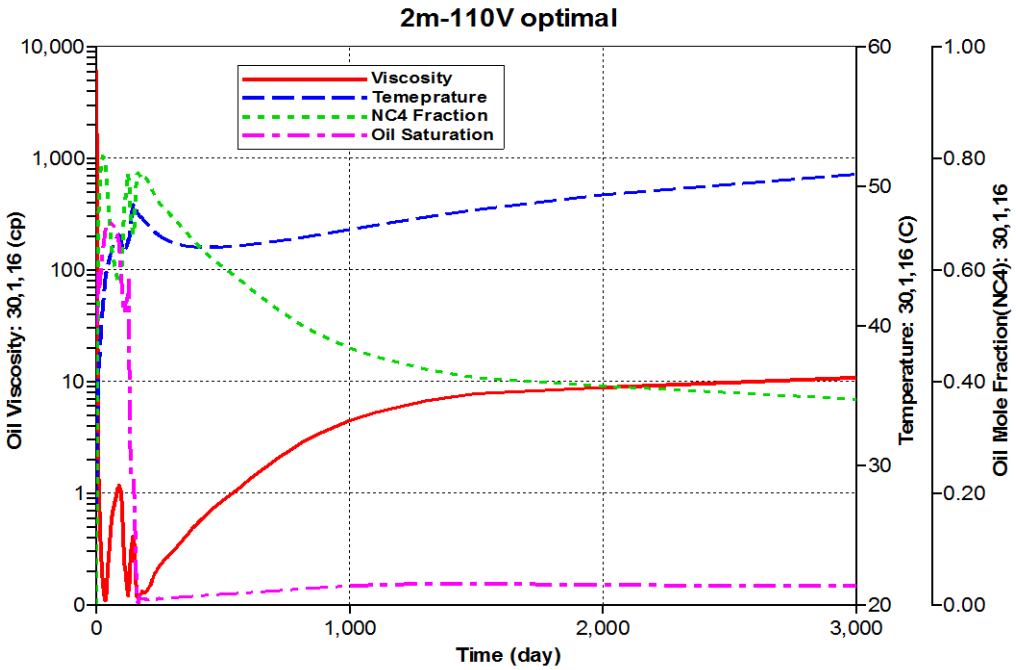

(a)

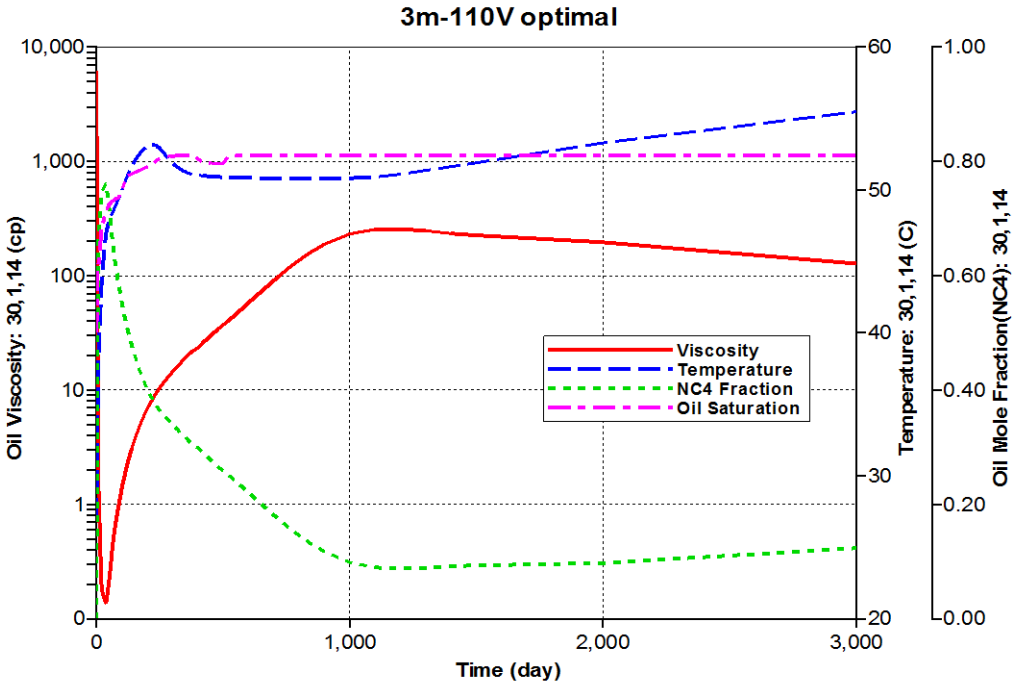

(b)

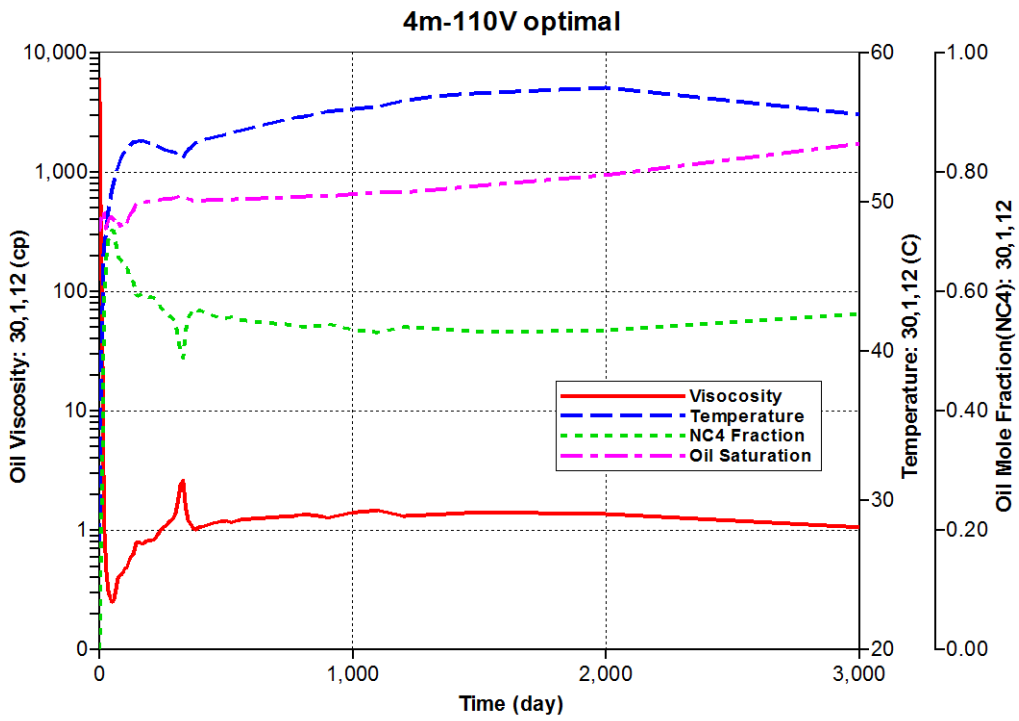

(c)

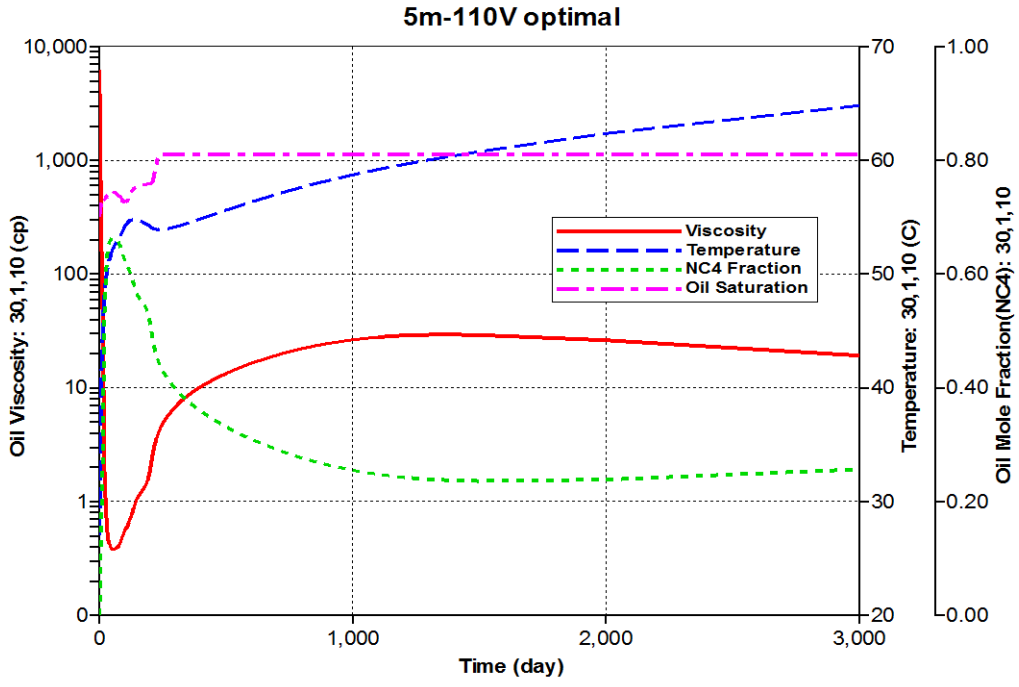

(d)

Figure 3-26 Viscosity change with time at injector position (a) 2 m, (b) 3 m, (c) 4 m (d) 5 m

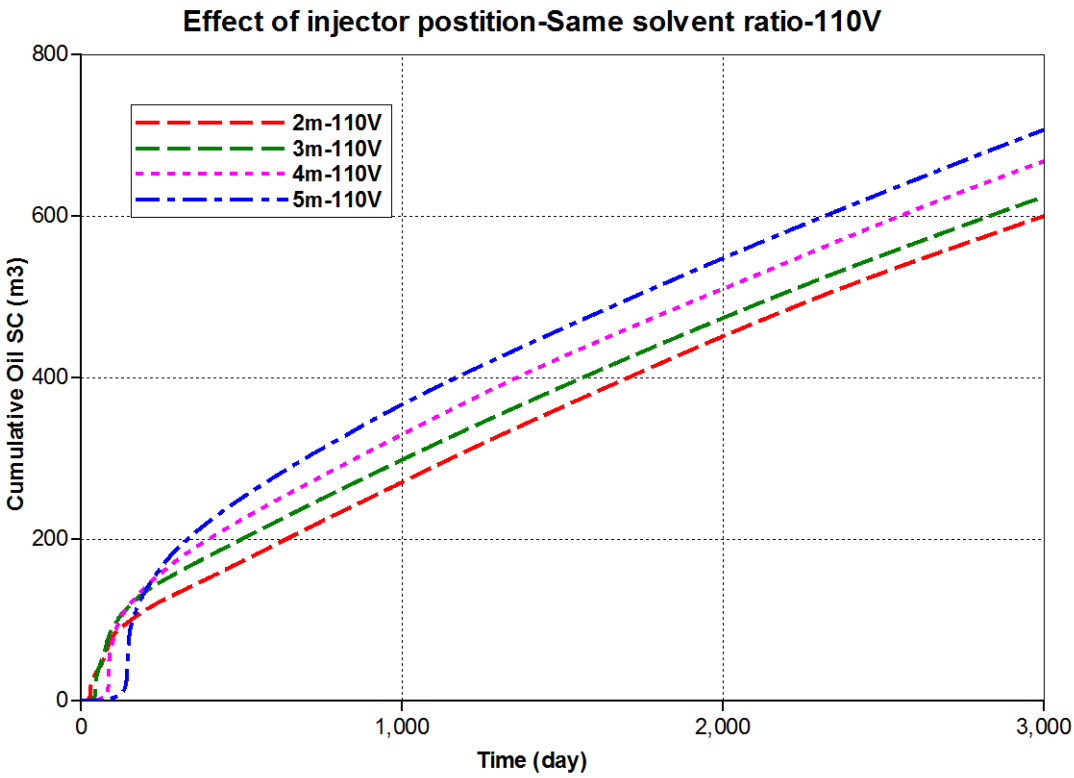

Figure 3-27 Comparison of cumulative oil in different injector position with the same solvent ratio at 110 V

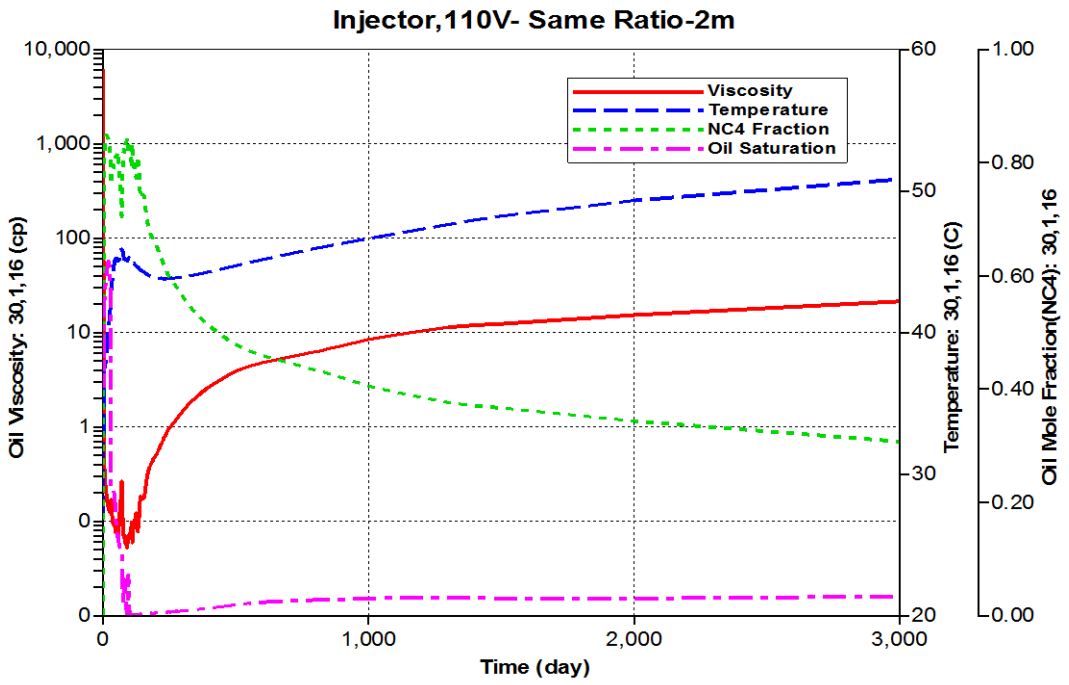
Injector,110V- Same Ratio-2m
Viscosity
Temperature
NC4 Fraction
Oil Saturation
Oil Viscosity: 30,1,16 (cp)
Temperature: 30,1,16 (C)
Oil Mole Fraction(NC4): 30,1,16
Time (day)
10,000
1,000
100
10
1
0
60
50
40
30
20
1.00
0.80
0.60
0.40
0.20
0.00
0
1,000
2,000
3,000

(a)

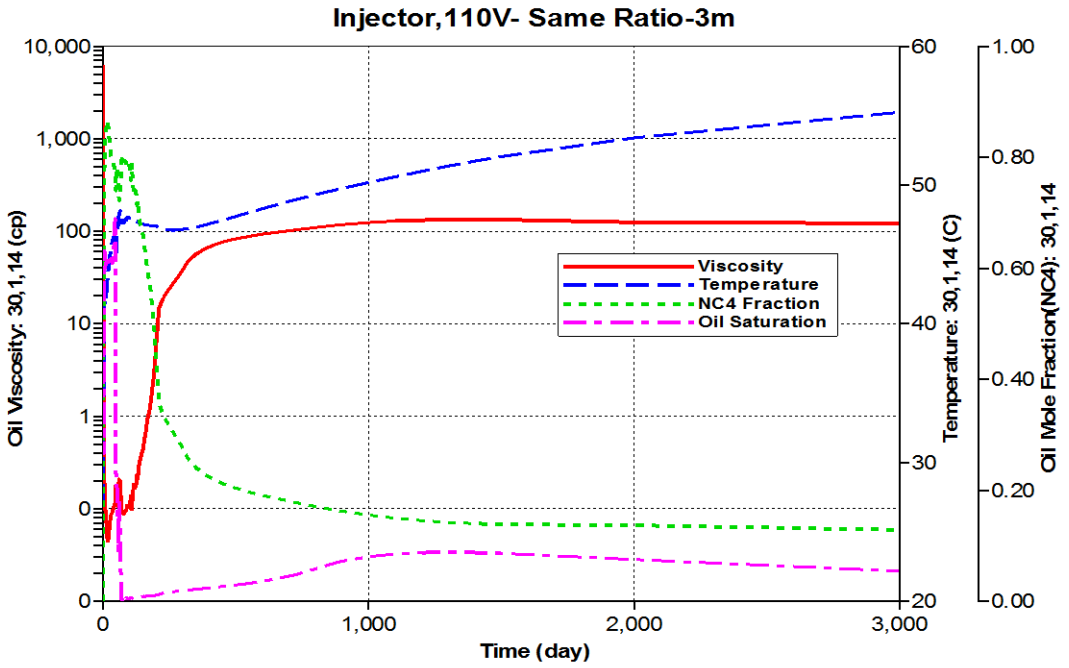
Injector,110V- Same Ratio-3m
Viscosity
Temperature
NC4 Fraction
Oil Saturation
Oil Viscosity: 30,1,14 (cp)
Temperature: 30,1,14 (C)
Oil Mole Fraction(NC4): 30,1,14
Time (day)
10,000
1,000
100
10
1
0
60
50
40
30
20
1.00
0.80
0.60
0.40
0.20
0.00
0
1,000
2,000
3,000

(b)

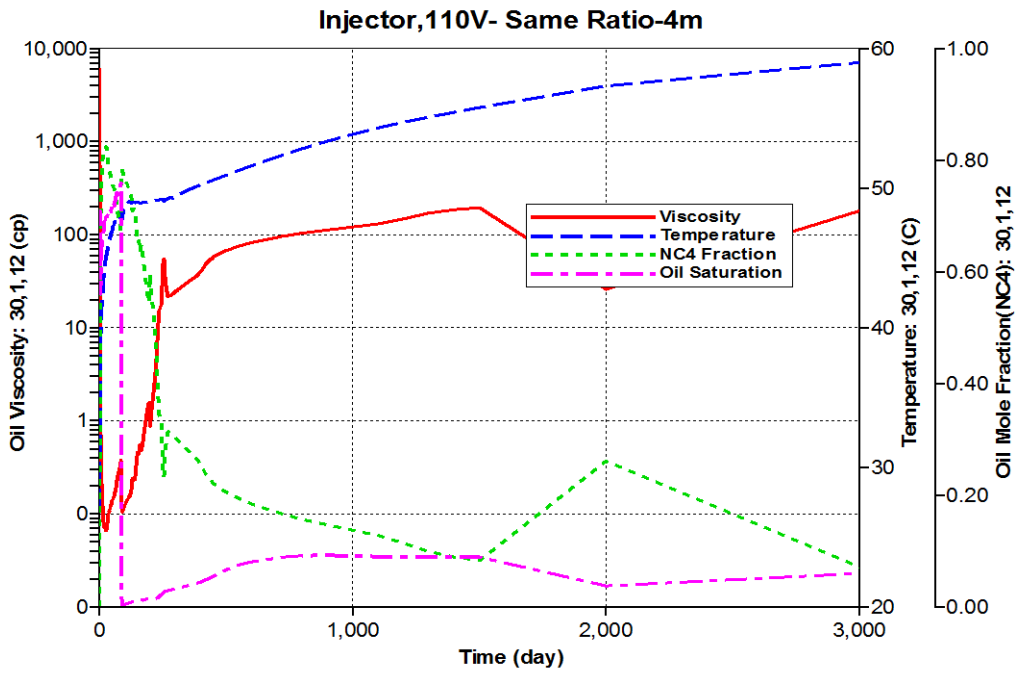

(c)

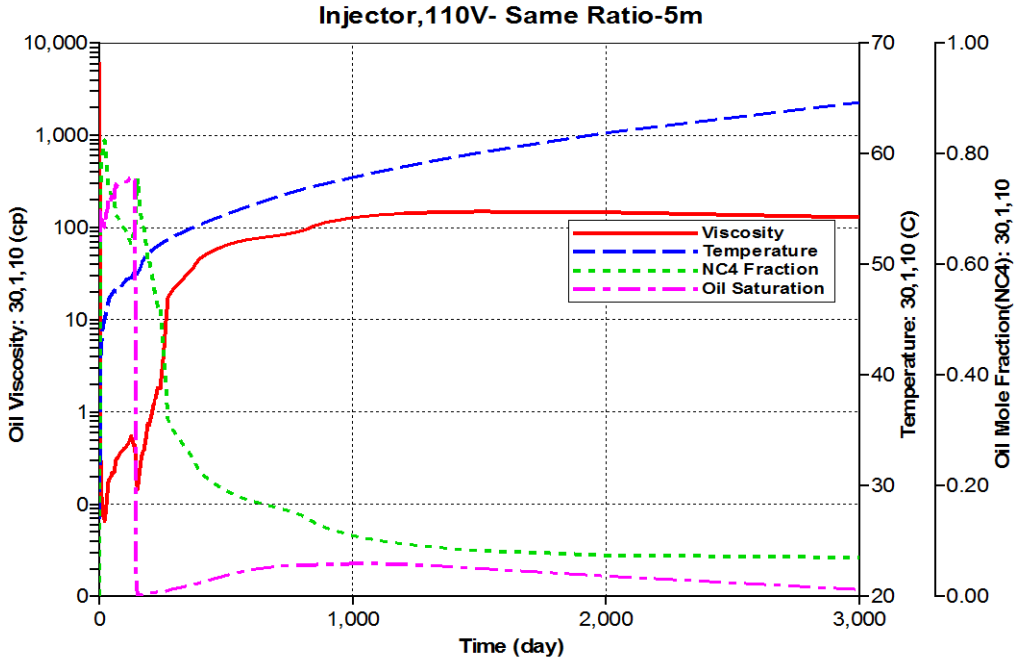

(d)

Figure 3-28 Viscosity change with time at injector location under the same solvent ratio at 110 V (a) 2 m; (b) 3 m; (c) 4 m; (d) 5 m

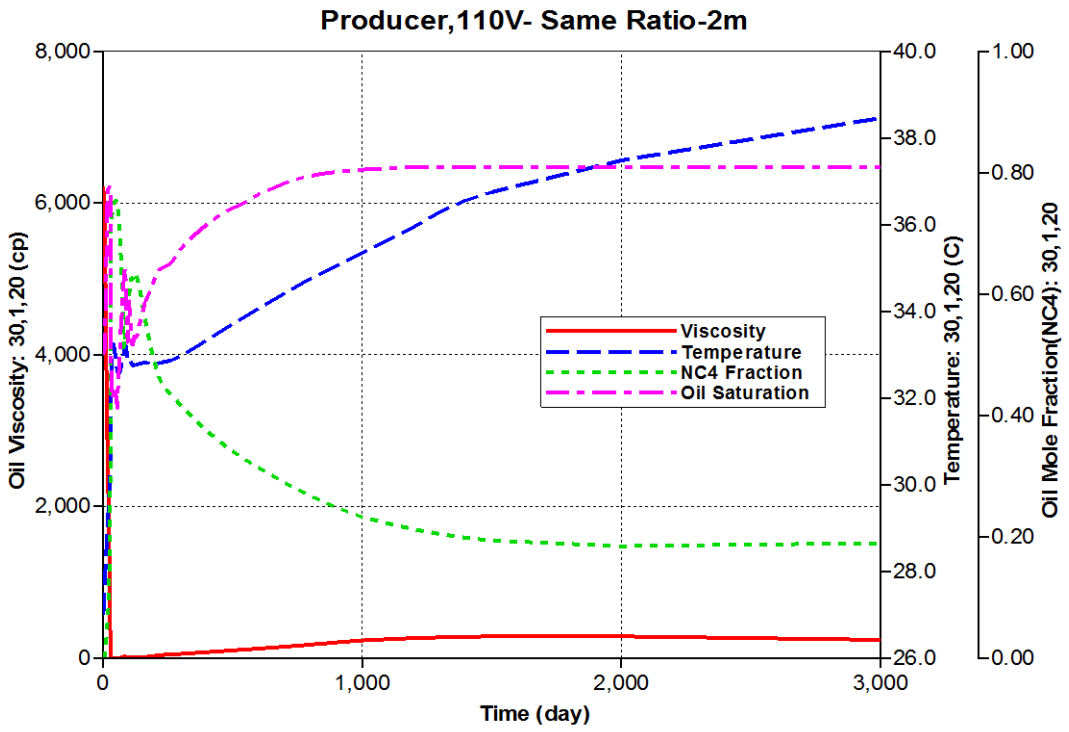
Producer,110V- Same Ratio-2m
Oil Viscosity: 30,1,20 (cp)
Temperature: 30,1,20 (C)
Oil Mole Fraction(NC4): 30,1,20
Time (day)
Viscosity
Temperature
NC4 Fraction
Oil Saturation
8,000
6,000
4,000
2,000
0
40.0
38.0
36.0
34.0
32.0
30.0
28.0
26.0
1.00
0.80
0.60
0.40
0.20
0.00
0
1,000
2,000
3,000

(a)

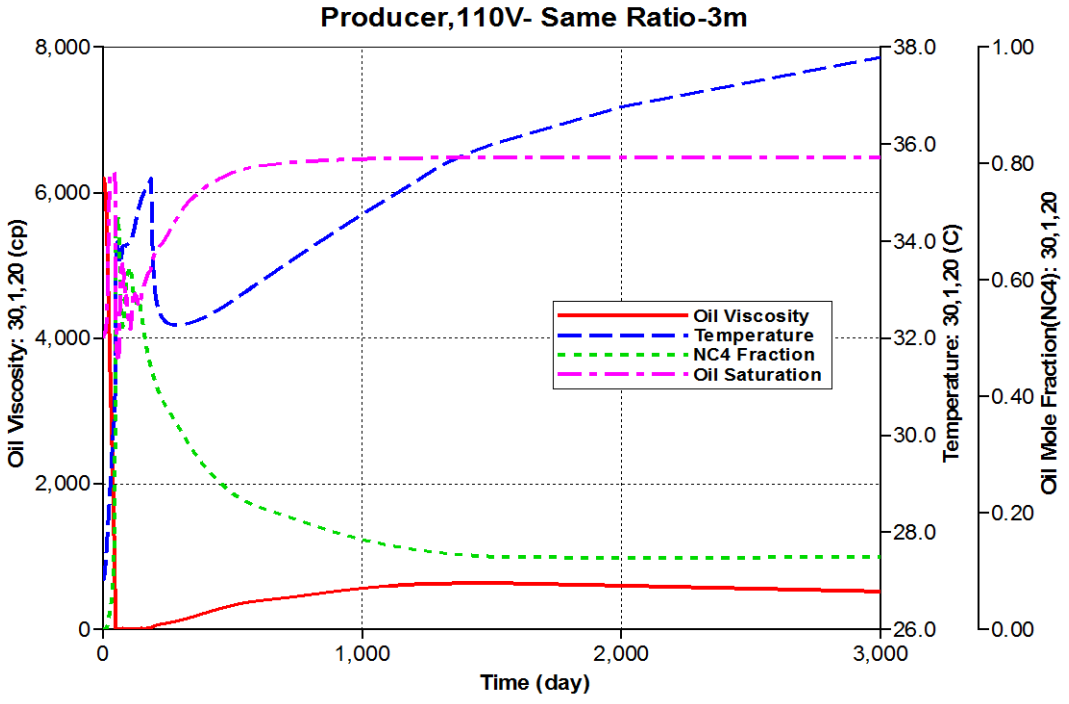
Producer,110V- Same Ratio-3m
Oil Viscosity: 30,1,20 (cp)
Temperature: 30,1,20 (C)
Oil Mole Fraction(NC4): 30,1,20
Time (day)
Oil Viscosity
Temperature
NC4 Fraction
Oil Saturation
8,000
6,000
4,000
2,000
0
38.0
36.0
34.0
32.0
30.0
28.0
26.0
1.00
0.80
0.60
0.40
0.20
0.00
0
1,000
2,000
3,000

(b)

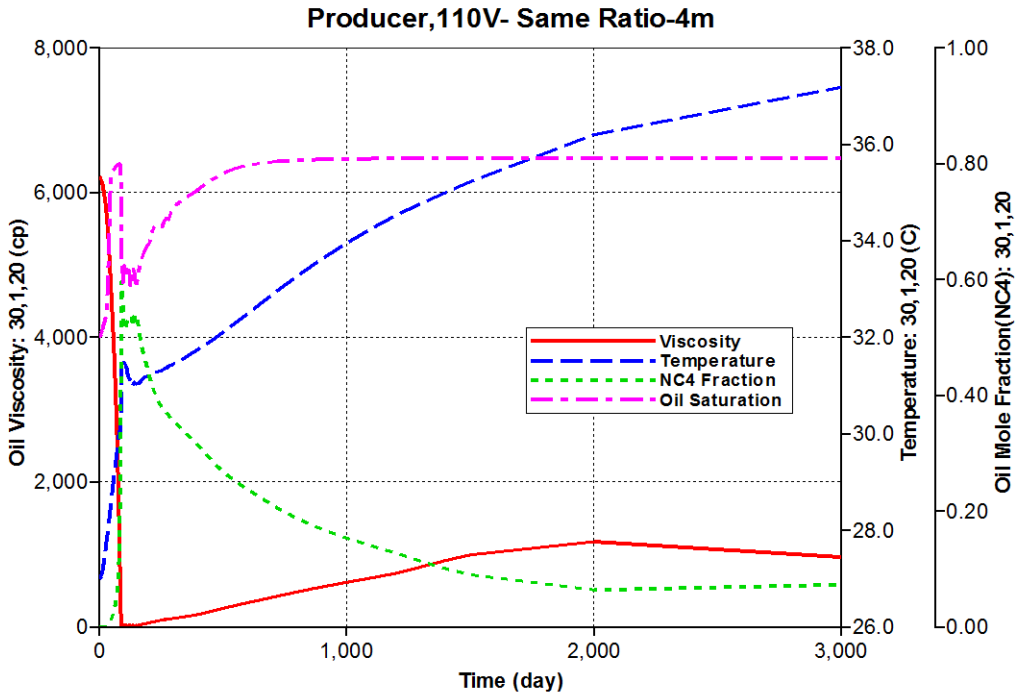

(c)

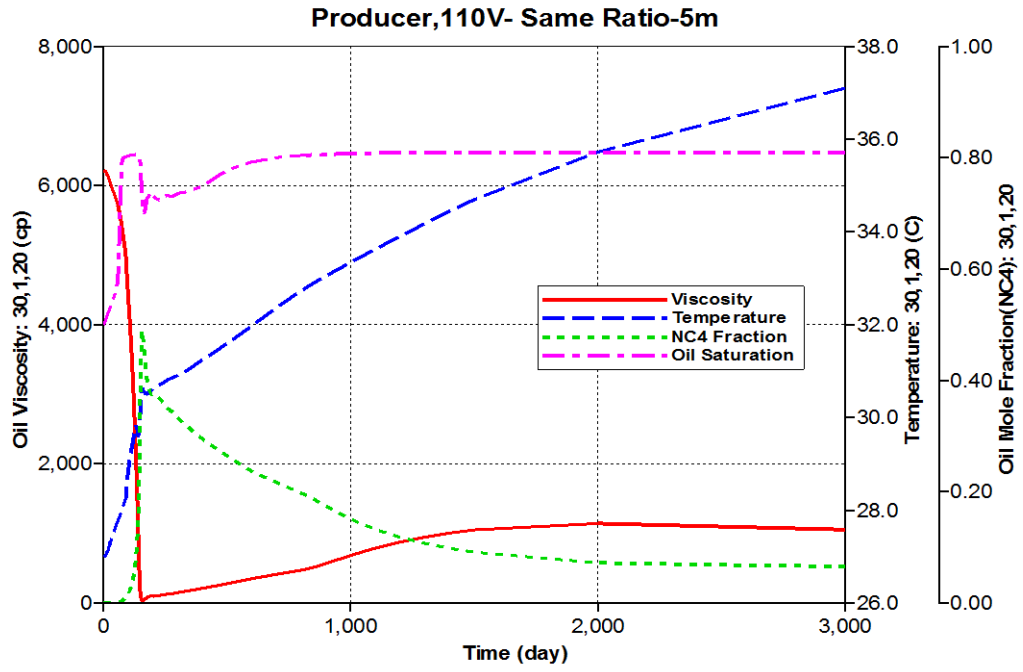

(d)

Figure 3-29 Comparison of viscosity with time at producer location under the same solvent ratio at 110 V (a) 2 m; (b) 3 m; (c) 4 m; (d) 5 m

3.2.4 Effect of Injection Pressure

In this scenario, 3 series are simulated.

- Series1: different pressure with same solvent ratio in 5000 md permeability
- Series2: different pressure with same solvent ratio in 10,000 md permeability
- Series3: different pressure with the higher solvent ratio in 5000 md permeability

Series1:

With the injector location fixed, the injection pressure is variable. In this study, the pressure of the injector position is 460 kPa, the solvent ratio is set as C1 (18%) and NC_4 (82%) under the reservoir pressure. The injection pressures simulated are 465 kPa, 470 kPa, 480 kPa, and 490 kPa; other parameters remained the same (the production pressure is 490 kPa). Figure 3-30 compares the simulation results and suggests that increasing the injection pressure will not necessarily increase the oil recovery; however, the higher the injection pressure, the faster the maximum oil rate will be reached. From the curves, the highest injection pressure (490 kPa) result in the highest cumulative oil production. Comparing the 465 kPa, 480kPa, and 490 kPa cases, the NC_4 distribution and oil saturation distribution at 1000 days are shown in Figure 3-31 (a), (b).

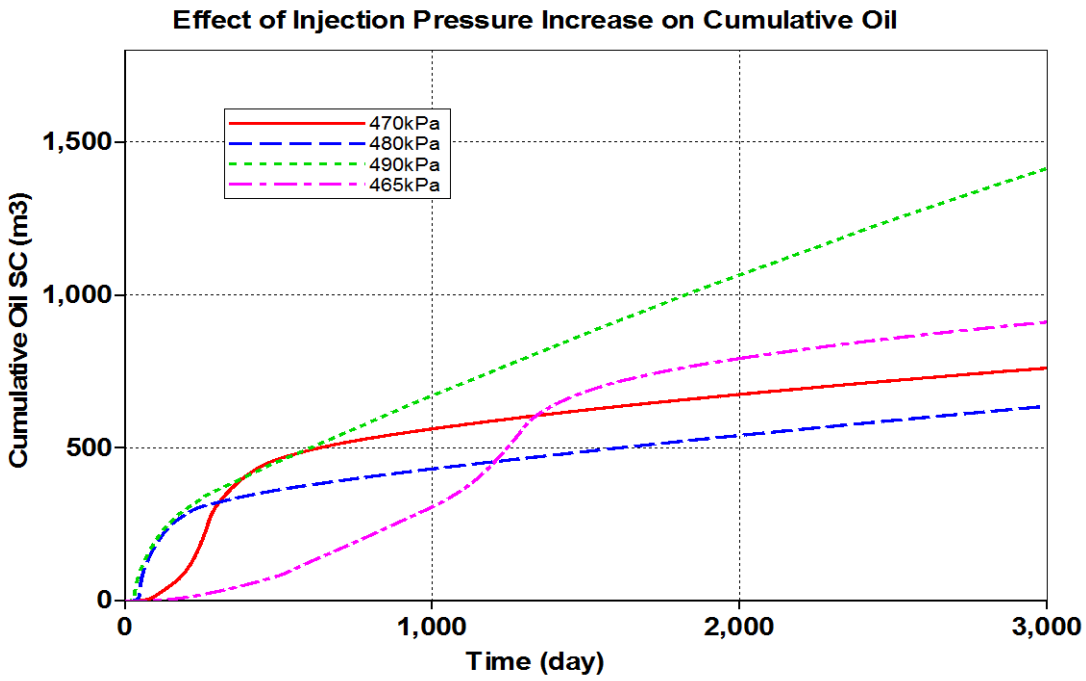
Effect of Injection Pressure Increase on Cumulative Oil
470kPa
480kPa
490kPa
465kPa
Cumulative Oil SC (m3)
1,500
1,000
500
0
0
1,000
2,000
3,000
Time (day)

(a)

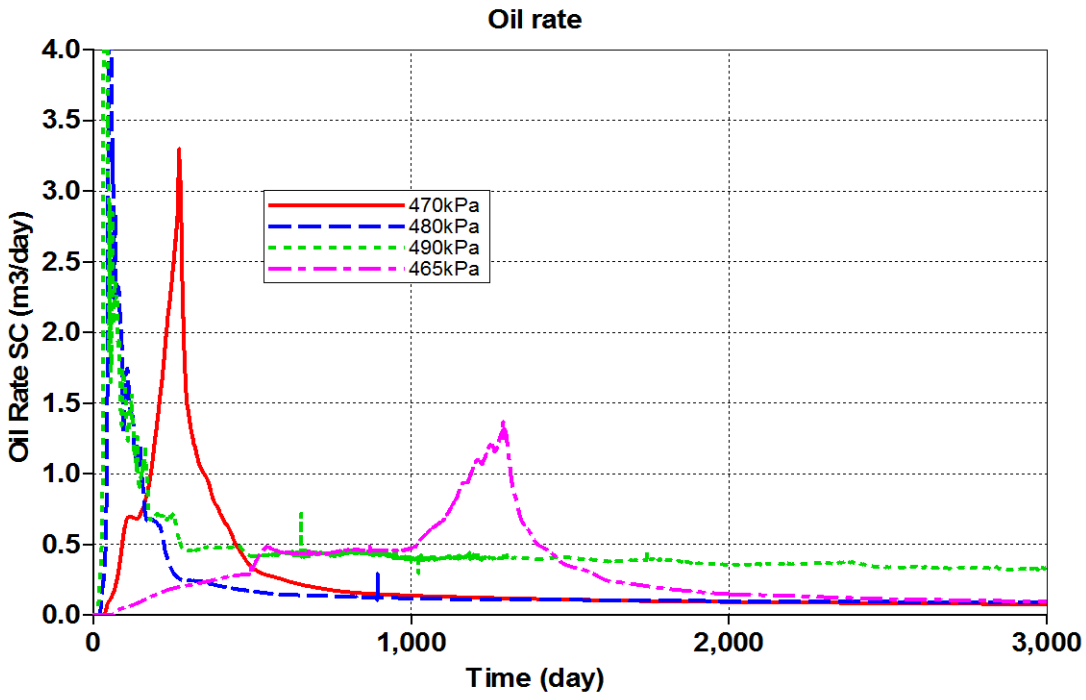
Oil rate
470kPa
480kPa
490kPa
465kPa
Oil Rate SC (m3/day)
4.0
3.5
3.0
2.5
2.0
1.5
1.0
0.5
0.0
0
1,000
2,000
3,000
Time (day)

(b)

Figure 3-30 Effect of injection pressure on (a) cumulative oil production and (b) oil rate

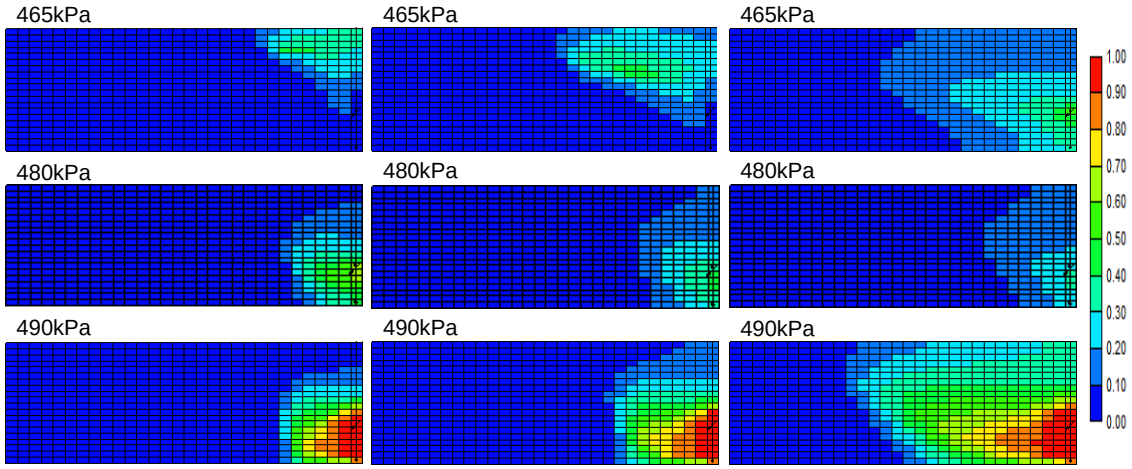

(a) 500 days, 1000 days, and 3000 days

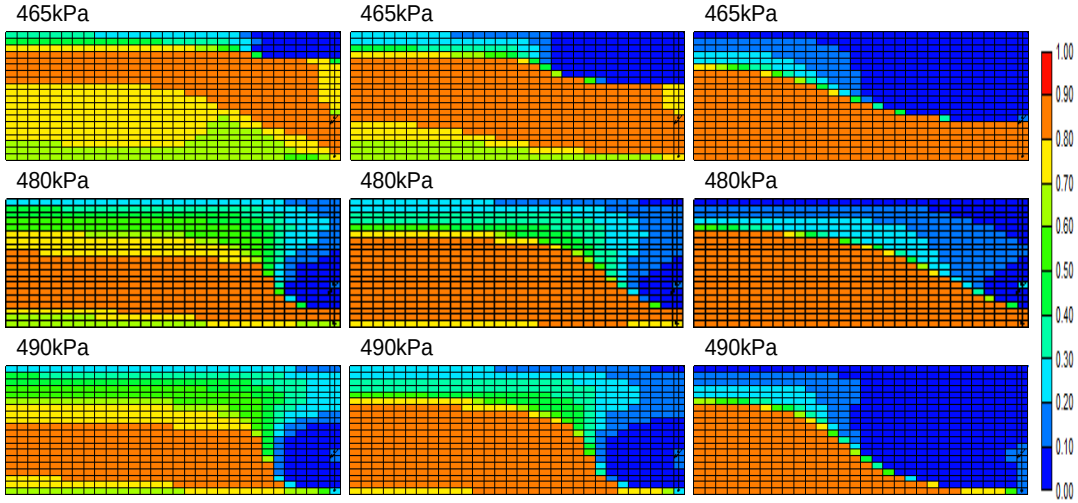

(b) 500 days, 1000 days, and 3000 days

Figure 3-31 NC_4 distribution (a) and oil saturation distribution (b) for different injection pressure at 500 days, 1000 days, and 3000 days

Figure 3-31 explains Figure 3-30 very well. When the injection pressure is low (465 kPa), the solvent will rise up and expand into a larger area on the top than with the injection pressure of 480 kPa because the pressure difference between the injector and the top reservoir layers; however, the highest injection pressure, 490 kPa, will transfer the solvent further in cross-section, higher and deeper in the vertical direction than the other two injection pressures. From the oil saturation distribution profiles, the slope of the tangent line of the chambers is descending from 490 kPa to 465 kPa and then 480 kPa in sequence.

The oil recoveries in this scenario are shown in the Table 3-6. The lowest oil recovery factor is 480 kPa case because the solvent injected concentrates around the injector and can not disperse into the reservoir effectively.

Series 2:

In this series, we tried a higher permeability value, 10,000 md. All the other parameters were kept the same as in Series 1. The cumulative oil productions and oil rates are shown Figure 3-32.

Series 3:

The solvent ratio is increased to 25% C1 and 75% NC_4 for all four injection pressures (465 kPa, 470 kPa, 480 kPa, and 490 kPa) to check the impact of different solvent ratios. The highest pressure, 490 kPa, still has the highest cumulative oil production, as verified above. The comparison is shown in Figure 3-33.

Table 3-6 Oil recovery comparison with different injection pressures

Injection Pressure (kPa)	Oil recovery
465	0.414
470	0.346
480	0.289
490	0.643

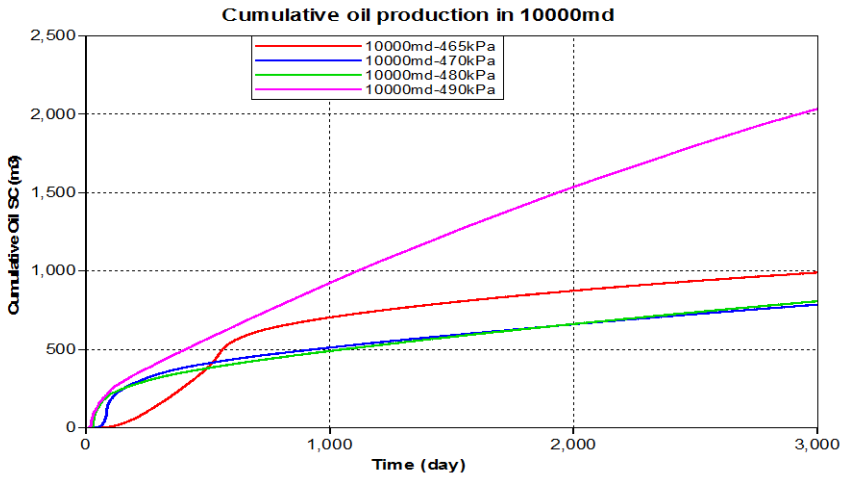

(a)

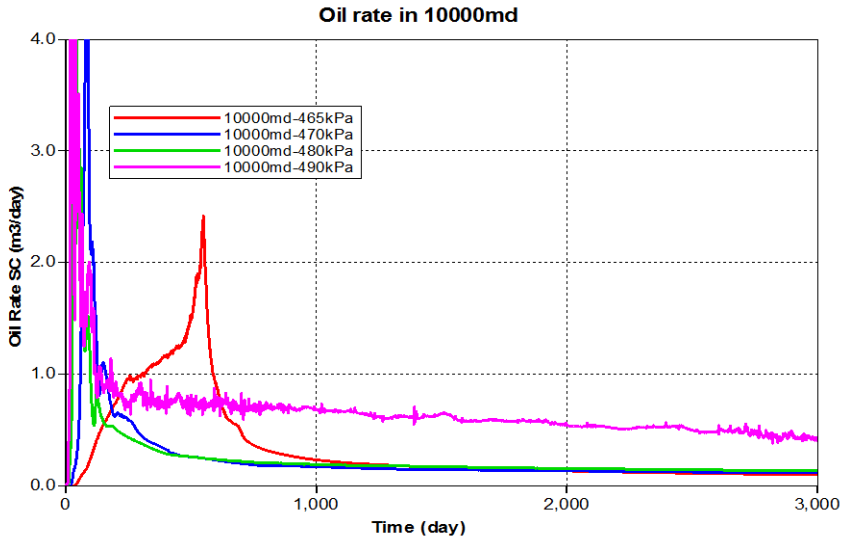

(b)

Figure 3-32 Comparison of high permeability in different injection pressure (a) cumulative oil production (b) oil rate

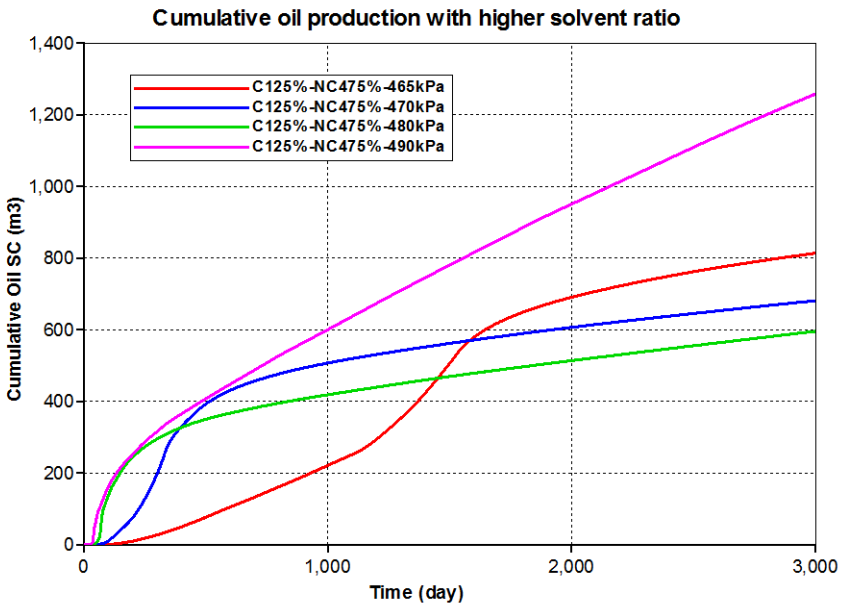

Figure 3-33 Comparison of cumulative oil production at different injection pressures with the same solvent ratio

From this scenario, as shown in Figure 3-33, the highest injection pressure (490 kPa) has the highest cumulative oil production regardless of the permeability or solvent ratio.

When the injection pressure is 465 kPa, the second highest cumulative oil production is achieved, but it has the lowest starting rate before 1500 days.

From all three series, the cumulative oil production lines have the same trend no matter the permeability or solvent ratio. The highest injection pressure presents the highest oil production and fastest staring oil rate among the 4 different injection pressure cases, and the lowest injection pressure, 465 kPa, shows the second cumulative oil production, but it has the lowest starting oil rate.

When the injection pressure is high, the solvent will spread up and down effectively and enlarge the diluted area where the temperature will not also increase too greatly because the heat caused by electricity will be delivered with fluid.

In the lowest injection pressure case, the solvent will rise up, not down, which will dilute the heavy oil in the top area. At the same time, the temperature increases quickly and reduces the viscosity around the injector.

The situation of all the three scenarios in which the NC_4 and temperature distribution has in common with that of base case keeps similar.

3.2.5 Water Saturation

As is well known, water plays an important role in electrical heating. In this section, the comparison is completed under different water saturations (Sw), 19%, 30% and 50% with the hybrid process. All the other parameters remained the same (solvent injection pressure and component ratio). Simulations of VAPEX were

conducted as well. From the simulation results, the hybrid process with lowest water saturation (19%) resulted in the highest oil recovery after 3000 days. The results are shown in Table 3-7 and in Figure 3-34.

According to the above table, the significant oil recovery change between the hybrid process and non-EH process occurred when the water saturation was 19%.

Comparing Figure 3-35 with Figure 3-36, because the temperature trends in both cases are totally different, the NC_4 distributions of both cases are different correspondingly. In both cases, the viscosity changes follow the theory explained above in 3.2.2. In Figure 3-36, although the NC_4 fraction is very low within 1500 days, the temperature increase results in viscosity reduction. In Figure 3-35, when the NC_4 reaches its maximum at around 1000 days, with the temperature decreasing all the time, the viscosity decreases to the lowest value.

Figure 3-37 explains Figure 3-35 and Figure 3-36, which show the NC_4 distribution at 1000 days and 2000 days, respectively. When the time is 1000 days, the temperature in 50% water saturation case is low, which cause the high NC_4 distribution in the reservoir. When the time is 2000 days, the situation is opposite.

Figure 3-38 and Figure 3-39 compare the NC_4 distribution over time. In the hybrid process, the NC_4 starts to spread from 1000 days and the chamber is growing transversely due to the temperature increase; however, the NC_4 chamber grows up-down and then touches the top of reservoir and the shape is very regular.

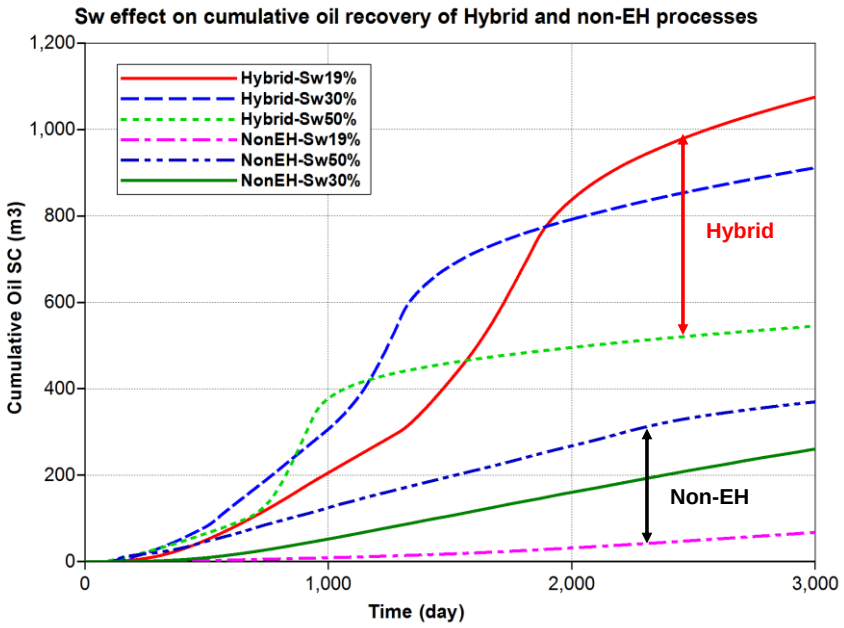

Figure 3-34 Effect of water saturation on cumulative oil recovery for Hybrid and Non-EH processes

Table 3-7 The oil recovery comparison between hybrid process and solvent injection only under different water saturations

Water Saturation	Oil Volume in Reservoir (m3)	Cumulative Oil Production		Oil Recovery	
		Hybrid Process	Solvent only	Hybrid Process	Solvent Only
19%	2540.7	1075.02	67.79	0.423	0.027
30%	2198.1	911.417	260.753	0.415	0.119
50%	1571.7	535.123	369.815	0.347	0.235

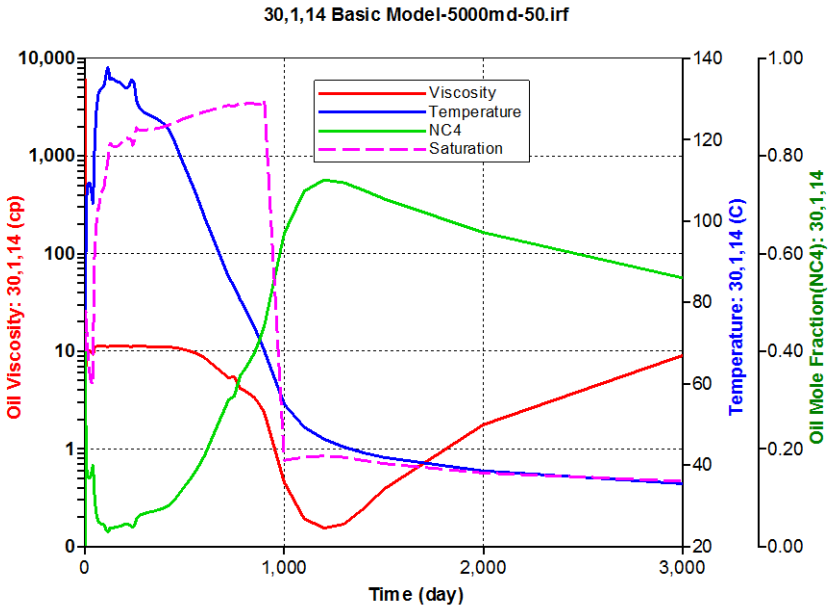

Figure 3-35 Viscosity changing with temperature and NC_4 changing in hybrid process with 0.5 water saturation

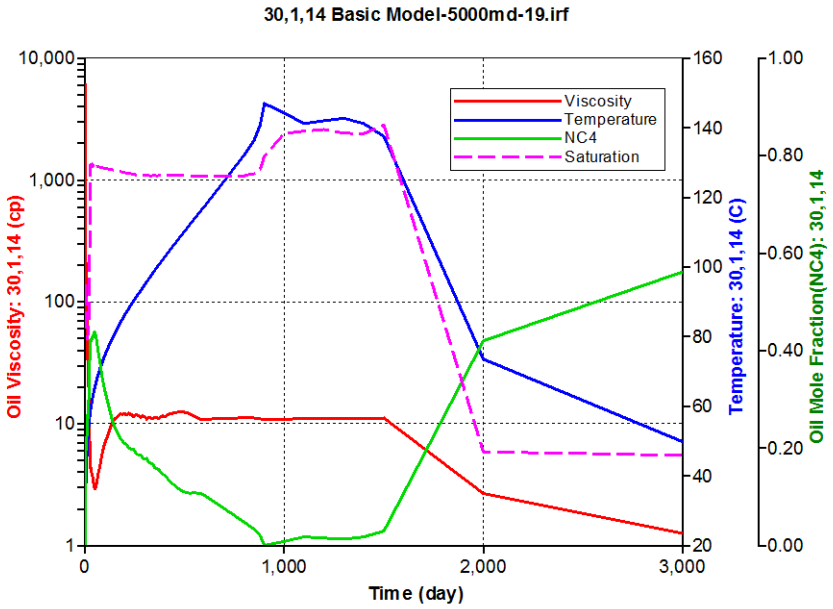

Figure 3-36 Viscosity changing with temperature and NC_4 changing in hybrid process with 0.19 water saturation

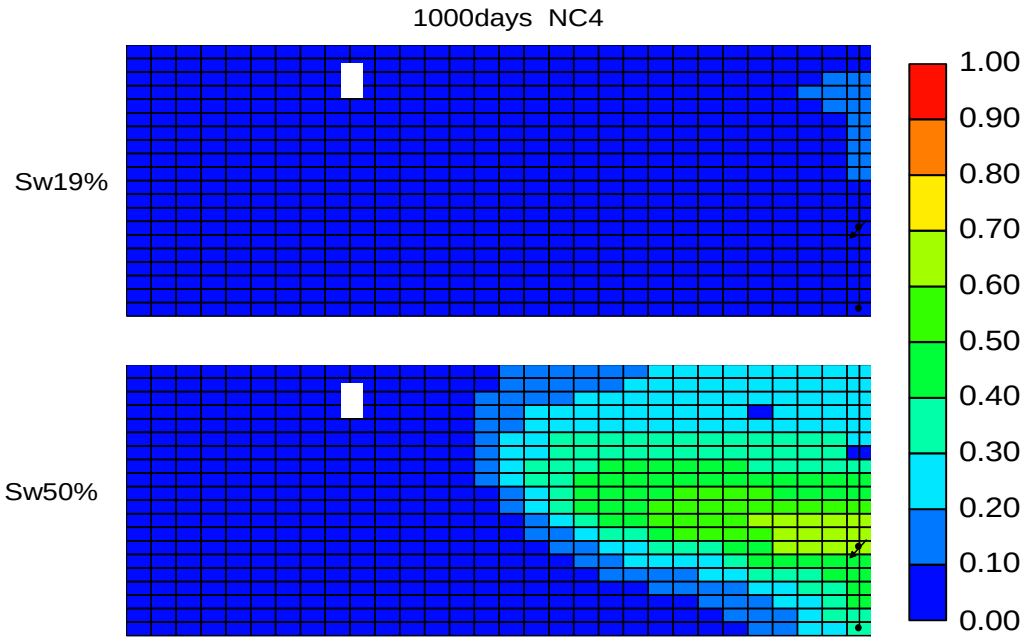

(a)

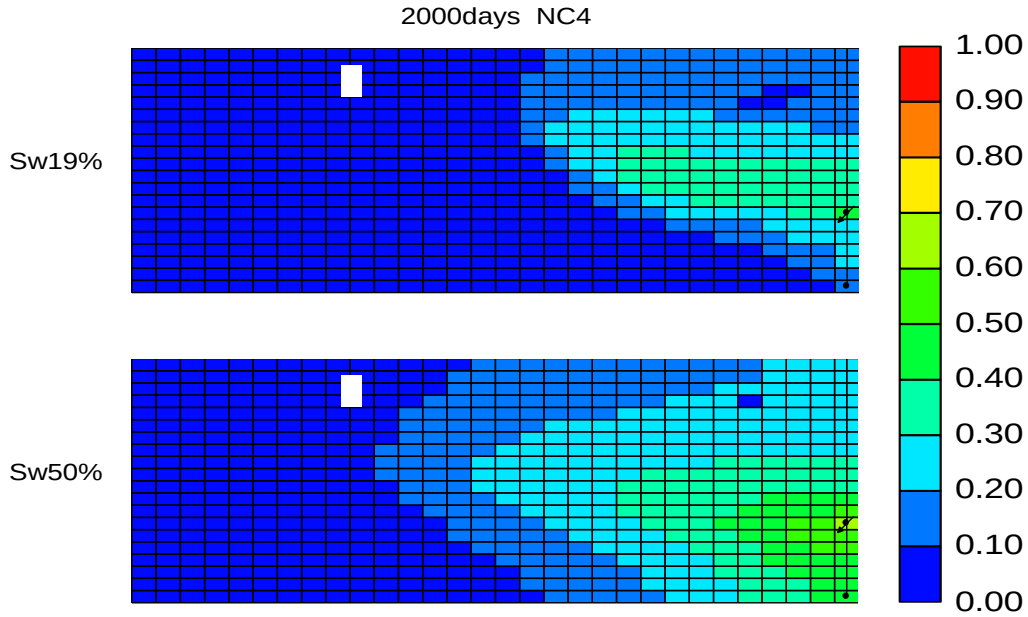

(b)

Figure 3-37 NC_4 distribution in Sw-19% and Sw-50% at (a) 1000 days and (b) 2000 days

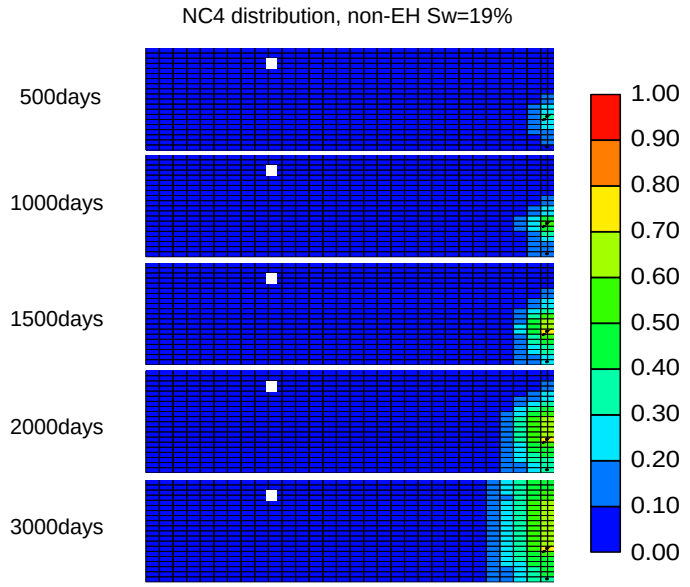

Figure 3-38 NC_4 changing with time in non-EH process with Sw=19%

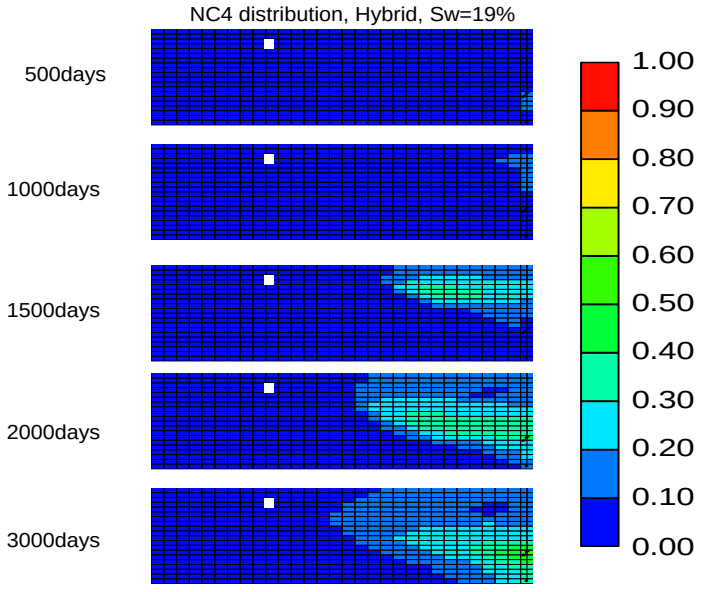

Figure 3-39 NC_4 changing with time in hybrid process with Sw=19%

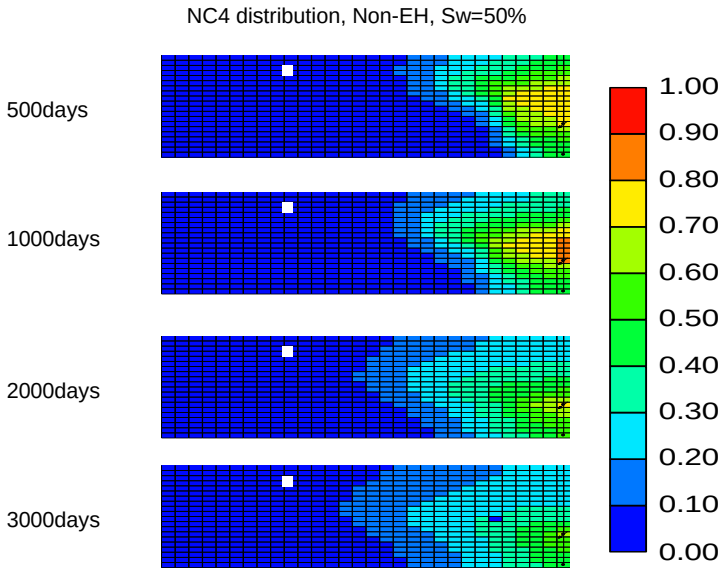

Figure 3-40 NC_4 changing with time in non-EH process with Sw=50%

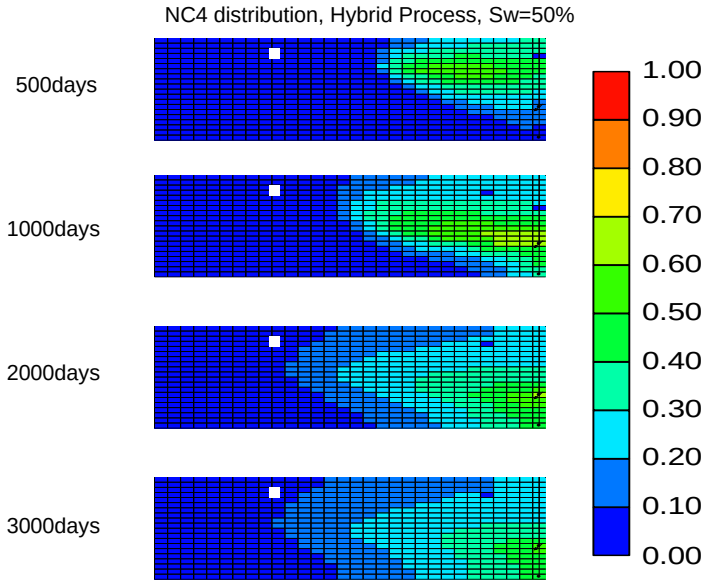

Figure 3-41 NC_4 changing with time in hybrid process with Sw=50%

Figure 3-41 has a similarly growing chamber of NC_4 as Figure 3-39. However, Figure 3-40 is a little bit different from Figure 3-38. Figure 3-40 has a larger NC_4 chamber than that of Figure 3-38 because the water in this area helps the solvent dissolve. When the water is produced, the light solvent easily moves into the unoccupied area from where the water was produced.

Although water plays a very critical role in the electrical resistive heating process, the low water saturation reservoir is more suitable for hybrid processes. When the water saturation is high, the temperature will not reach a very high value because most electrical energy input would transfer out of the reservoir with the fluid.

3.2.6 Lateral Pattern

In this scenario, we simulated two different permeability values, 1000 mD and 5000 mD. In the lateral pattern, the injector is drilled in the far top of the reservoir in Block (1,1,1), in which the injection pressure is set as 490 kPa and all the other parameters remain the same.

From the cumulative oil point of view, the lateral pattern in a high permeability reservoir shows a slow cumulative oil recovery in the first 1700 days, but then the cumulative oil recovery rises rapidly; however, the low permeability reservoir presents a steady climb in both the base case and lateral pattern case. The cumulative oil results are shown in Figure 3-42. This situation is easily understood from the viscosity distribution. Figure 3-43 (a) and Figure 3-43 (b) show the viscosity distribution in 1500 days and 2000 days for both cases. In the high

permeability case, the viscosity reduction is caused by the temperature increasing over 1700 days, followed by the NC_4 solvent dissolving into the heavy oil.

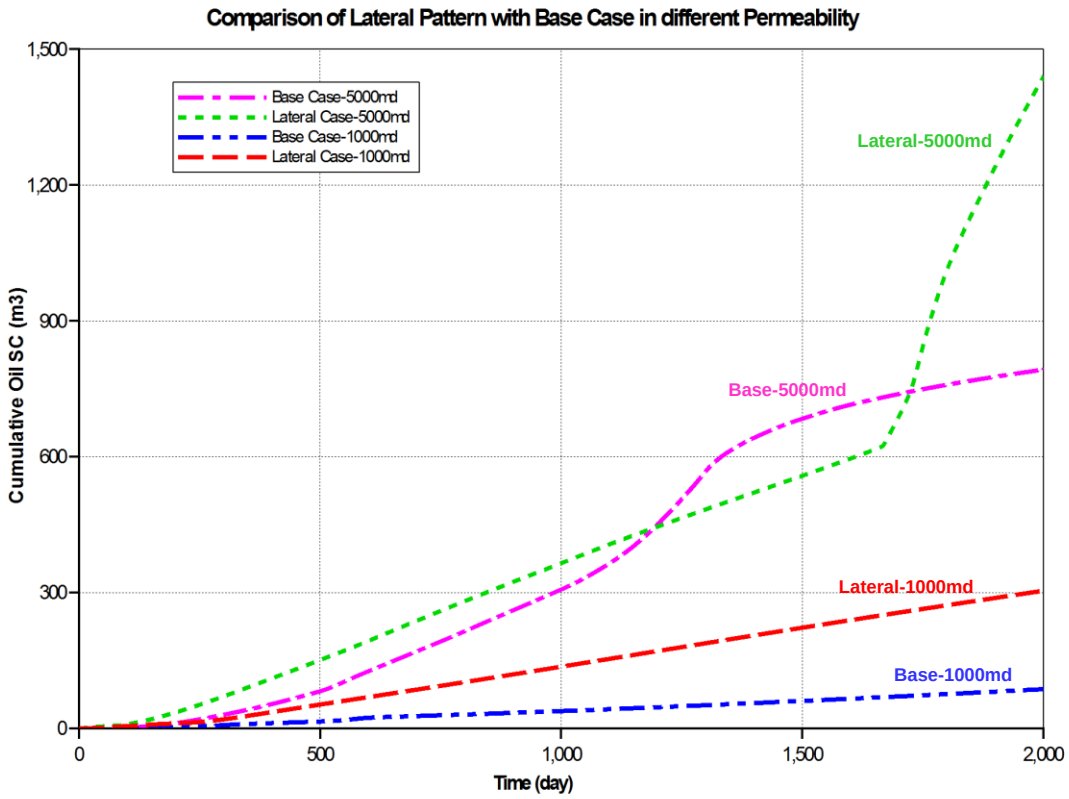

Figure 3-42 Comparison of cumulative oil of lateral pattern and base case at 1000 md and 5000 md

In the low permeability (1000 md) simulations, because the pressure of the injector is higher than the local reservoir pressure, the downward driving force assists gravity drainage of diluted oil to the producer.

Figure 3-43 (a) presents the oil viscosity distribution in 1500 days and Figure 3-43 (b) shows the oil viscosity distribution in 2000 days. When the NC_4 dissolves and reduces the viscosity on the top of the reservoir, at the same time, the temperature increase causes the viscosity reduction as well, as shown in Figure 3-43 (a). Once the two affected areas integrate, which means that the solvent injection area and electrical heating area connect, as in Figure 3-43 (b), the oil recovery will increase rapidly.

Obviously, in the high permeability reservoir (5000 md), the lateral pattern represents a better performance than the base case. In the lateral pattern, the electrical heating and solvent injection play their own roles in areas that could lead to greater viscosity reduction across larger areas. Therefore, the cumulative oil increases correspondingly. The injector is set in the mid-left side in the following case. The position is shown in the Figure 3-44. The comparison of cumulative oil production between top-left and mid-left is shown in Figure 3-45. Figure 3-46 and Figure 3-47 show the viscosity distribution at 500 days, 1000 days, and 2000 days in two different injector location cases. There is a connection between the solvent affected area and heating affected area in the top-left injection position. However, this does not occur in the case with the injector located at the mid-left side. Then, Figure 3-47 explains Figure 3-45 very well. At 2000 days, the cumulative oil jumps in the case with the injector in the top left.

Obviously, when the injector is located at the top left in the 3-D model, there is high oil cumulative production in the simulation period because the solvent injection is prone to spread horizontally, which enlarges the solvent diluted area.

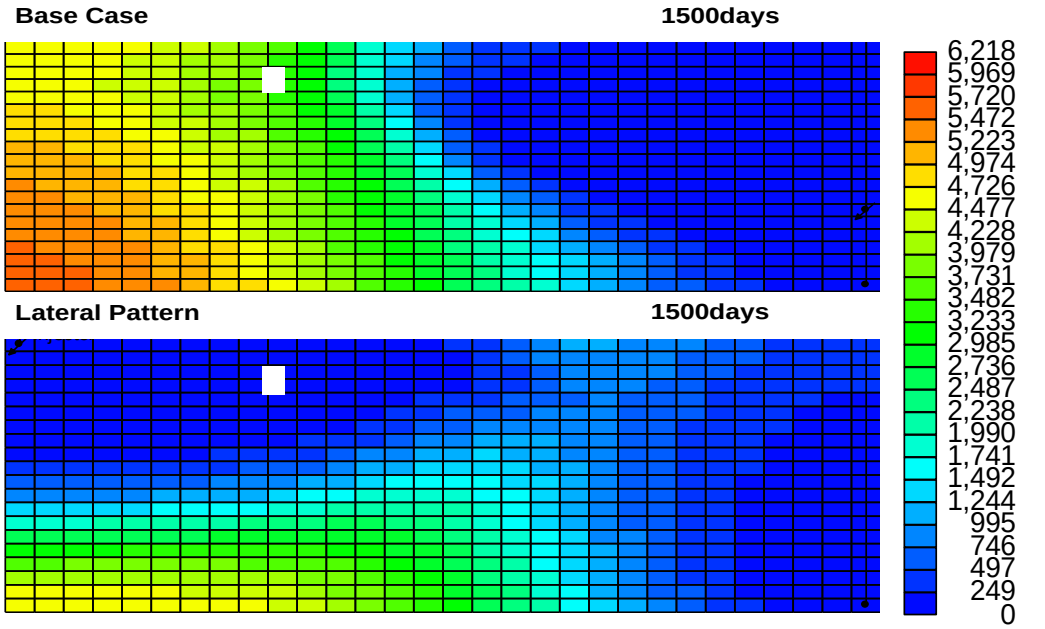

(a)

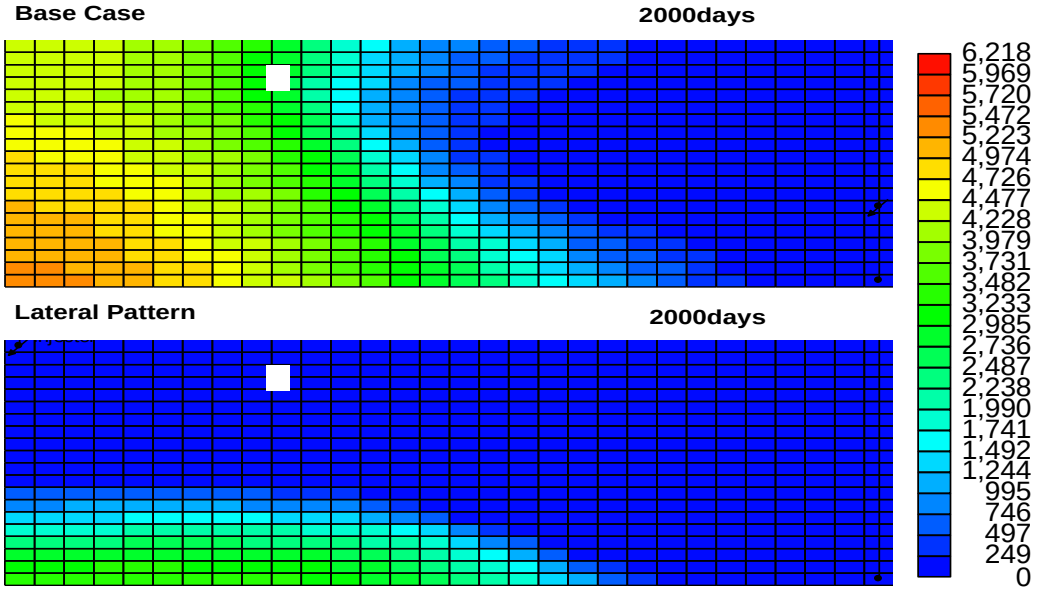

(b)

Figure 3-43 Viscosity Distribution comparison of Base case with Lateral Case

(a)1500 days; (b) 2000 days.

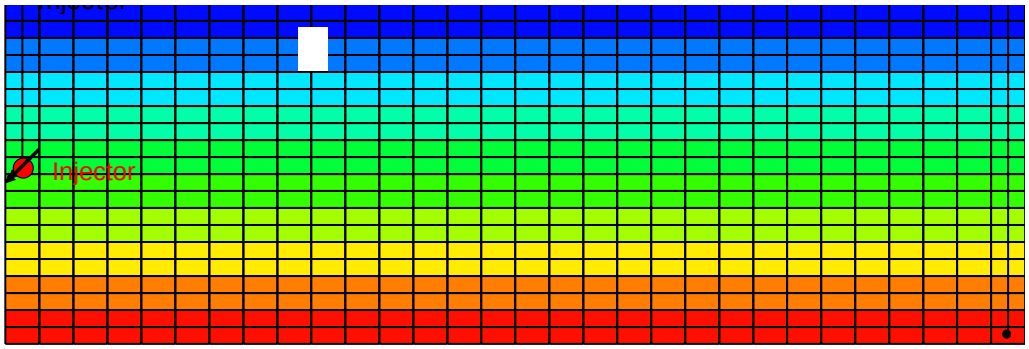

Figure 3-44 Injector in the Mid-Left position

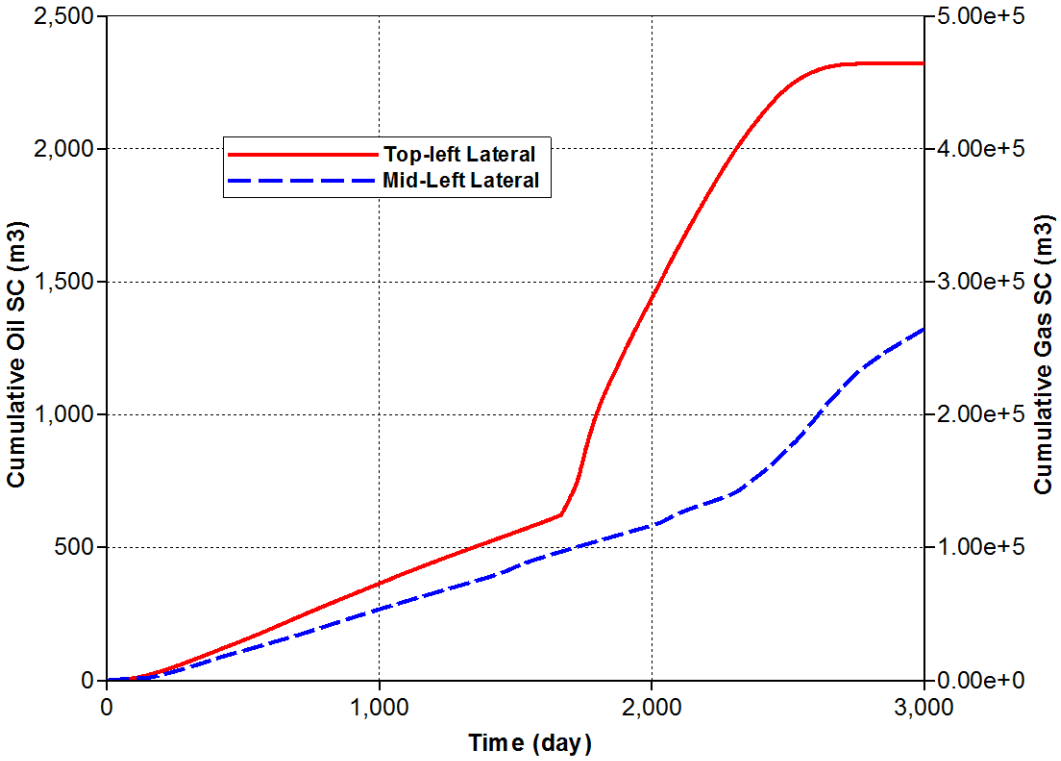

Figure 3-45 Comparison of cumulative oil recovery with different injector positions

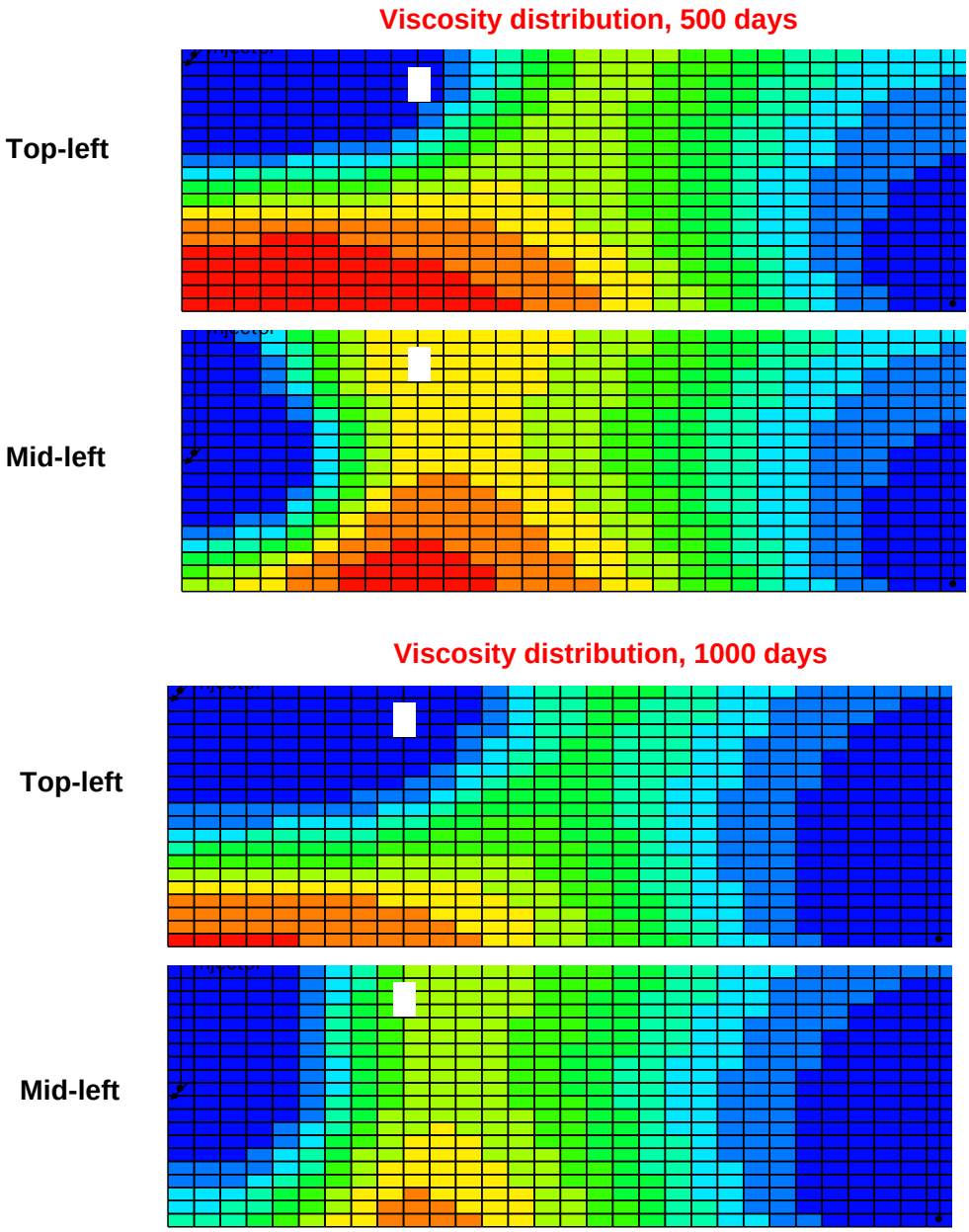

Figure 3-46 Comparison of viscosity with different injector positions at 500 days, 1000 days

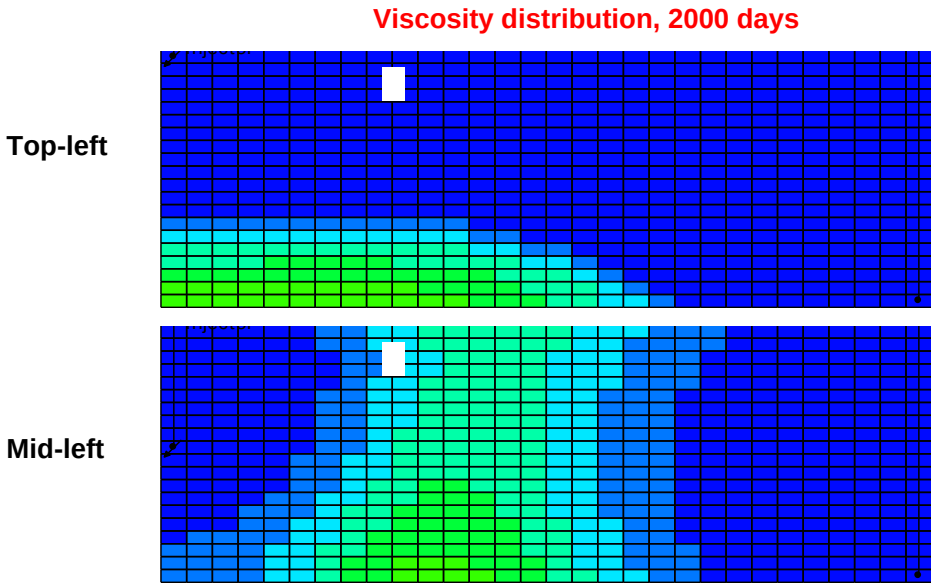

Figure 3-47 Comparison of viscosity with different injector positions at 2000 days

3.2.7 Heterogeneity Effect

Most of the VAPEX-related simulations in the literature were done with homogeneous reservoirs. However, in reality, all reservoirs are heterogeneous. In order to simulate the effect of reservoir heterogeneity on the hybrid process performance and the well conformance due to heterogeneity, the permeability is reduced to 500 md in some layers in the k and j directions.

In this scenario, two series were simulated:

Series 1: The permeability of three layers (layer-4,5,6) in j-direction is changed from 5000 md to 500 md, and the electrodes are installed in these three blocks in the injector to check the well conformance due to heterogeneity, as shown in Figure 3-48 (a).

Series 2: The permeability of layer-10 in the k-direction is changed to from 5000 md to 500 md, which is shown in Figure 3-48 (b); the electrode is still located in the injector.

Both reservoir initial conditions and producer operative conditions are the same as those used before. The operation voltage is 220 V.

Figure 3-49 and Figure 3-50 show the oil recovery factor and oil rate comparisons for the heterogeneous reservoir under the solvent injection and hybrid process cases.

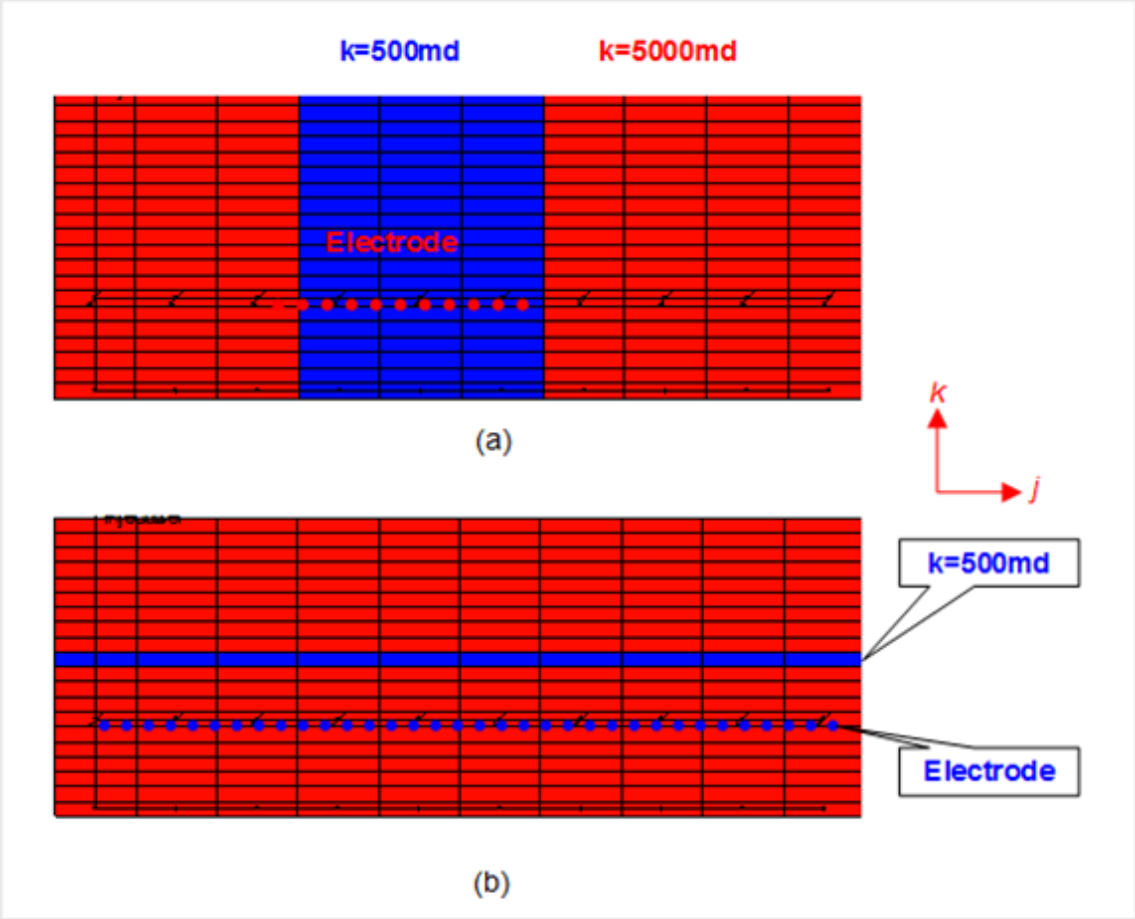

Figure 3-48 Permeability distributions in heterogeneity model (a) j-direction; (b) k-direction

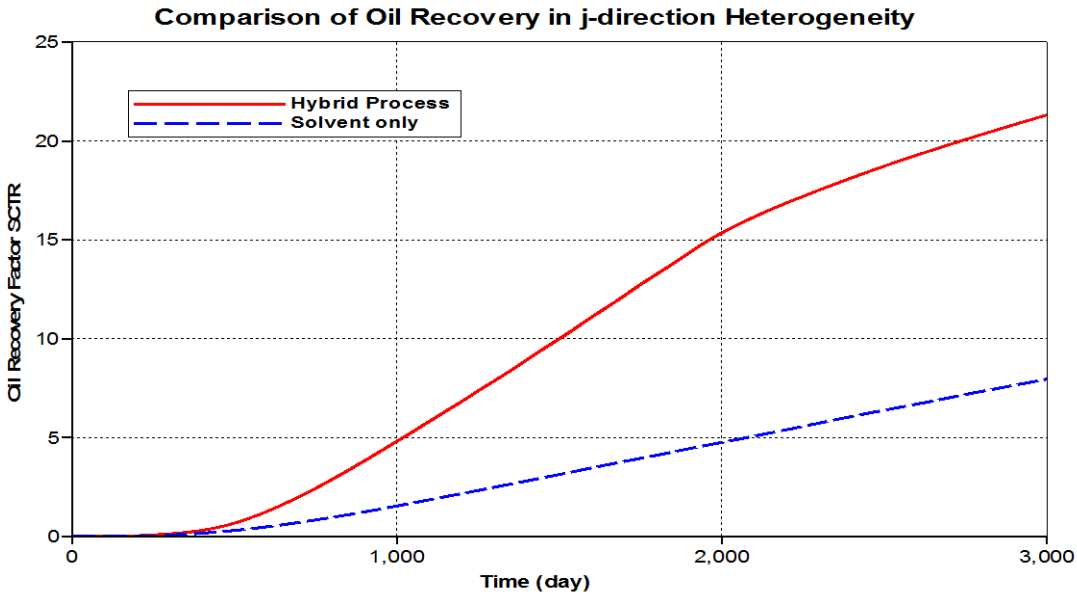

(a)

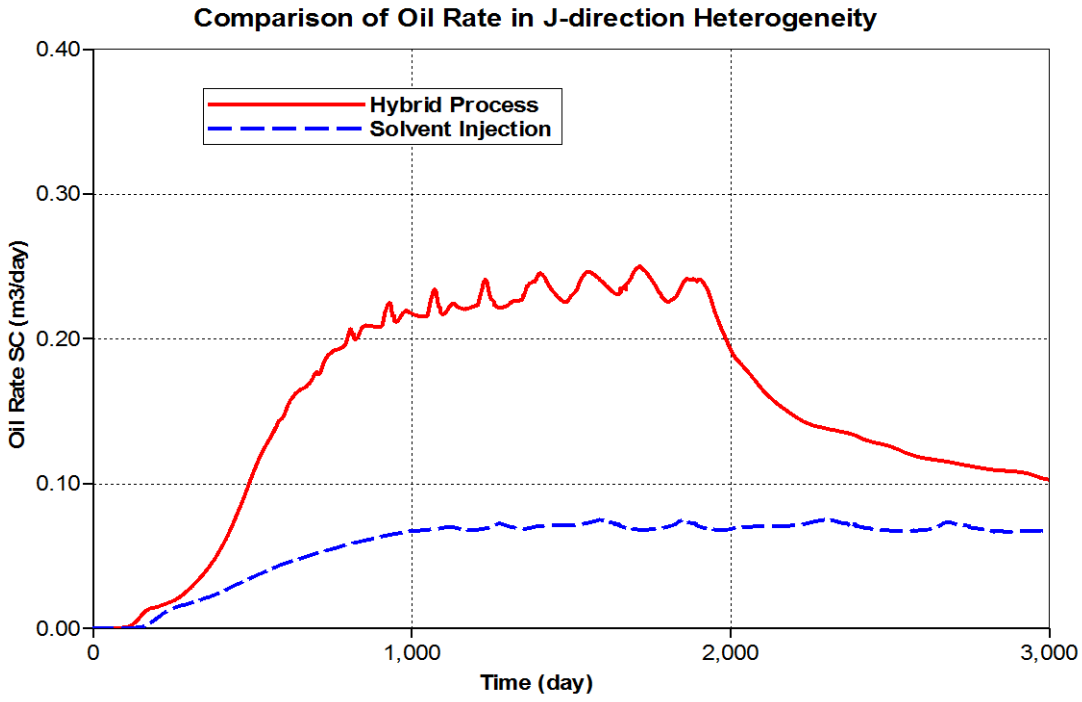

(b)

Figure 3-49 Comparison of hybrid process and solvent injection: (a) oil recovery factor and (b) oil rate [j-direction]

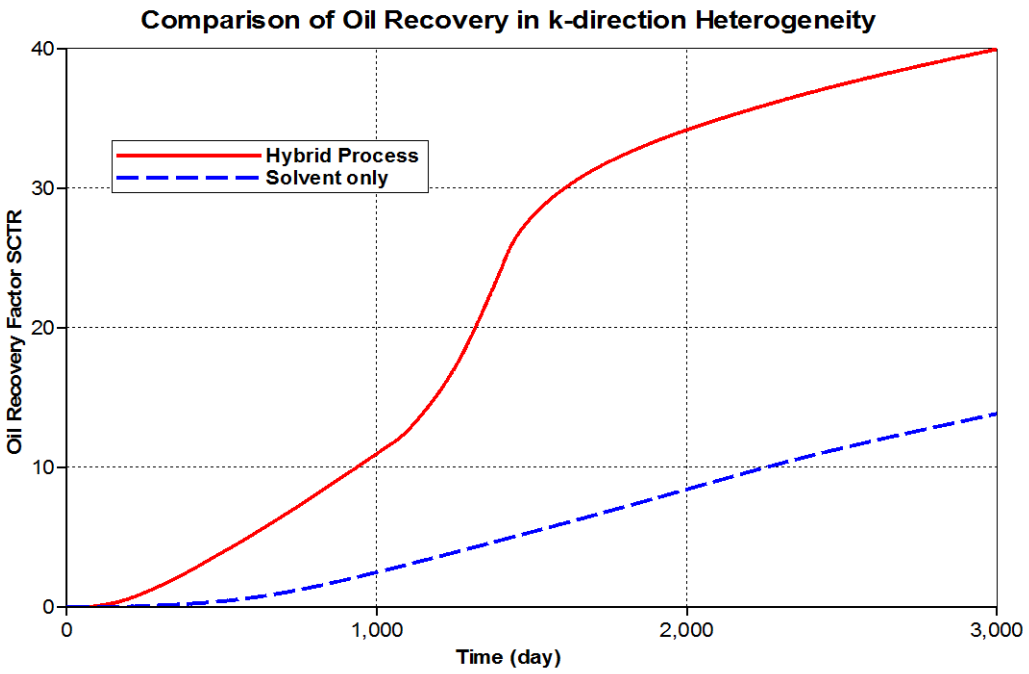

(a)

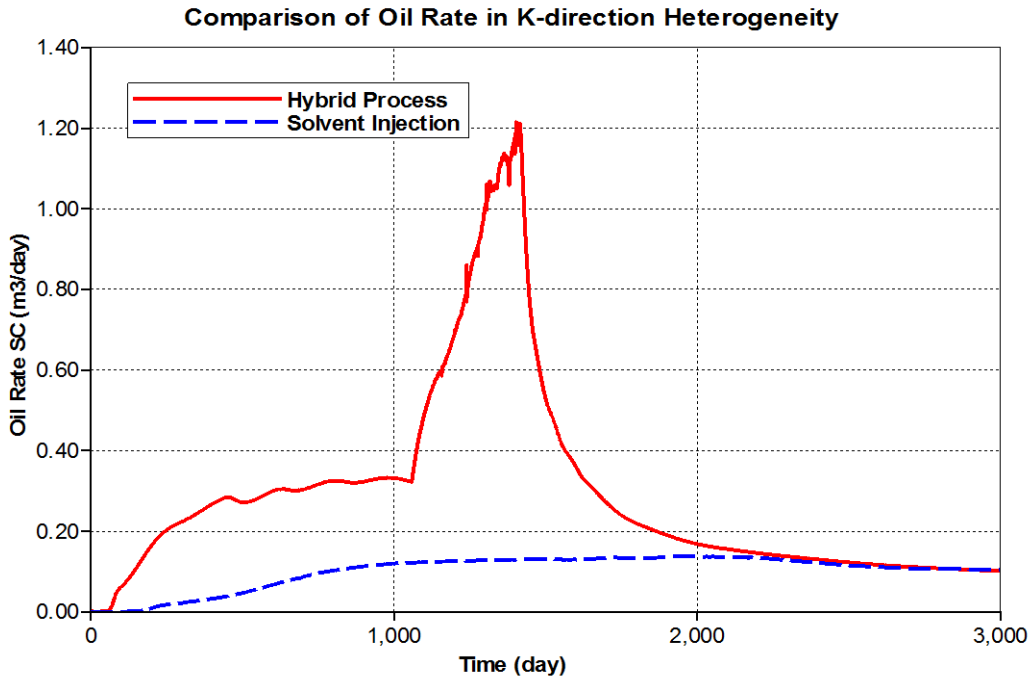

(b)

Figure 3-50 Comparison of hybrid process and solvent injection: (a) oil recovery factor and (b) oil rate [k-direction]

Apparently, the hybrid processes in both series recover more oil than the solvent injection processes due to the presence of electrical energy input. Both hybrid processes have around 3 times more than those with solvent injection processes at 3000 days simulation.

In Series1, when the ERH-S is applied, the temperature in three layers increases, which reduces the viscosity. Figure 3-51 shows the NC_4 distribution comparison between the hybrid process and solvent only process. The oil viscosity distributions from the left view and top view are shown in Figure 3-52 and Figure 3-53. From Figure 3-52 and Figure 3-53, the oil viscosity reduction area and extent of the hybrid process are greater than that of the solvent injection alone process. However, from the Figure 3-51, we can see that the NC_4 distribution is similar in both processes. Following Figure 3-54 and Figure 3-55, the electrical resistive heating is the main cause of the oil viscosity reduction. Because the electrode is set only in layer 4-5-6 in the j-direction, the temperature of both sides of the electrode increases, which can lead to improved NC_4 distribution. In Series 2, Figure 3-56 and Figure 3-57 present viscosity changing with time in block (30,1,9), which is located above the low permeability layer, and block (30,1,20), which is located in the producer position. In Figure 3-56 (a), the oil viscosity in block (30,1,9) changes with the temperature increase and NC_4 fraction increase in the first 80 days, and then, with the temperature continuously increasing, the NC_4 fraction decreases. Combining these two influencing factors, the oil viscosity keeps almost constant until around 1100 days. Comparing Figure 3-56 (a) and Figure 3-56 (b), the oil viscosity above the low permeability layer could change dramatically due to the

electrical energy transferring to upper layers. The Figure 3-57 agrees with Figure 3-50 very well.

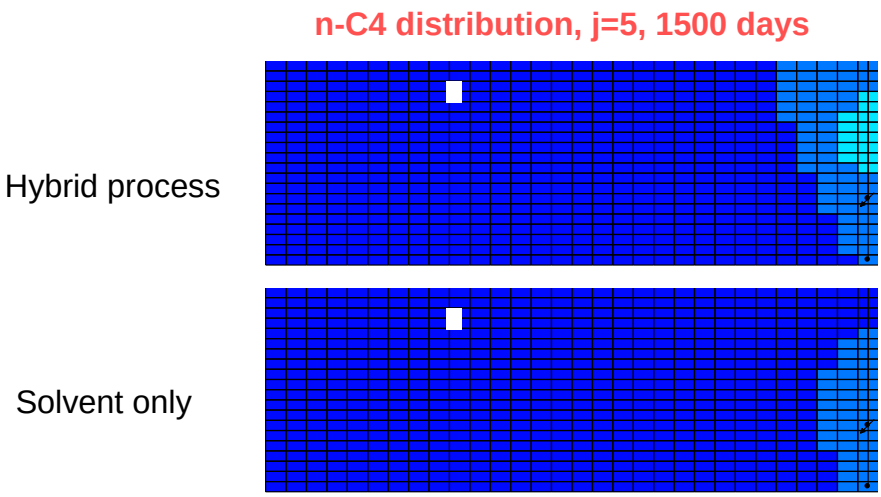

Figure 3-51 Comparison of NC_4 distribution in layer 5 in j-direction at 1500 days

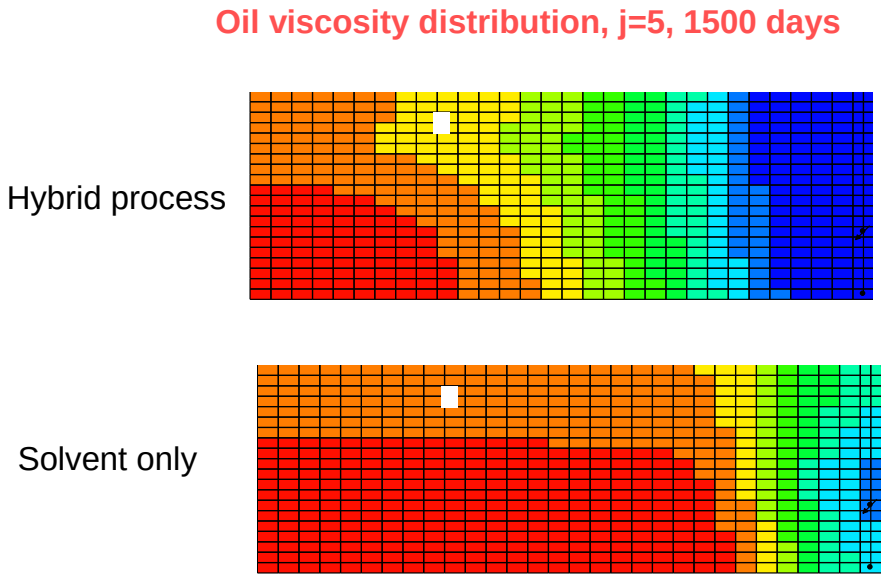

Figure 3-52 Comparison of oil viscosity in Layer 5 in j-direction at 1500 days

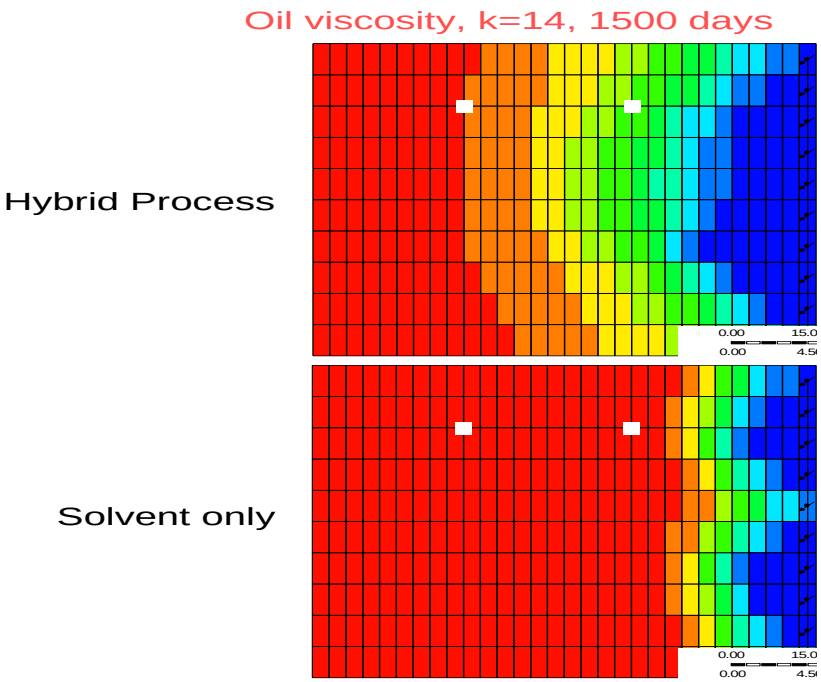

Figure 3-53 Comparison of oil viscosity in Layer 14 in k-direction at 1500 days

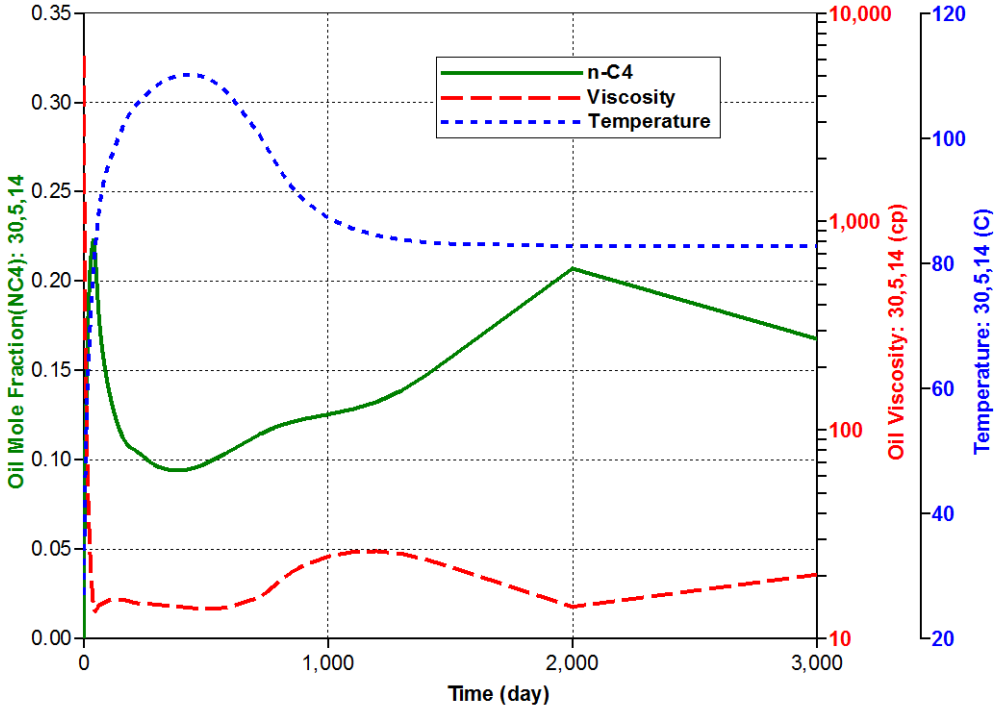

Figure 3-54 Parameters changing with time in block (30,5,14) in hybrid process

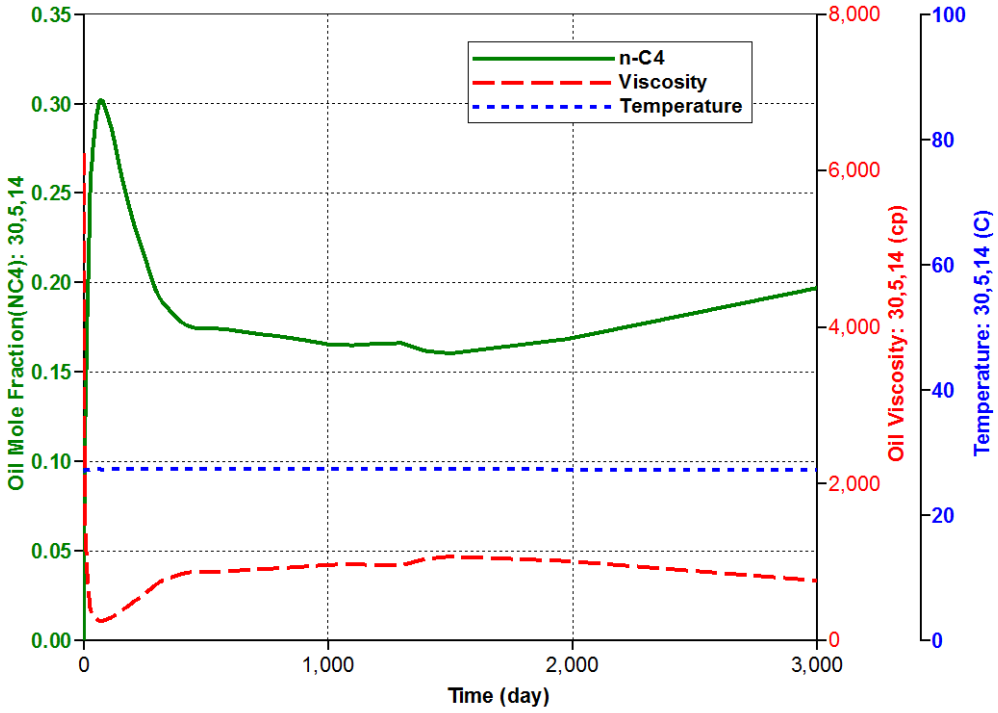

Figure 3-55 Parameters changing with time in block (30,5,14) in solvent injection only

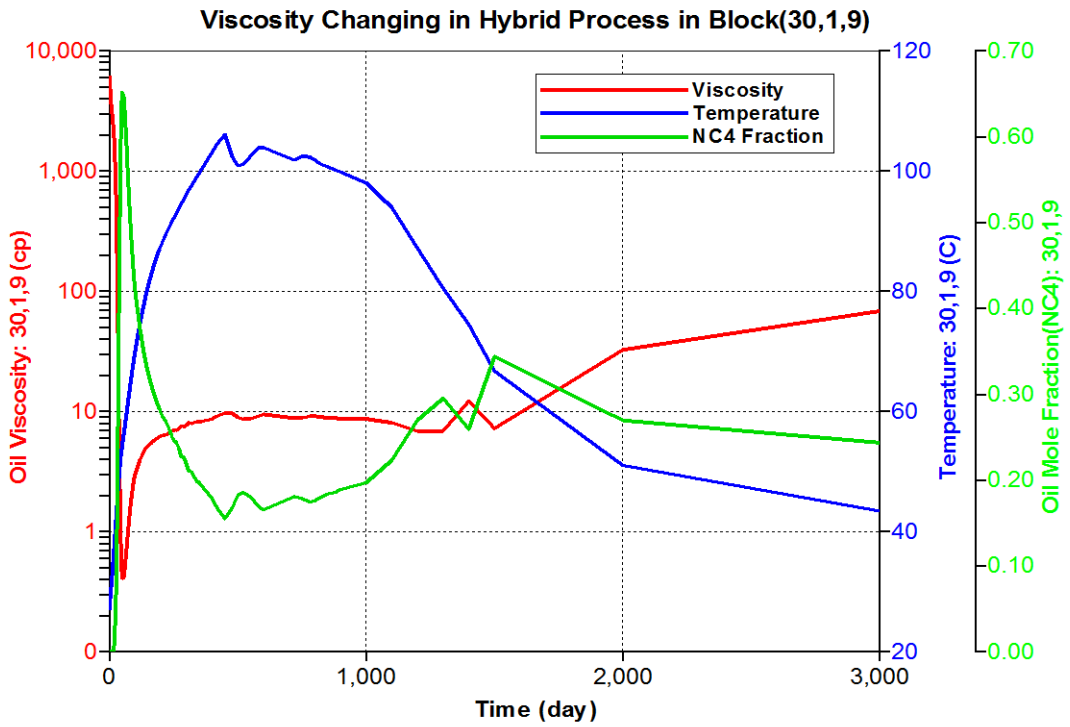

(a)

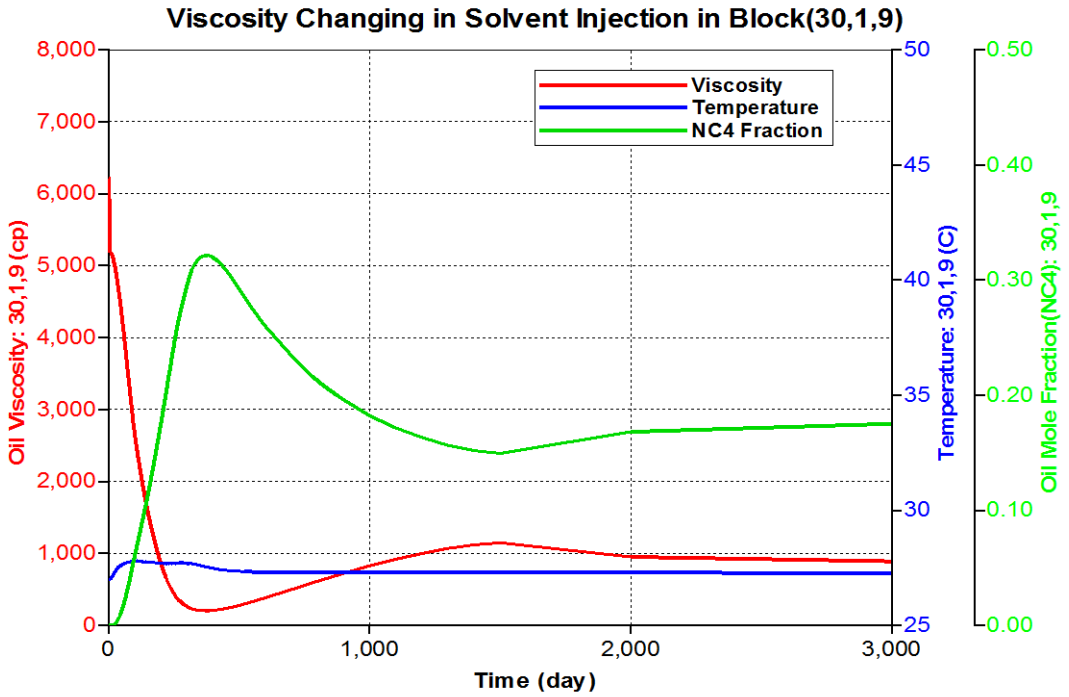

(b)

Figure 3-56 Viscosity changing in block (30,1,9) in k-direction heterogeneity situation (a) hybrid process (b) solvent injection

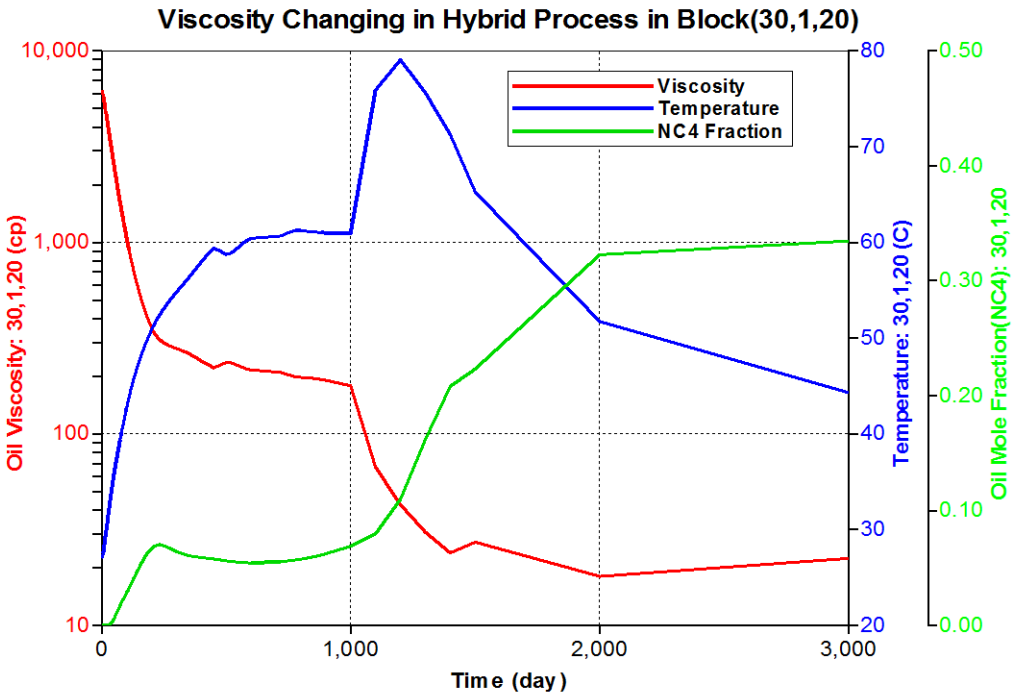

(a)

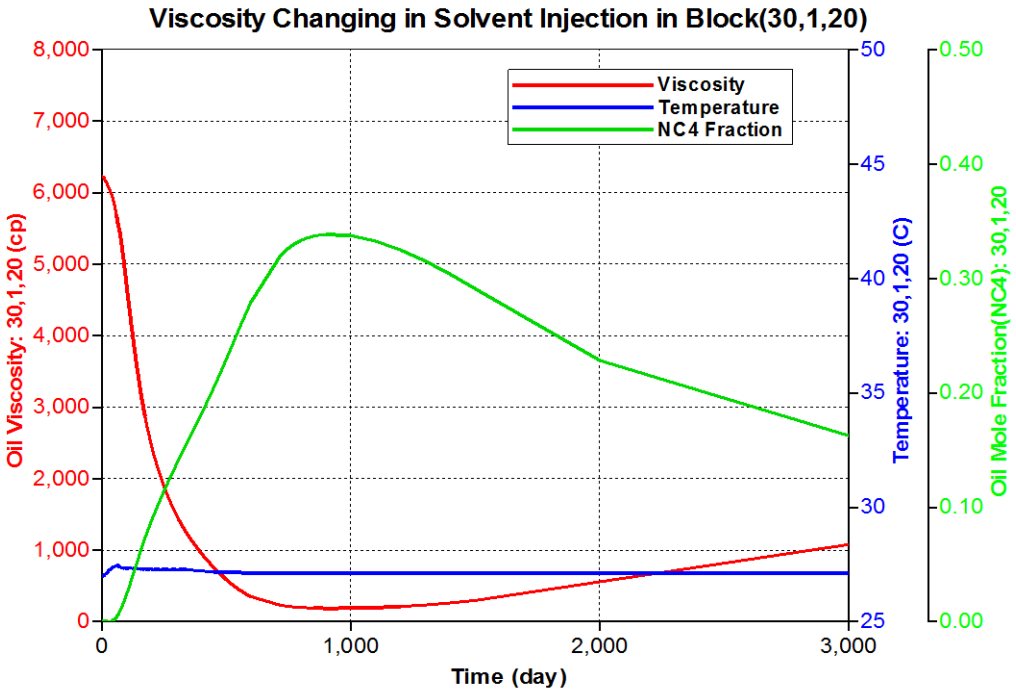

(b)

Figure 3-57 Viscosity changing in block (30,1,20) in k-direction heterogeneity situation (a) hybrid process (b) solvent injection

In order to understand this hybrid process, the following discussion includes the heterogeneity and base cases in the hybrid and solvent injection only processes.

k-direction

In this scenario, four cases are compared: Base case-ERH-S, Heterogeneity-ERH-S, Base case-Solvent injection only, and Heterogeneity-Solvent injection only.

The comparison of oil recovery factor in the four cases is shown in Figure 3-58. For the hybrid process in the heterogeneity and base cases, there is little difference between them, which demonstrates that the low permeability layer has a small impact on the hybrid process.

Also, from Figure 3-59, the NC_4 distribution in the heterogeneity-solvent only case is better than that of the base solvent injection-only case, which is due to the NC_4 spreading horizontally, not vertically. Correspondingly, the viscosity reduction profiles at that time are shown in Figure 3-60.

From this section, the hybrid process shows a very good result when used in heterogeneity reservoirs.

When the low permeability zones exist, the heat can help to reduce the viscosity of the low permeability zones, and then, when the temperature drops to some degree, it helps increase the solvent solubility, so the solvent injection reduces the viscosity continually.

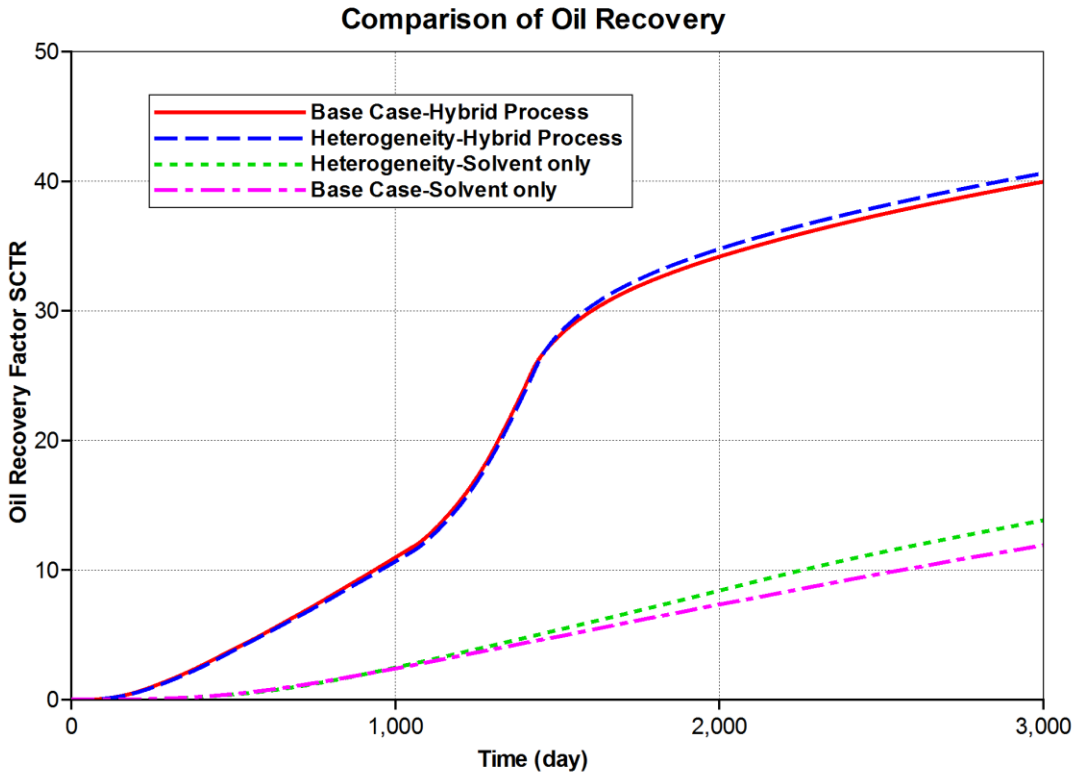

Figure 3-58 Comparison of oil recovery of ERH-S and solvent injection only between heterogeneity and base case

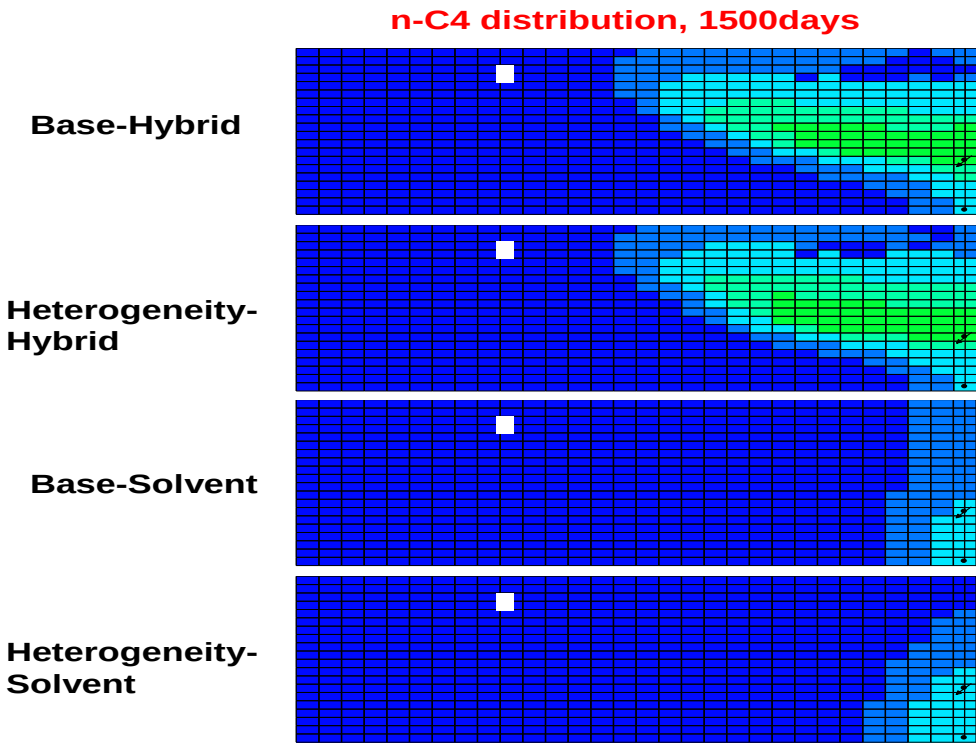

Figure 3-59 NC_4 distribution at 1500 days in four cases

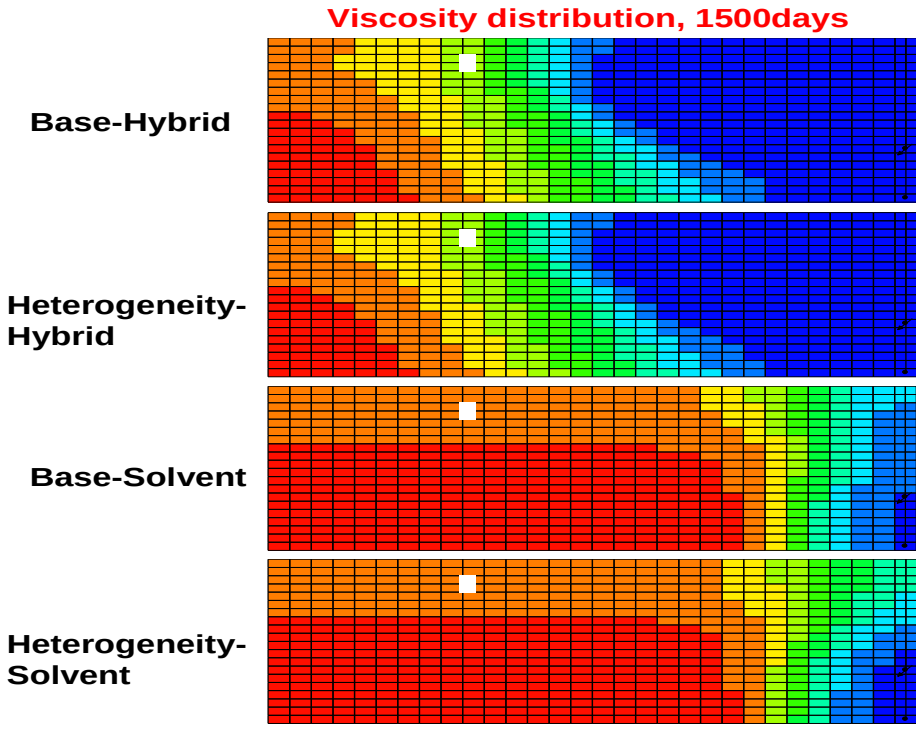

Figure 3-60 Viscosity distribution at 1500 days in four cases

3.2.8 Energy analysis

In this section, the energy efficiency is analyzed simply by referring to the electricity input and gas consumption.

We compared the different cases with the same reservoir conditions and different voltage values. The cumulative oil production, cumulative electricity energy input, and cumulative solvent injection are compared in Figure 3-61. From this figure, the gas consumption of VAPEX is the highest in all 5 cases, and the 240 V of hybrid process is the lowest. However, the electricity consumption is lowest in the 110 V hybrid process case.

Figure 3-61 Comparison of gas and electricity consumption between ERH-S and VAPEX

CHAPTER 4

NUMERICAL INVESTIGATION OF SOLVENT AND STEAM HYBRID PROCESSES

The more typical type of thermal process is to inject steam to heat the reservoir and reduce oil viscosity. Among the different well-known and popular processes that involve the injection of steam into the reservoir, SAGD and CSS processes are chosen in this chapter primarily because both are applied on a large scale and are successful in commercial projects. Then, based on the SAGD and CSS model, SAGD-S and CSS-S are investigated and compared with SAGD and CSS, respectively. SAGD with solvent and CSS with solvent are also simulated by CMG STARS with the same basic reservoir model.

4.1 SAGD-S

4.1.1 Model description

The STARS simulator from CMG (Computer Modeling Group) is used for SAGD simulations. All the reservoir parameters are shown in Table 4-1, which are the same as those of the basic reservoir applied in ERH-S. The injector is then assigned to the corresponding layer in the ERH-S model and the producer is placed below the injector with the same spacing as that of the well pairs in the basic ERH-S model. (The locations of the injector and producer are same as the locations of the injector and producer in ERH-S.)

Table 4-1 Basic Reservoir Parameters

Parameters	Value
Reservoir Dimension	30 m × 30 m × 10 m
Permeability	5000 md(in Base Case)
Porosity	0.35
Initial water saturation	30%
Oil Viscosity @ 27°C	6217.86 cp
Production pressure	2100 kPa
Injection pressure	2200 kPa

For steam injection, 80% quality 210^{o}C steam at 2200 kPa is injected, which is slightly higher than the initial reservoir pressure at 2100 kPa. In order to compare this SAGD process with the hybrid process, 3000 days are set for the production period, which is applied in oil industry for SAGD lifetime production. The temperature range in the middle of the injector and producer reached 60-90^{o}C when the start-up period finished. The pressure is set as 2100 kPa.

In terms of solvent selection, hexane and butane are chosen to be injected with steam in a vapour phase because hexane has the closest vapourization temperature to the injected steam temperature (210^{o}C at an operating pressure of 2.2 MPa) and butane was chosen to compare the efficiency with lower vaporization temperature. The process is then compared with ERH-S. Condensed solvent around the interface of the steam chamber dilutes the oil and, in conjunction with heat, reduces its viscosity.

4.1.2 Sensitivity Analysis

Thick Oil Reservoir

Another reservoir model with 30 meters in thickness, which is 20 meters thicker than the original model, is built and all the reservoir parameters are based on the original model. The well distance is kept the same as that in the thin reservoir, which is 3 meters, and the well spacing is 30 meters. Figure 4-1 shows the oil rate in this thicker reservoir (30 meters) and displays a jump of oil rate after 1600 days of simulation.

Three blocks are chosen to check the parameter changes with time, block (22,1,1) on the top of the reservoir, block (21,1,10) inside of the reservoir, and block

(1,1,10) at the left boundary of the reservoir. The locations for the three blocks are shown in Figure 4-2.

Figure 4-3, Figure 4-4 and Figure 4-5present the temperature, oil viscosity, and oil saturation change with time in block (21,1,10), block (22,1,1), and block (1,1,10), respectively. There are two oil saturation jumps in Figure 4-3 because of the oil gravity and re-fill. In the simulation over 1600 days, the temperature in block (21,1,10) increases and causes the viscosity to decrease. From the temperature perspective, after the steam chamber reaches the top of the reservoir, the heat loss to the overburden is slower than the heat accumulation in the chamber, which causes the temperature to increase inside of the reservoir. Compared to block (21,1,10), block (22,1,1) presents a very small increase of temperature after the chamber reaches the top of the reservoir due to the heat loss to the overburden.

Given that the well spacing is enlarged to 100 meters, after the steam chamber reaches the top of the reservoir and expands horizontally across 30 meters of the reservoir, the heat losses to the overburden are the same as the heat losses in the case of 30 meters well spacing. However, in the case of 100 meter well spacing, the heat keeps transferring horizontally after the steam chamber reaches 30 meters instead of accumulating in the reservoir of the case of 30 meters well spacing. Figure 4-6 displays the temperature distributions in different well spacing cases. In the same location of two cases, block (1,1,1) in 30 m well spacing and block (71,1,1) of 100 m well spacing, the temperature for two blocks shows differences after the steam chamber reaches the boundary of the 30 m well spacing (shown in Figure 4-7).

When the steam chamber touches the left boundary of the reservoir, because there is no heat loss to the left boundary, the heat accumulates within the steam chamber boundary and the steam chamber travels downwards. The temperature in the left boundary increases with corresponding steam continuous injection. The jump in the oil saturation is due to the oil re-infill under the gravity effect.

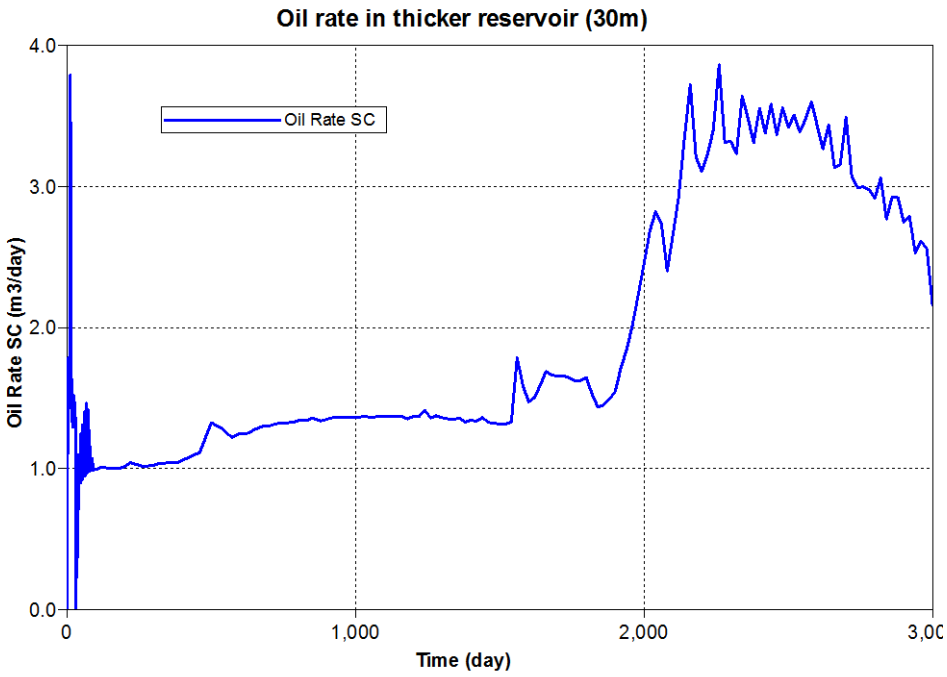

Figure 4-1 Oil rate in thicker oil reservoir with SAGD process

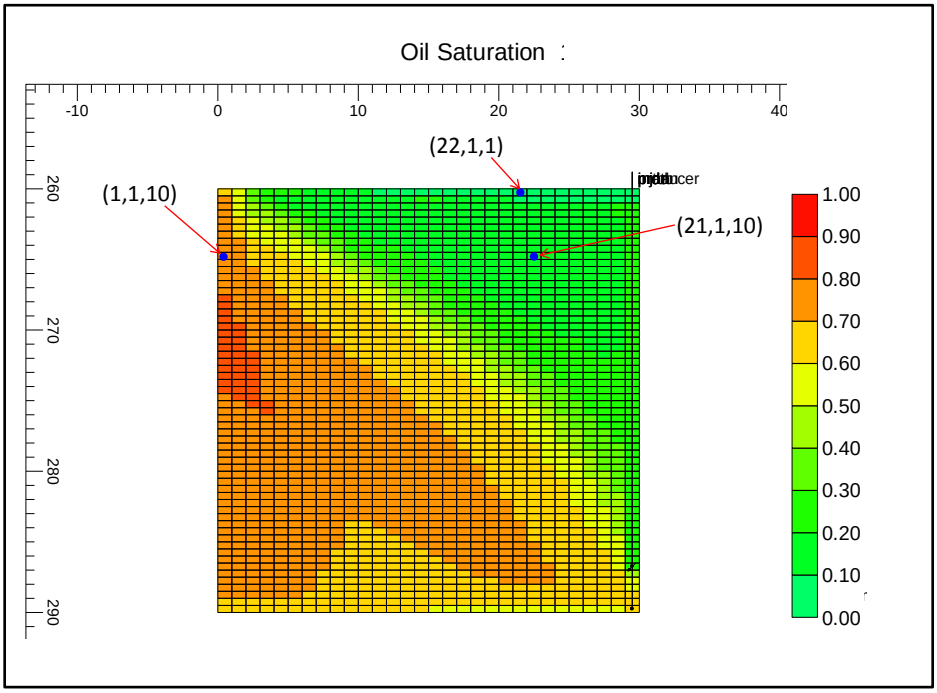

Figure 4-2 Three block (22,1,1), block (21,1,10), and block (1,1,10) marked at the reservoir with oil saturation profile at 1500 days of simulation

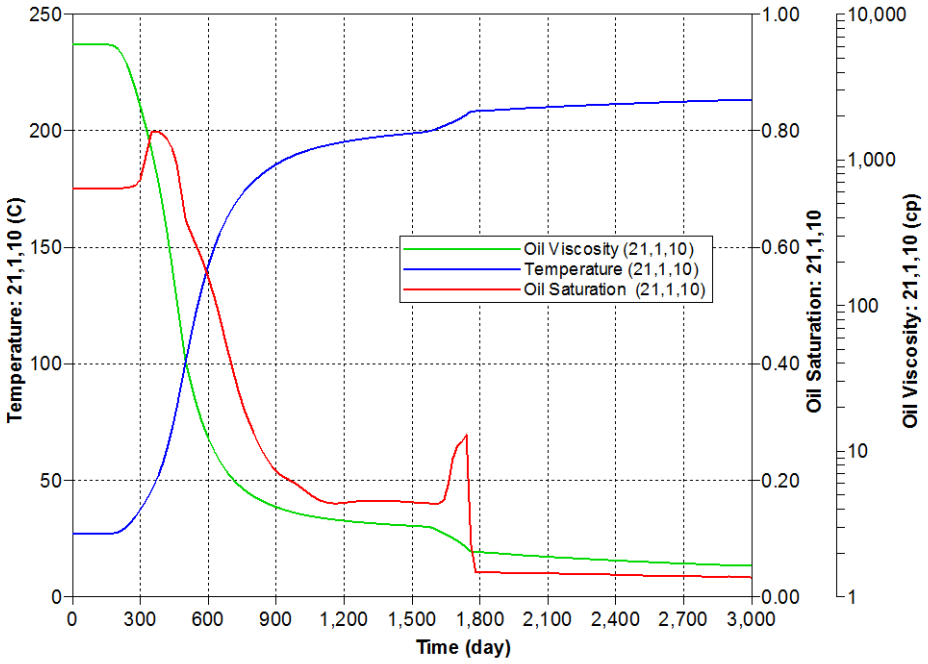

Figure 4-3 Parameter changes with time in block (21,1,10)

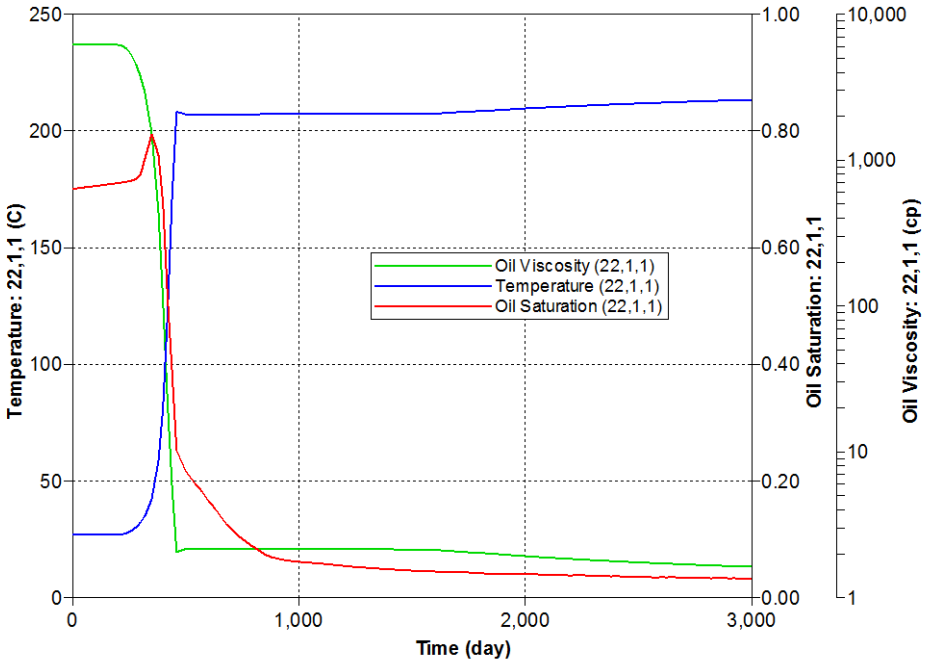

Figure 4-4 Parameter changes with time in block (22,1,1)

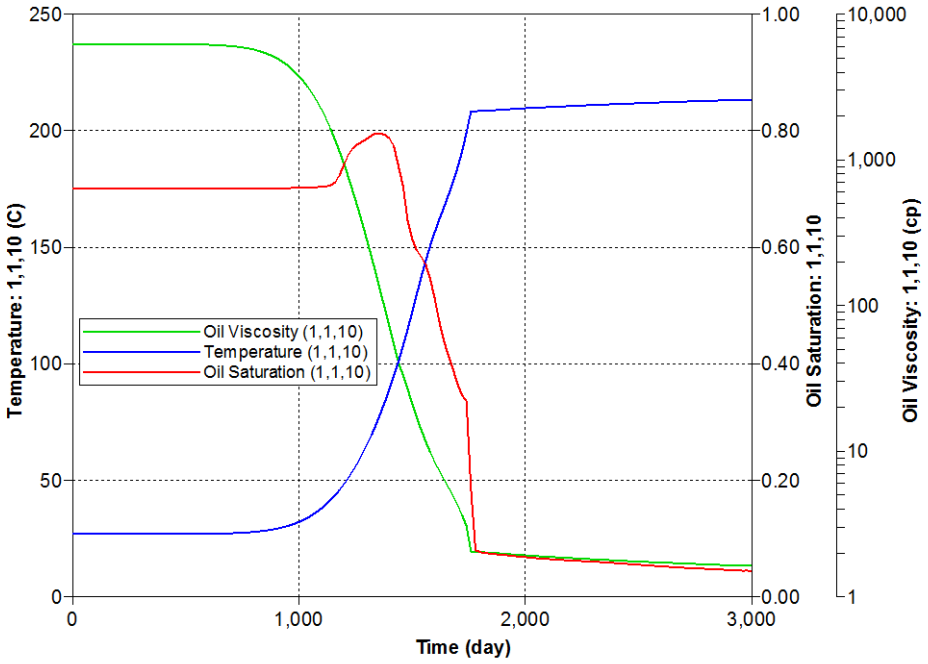

Figure 4-5 Parameter changes with time in block (1,1,10)

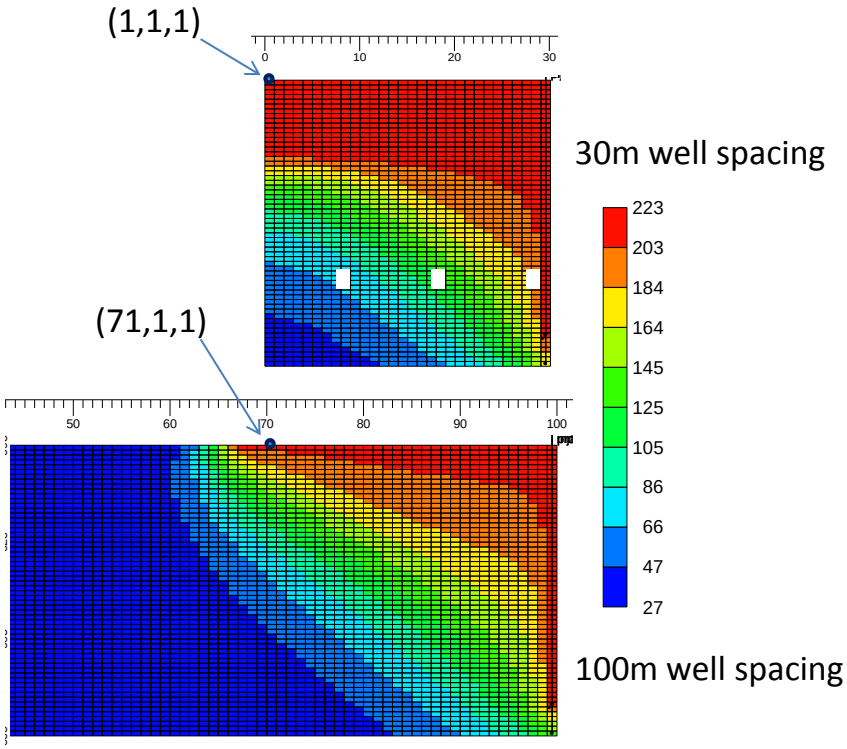

Figure 4-6 Temperature distribution in different well spacing cases after 1900 days of simulation

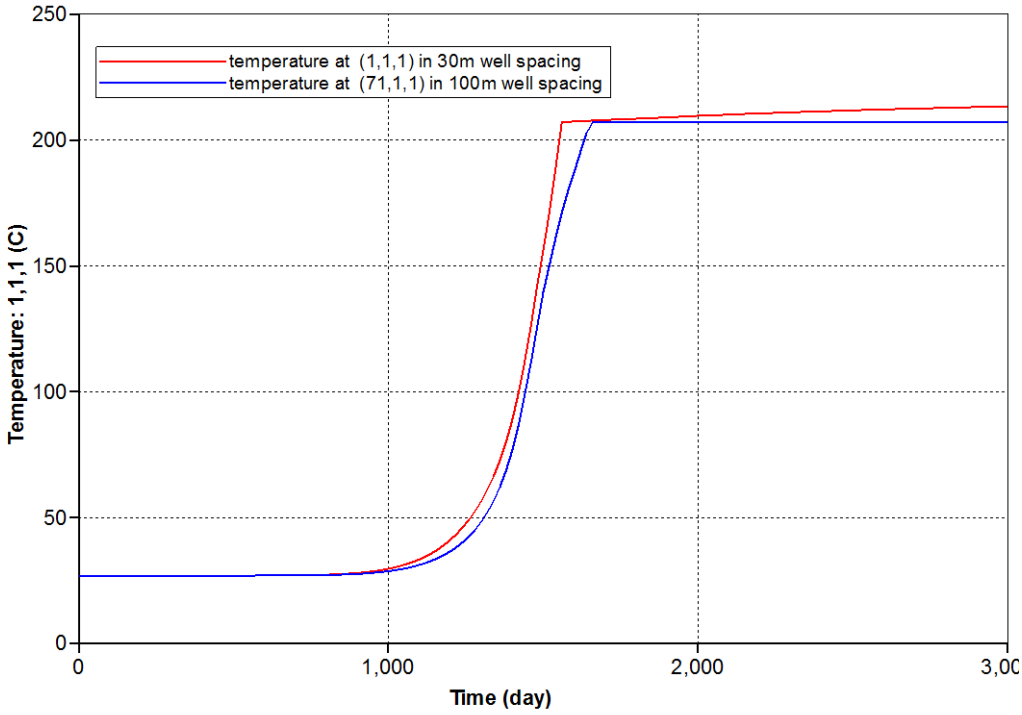

Figure 4-7 Temperature trend in block (1,1,1) of 30 m well spacing and block (71,1,1) of 100 m well spacing

Cumulative Oil Production

Figure 4-8 presents the cumulative oil production for SAGD, SAGD with butane (5%, 10% and 15% volume C_4H_{10}), and SAGD with hexane (5%, 10% and 15% C_6H_{14}). It is clearly shown that the SAGD process yielded a little bit higher cumulative oil production than all the cases of SAGD with solvent. With the solvent volume increase, the cumulative oil production decreases after 3000 days simulation. However, in the middle of the simulations, SAGD has higher cumulative oil production than SAGD-S, and the corresponding oil rate profiles of SAGD and SAGD-S are presented in Figure 4-9. In Figure 4-9, the oil rate increases sharply after 1200 simulation for all the cases, which is different with the traditional SAGD oil rate profile because of the limitation of the thickness of the reservoir. With small reservoir thickness, the steam can easily travel horizontally and vertically and cover the whole area of the reservoir, and then the production rate reaches the peak after 1400 days of simulation.

In Figure 4-9, the oil rate of SAGD is higher than these of SAGD-S processes; also, it is faster to reach peak oil rate than other SAGD-S processes. One of the main reasons behind this phenomenon is that with more solvent accumulation at the edge of the steam chamber, solvent in gas phase acts as an insulator and deteriorates heat transfer from steam to cold bitumen. The temperature profiles at the end of 58 days of simulations for SAGD and SAGD-S (C_4H_{10}-15%) is shown in Figure 4-10, in which the temperature in SAGD already touches the top of the reservoir. However, the temperature of SAGD with butane does not touch the top of the reservoir yet. After the steam chamber reaches the boundary of the reservoir at

1000 days simulation, the temperature profiles of SAGD and SAGD with butane (C_4H_{10}-15%) are presented in Figure 4-11. More injected solvent detained in the reservoir delays the growth of the chamber due to the isolation properties of the solvent in gas phase, which causes the temperature to propagate slowly. Figure 4-12 gives the C_4H_{10} distribution profiles for different solvent volume injections. The temperature profiles at the end of 1000 days of simulation demonstrates corresponding differences in cumulative oil production and oil rate between low solvent volume and high solvent volume injected.

In these simulations of SAGD and SAGD-S with different solvent volumes, the CDOR decreased slightly with increased solvent injection volume in the injected steam ((Table 4-2) up to 15% volume percentage in steam). From the CSOR perspective, all the CSORs are a bit higher than in ordinary economical CSOR (2.8-4.0) (Jiang et al., 2010) due to the small thickness of the reservoir. However, the CSOR is decreased significantly with the solvent volume increased in the steam injected. For the solvent type, the C_6H_{14} is slightly better than C_4H_{10} because the vapourization temperature of C_4H_{10} is significantly lower than the steam temperature, which is similar to the vapourization temperature of C_6H_{14}. Then, from the simulation results, the conclusion is drawn that C_4H_{10} is not good for co-injection with steam because of the large difference between dew point conditions and the steam injection conditions.

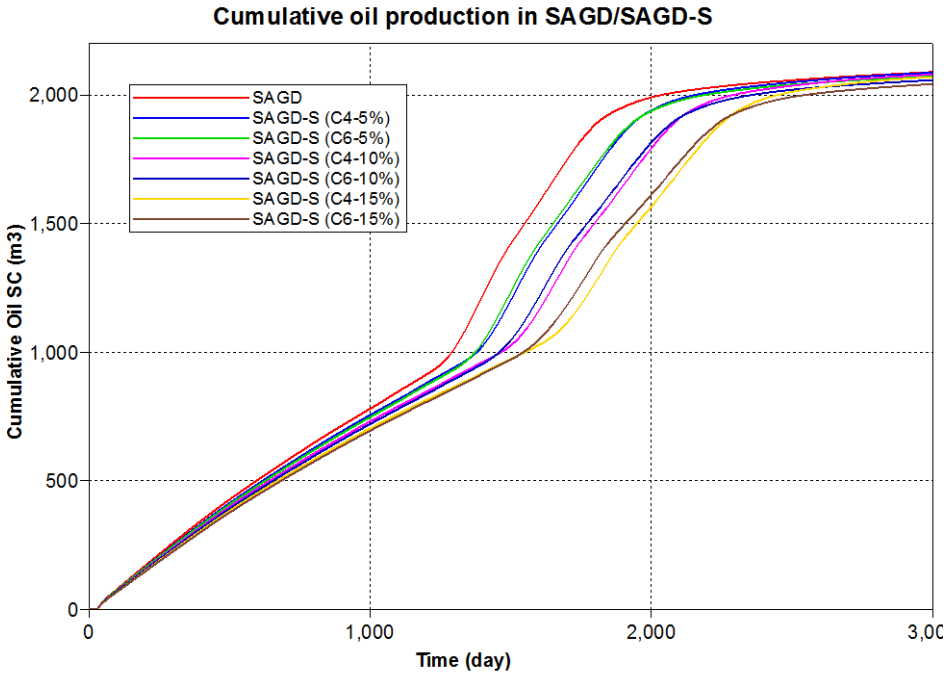

Figure 4-8 Cumulative oil production profiles for SAGD and SAGD-S (with different solvents and different solvent volumes) after 3000 days of simulation

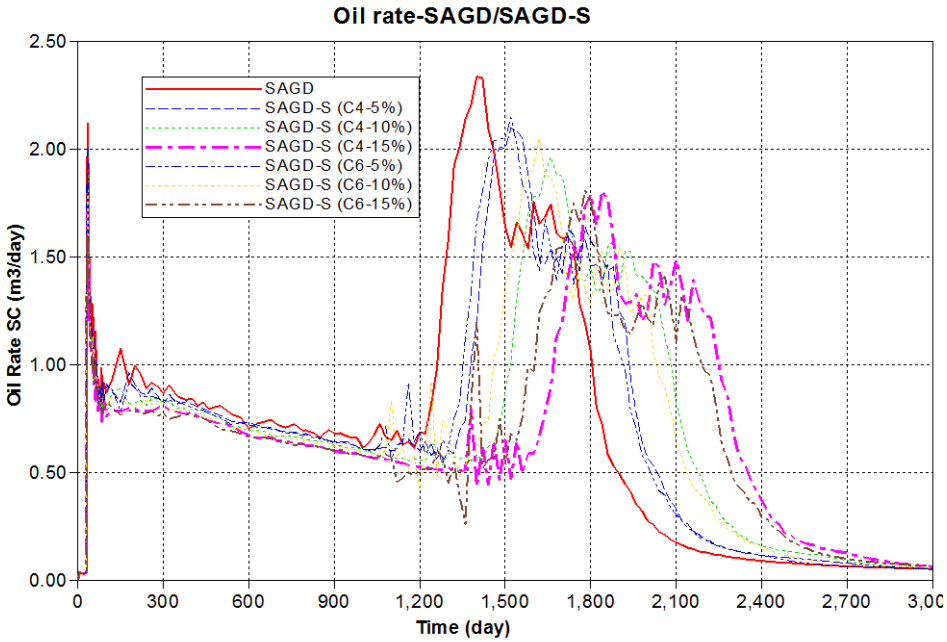

Figure 4-9 Oil rate profiles in SAGD and SAGD-S (with different solvent volume)

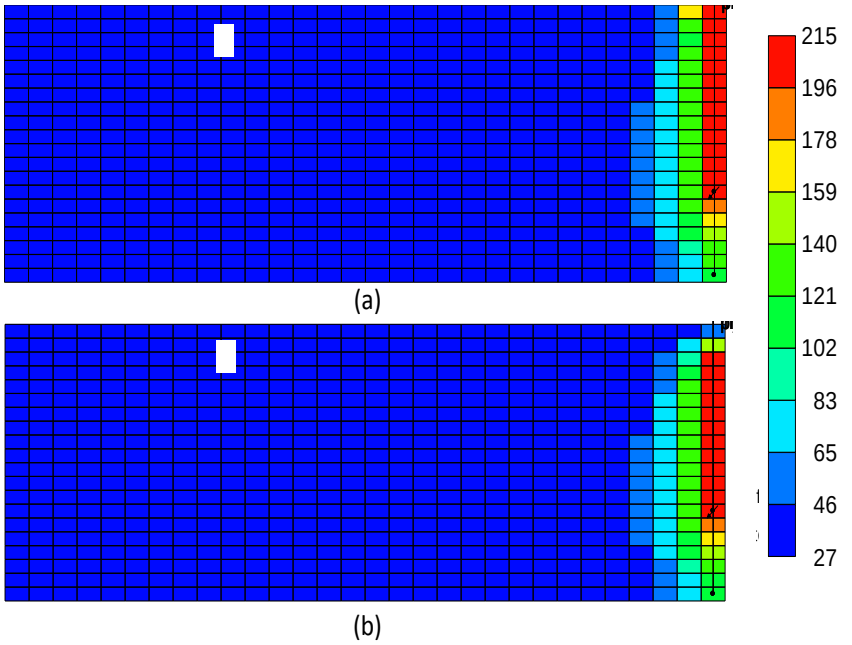

Figure 4-10 Temperature profile at the end of 58 days of simulation- (a)SAGD; (b) SAGD with butane (C_4H_{10}-15%)

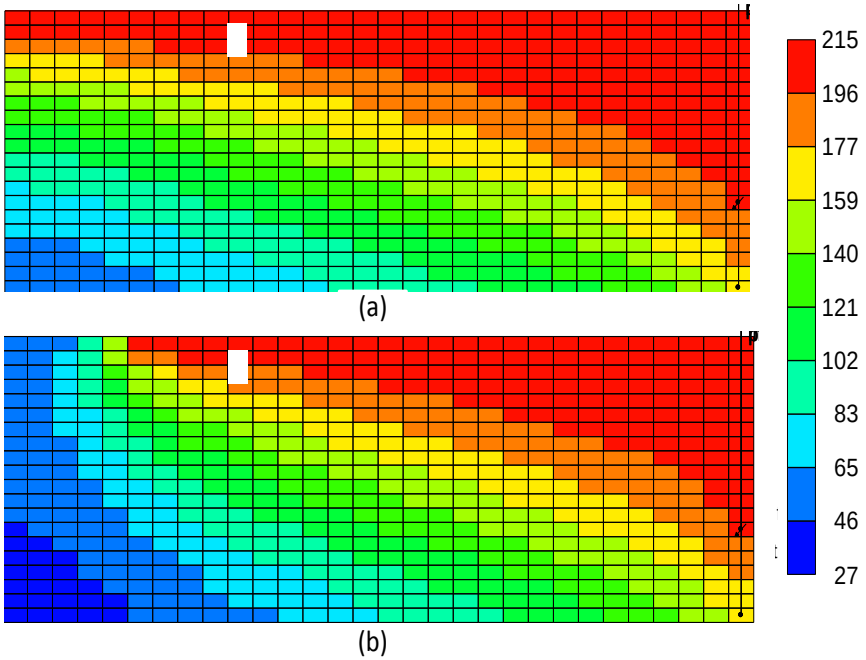

Figure 4-11 Temperature profiles at the end of 1000 days of simulation: (a) SAGD; (b) SAGD with butane (C_4H_{10}-15%)

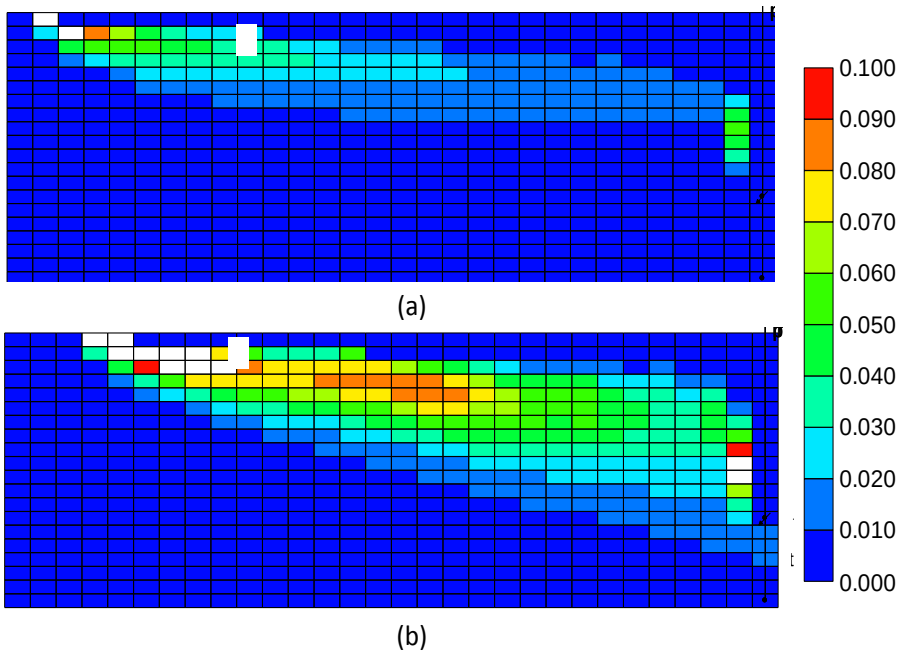

Figure 4-12 Gas mole fraction (C_4H_{10}) in SAGD-S processes at the simulation of 1000 days

(a) 5%- C_4H_{10}; (b) 15%- C_4H_{10}

Table 4-2 Effect of solvent volume on SAGD and SAGD with solvent processes

	SAGD	SAGD with solvent processes					
		C_4H_{10}			C_6H_{14}		
		5%	10 %	15 %	5%	10 %	15 %
CDOR(m^3 /day)	0.6965	0.6956	0.6932	0.6900	0.6911	0.6860	0.6809
CSOR(m^3 /m^3)	5.43	5.17	4.92	4.67	5.20	4.97	4.73
Net solvent to oil ratio m^3/m^3)	0	0.269	0.540	0.815	0.271	0.546	0.826

4.2 CSS-S

4.2.1 Model description

CSS in oil reservoirs involves injection of heat in the form of high pressure steam. The four operating constraints that control the flow of heat in the reservoir are steam volume, injection rate, steam quality, and steam temperature. Given that steam fracture occurs in the first 3 cycles, the injected volume of steam has to be large enough to contact and mobilize an economic amount of bitumen. In the beginning of the production, the steam and steam condensate is produced relatively highly and rapidly over days. After some time, oil production increases, and it peaks and then declines as the pressure in the reservoir falls. Generally, the ratio of length of injection, soaking, and production is 10%, 10%, and 80%. With more oil produced, the amount of steam per cycle increases and the length of the production period grows in order to maintain the production and chamber growth. Below, CSS and CSS-S processes are investigated.

In the CSS model, the well is placed in the bottom of the reservoir, which is in the same location as the injector in the ERH-S process. All the other reservoir parameters are presented in Table 4-1, which are applied in the ERH-S reservoir. In the CSS simulation, the flow conditions are quite different from the SAGD simulation. The steam injection rate under reservoir conditions are too low, and the injection pressure must be increased until parting occurs to achieve a high injection rate. In this model, the CSS process in the simulation is a multi-cycle single well operation. It considers a vertically fractured along with the wellbore. The fracture occurs when the injection pressure is larger than that fracture pressure. Current

reservoir simulation models cannot take into account the complexity of steam fracturing together with fluid flow as is encountered in CSS. It is still unclear how geo-mechanics should be modeled to represent steam injection with fracturing in the reservoir. For the fracture modeling, methods from CNRL are applied. Once the injection pressure reaches the fracture pressure in the beginning, the injection rate/injection volume is very high and the production rate is high correspondingly, which causes both localized fracturing and widespread pore-volume increases in the formation. The resulting complex geo-mechanical behaviour determines the initial steam flow paths and provides significant drive energy during CSS operations. In all of the CSS simulations, dilation and re-compaction are simulated based on the Beattie-Boberg model.

In the Beattie-Boberg model, it is assumed that elastic conditions apply (pore pressure increases quickly with steam injection) until a specific pressure (PDILA) is reached, at which point the pores expand (dilation) with continued steam injection. During production, the pores stay dilated until the pressure falls below another specified pressure (PPACT). At this time, the pores start to shrink (re-compact) as the pressure decreases further due to continued fluid production. In the simulations of CSS and CSS-S in this section, values for the Beattie-Boberg properties are used (Table 4-3).

Table 4-3 Beattie-Boberg Properties for the HPCSS model

CRD	2.0E-5
PBASE (kPa)	2000
PDILA (kPa)	6000
PRPOR	2000
PERMULI	15
PERMULJ	15
PERMULK	15
PORRATMAX	1.02
PPACT (kPa)	2100

PBASE = Reference pressure

CRD=Dilated rock compressibility

PDILA= Pressure at which dilation begins

PORRATMAX=Maximum relative porosity increase in a block=maximum permitted porosity/initial porosity.

PPACT =Pressure at which re-compaction begins.

PERMI,J,K=absolutely permeability in the I direction after allowance for dilation.

PERMI,J,K=PERM initial *ePERMULI * (Φ-Φinitial)/(1-Φinitial)

Fracture

Two types of pressure induced fractures are created during the course of the simulation. Vertical fractures are created during periods of high pressure steam injection while it is believed that the minimum principal stress in the reservoir is horizontal, generally in the early part of CSS operations. A horizontal fracture is created during sustained CSS operations.

During the early cycles, vertical fractures are created because of the high injection rate and pressure. Arthur and McGee presented the CSS analytical model, which included the vertical fracture at the wellbore. They used the total pay thickness (100%) for the fracture height (McGee et al., 1987). Due to the reservoir heterogeneity, Leshchyshyn reported a fracture height of less than 50% of continuous net pay height. In our model, the pay thickness is used as the height of the fracture (Leshchyshyn et al., 1994). For the horizontal fracture, a problem in the STARS dilation modeling feature was identified, and it effectively prevented rapid propagation of the high permeability fracture. In order to offset this issue, the PFRAC was set up in such a way as to force rapid propagation of a high permeability pathway in layer #14 from the horizontal well in the first cycle. The rapid propagation along the horizontal direction is limited by the successively reduced fracture pressure relative to the upstream grids.

The fracture in the model is set manually and the propagation of different layers and directions are determined by Transmissibility Multipliers (PTRANSI, PTRANSJ and PTRANS K) and Lower/Higher reference pressure (PFRAC/PFRACF).

The fracture pressure of the reservoir is set as 6 MPa (Encana, Christina Dilation Scheme application, 2009). During CSS, the maximum wellhead injection pressure (WHP) is set at 7 MPa, which is higher than the fracture pressure of the reservoir.

A 70% quality and 303^{o}C steam at 7 MPa is injected from the well. In the first cycle, the injection pressure is set as the first constraint during the injection period, and the surface steam rate is set as the second constraint. For the production period, surface liquid rate (30 m^3) is set as the first constraint, and bottomhole pressure (BHP) is set as the second constraint. The solvents considered are C_6H_{14} and C_4H_{10}.

4.2.2 Sensitivity Analysis

Solvent selection and volume

Figure 4-13 displays cumulative oil production in CSS and CSS-S (different solvents with different volumes). At the end of 3000 days of all simulations, CSS-S with 5% volume of C_6H_{14} obtains the highest cumulative oil production. However, the CSS process only attains the second smallest oil production (CSS-S with 15% volume of C_4H_{10}).

C_6H_{14} has a higher diffusion coefficient than C_4H_{10} in high temperature profiles and, consequently, can disperse more quickly in the reservoir.

During the solvent injection into the reservoir with steam, the solvent mole fraction in the oil phase increased as a result of dissolution. Over time, a high C_6H_{14} mole fraction in oil phase is obtained as compared to the C_6H_{14} mole fraction in gas phase.

Compared with C_6H_{14}, C_4H_{10} has a lower saturation temperature. In the HPCSS-S process, the temperature in the reservoir is above 100^oC most of the time because of continuous steam injection, which causes the C_4H_{10} to barely dissolve into the heavy oil.

During CSS-S with different solvent volumes, when the solvent takes more volume percentage in the steam, less steam will be injected and, correspondingly, less heat will be transferred into the reservoir. Also, Figure 4-14 shows the C_6H_{14} mole fraction in the gas profile. With more C_6H_{14} injected, more vapour solvent acts as an insulator, which can detain steam propagation between the cold heavy oil and steam chamber. Correspondingly, at the end of 1100 days of simulation, the high temperature zone in 5% volume of C_6H_{14} reaches the boundary of the reservoir laterally (Figure 4-15). In contrast, the high temperature zone in high solvent volume injected (15%) only reaches the edge of the boundary.

For all three solvent volume percentages injected (5%, 10% and 15%), 5% shows the best cumulative oil production. Compared to the same volume of C_4H_{10}, C_6H_{14} shows a higher CDOR and lower CSOR. With the increase of solvent volume in steam, the net solvent to oil ratio for 5% volume of C_6H_{14} is the lowest of all the CSS-S processes. The results of the CSS and CSS-S simulations show that C_6H_{14} is an effective solvent for the given operating conditions. C_6H_{14} can not only reduce the CSOR but also increase the CDOR with 5%, 10%, and 15% volume injected.

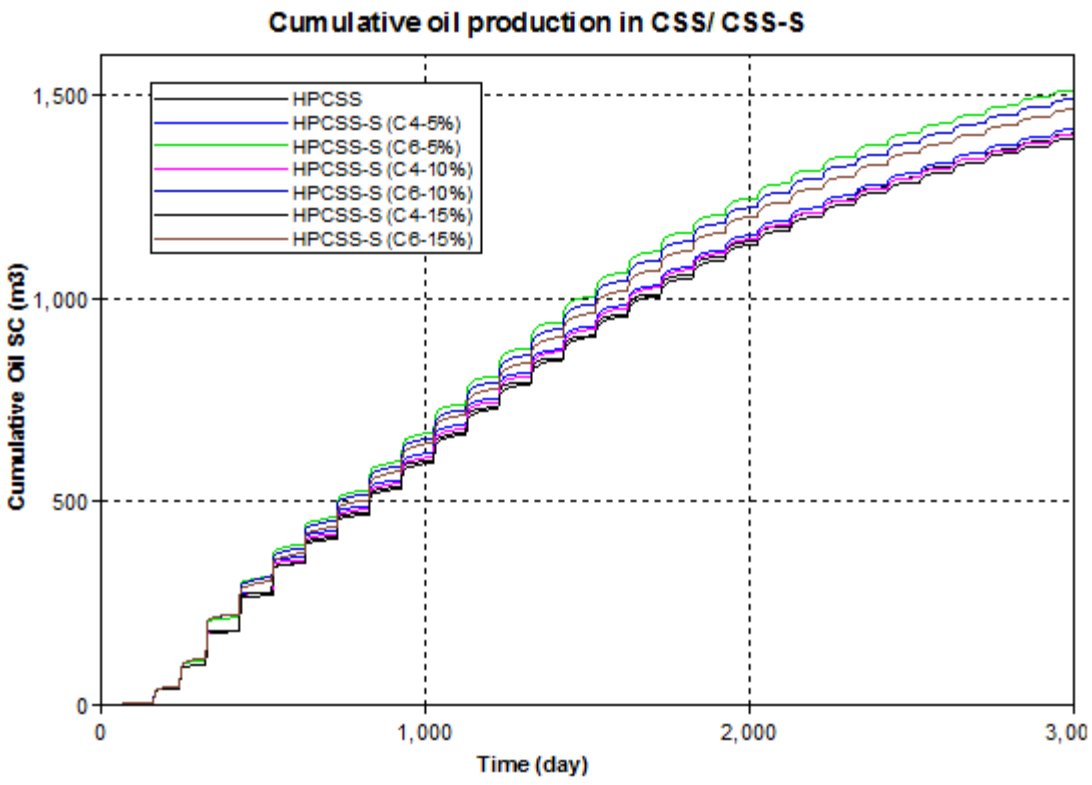

Figure 4-13 Cumulative oil production in CSS and CSS-S (different solvent volumes)

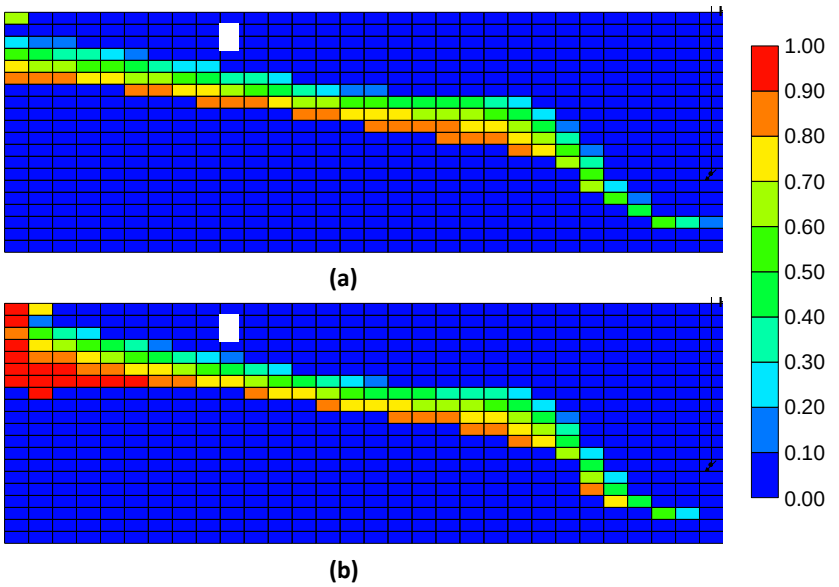

Figure 4-14 Gas mole fraction (C_6H_{14}) at the end of 1100 days of simulation: (a) 5% volume of C_6H_{14}; (b) 15% volume of C_6H_{14}

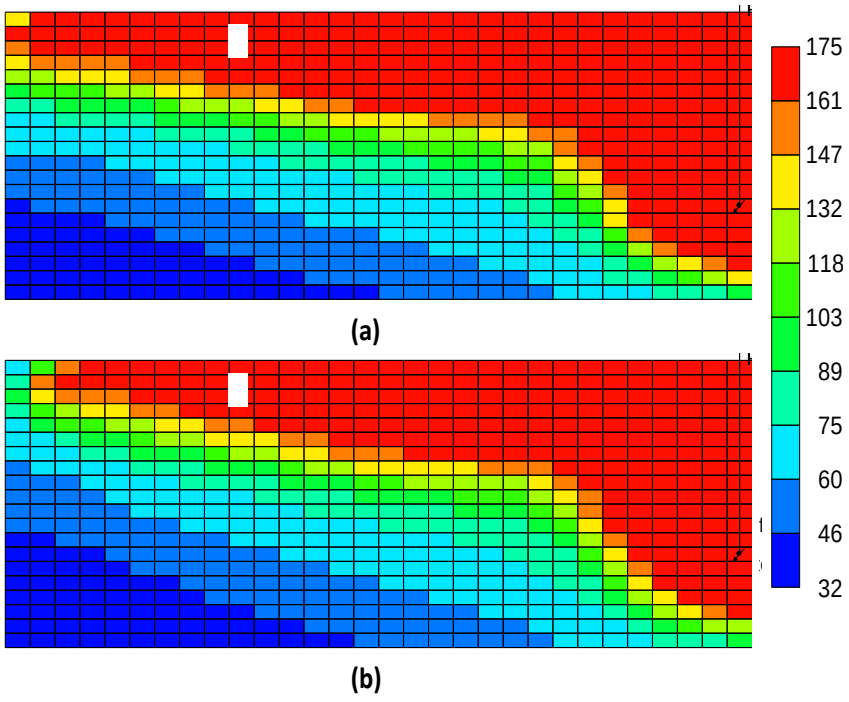

Figure 4-15 Temperature profile after 1100 days of simulation with different solvent volumes injected: (a) 5%- C_6H_{14}; (b) 15%- C_6H_{14}

Table 4-4 Effect of solvent volume on CSS/CSS with solvent process

	CSS	CSS-S					
		C_4H_{10}			C_6H_{14}		
		5%	10%	15%	5%	10%	15%
CDOR(m^3/day)	0.4681	0.4718	0.4673	0.4642	0.5038	0.4956	0.4882
CSOR(m^3/m^3)	9.70	9.17	8.81	8.41	8.62	8.33	8.03
Net Solvent to Oil ratio(liquid m^3/m^3)	0	0.485	0.978	1.491	0.454	0.921	1.418

Effect of soaking time

Based on the solvent selection and volume results, C_6H_{14} in 5% volume is chosen as the solvent injection for different time ratios. In previous simulations, the time ratio of injection, soaking, and production is 10:10:80. In this section, two time ratios of 10:5:85 and 10:20:70 are simulated for comparison. Figure 4-16 presents the cumulative oil production difference between CSS-S (5%) with different soaking times. Under the same injection time, the cumulative production improves with the increase in soaking time. The main reason behind this phenomenon is that the solvent dissolution into the heavy oil increases (shown in Figure 4-17), while the temperature remains very similar (shown in Figure 4-18). From the results, given the same injection time, the cumulative oil production increases with increase in the soaking time.

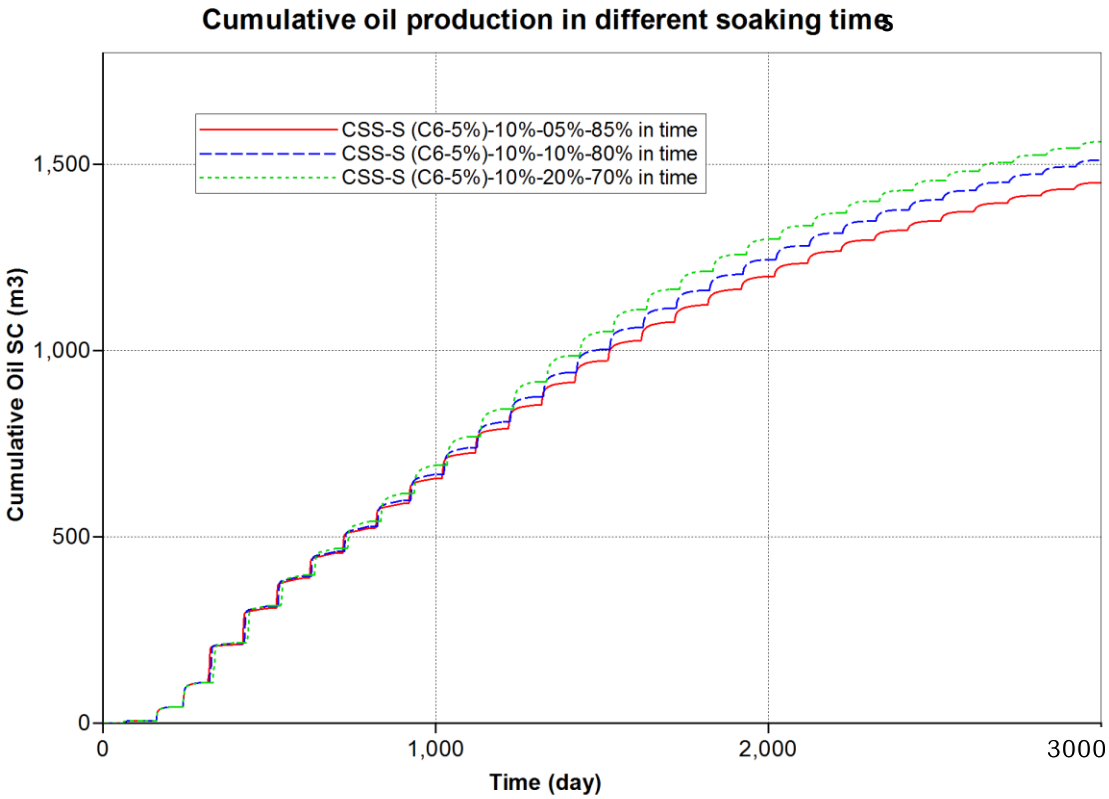

Figure 4-16 Cumulative oil production in CSS-S (5%-C_6H_{14}) with different soaking times

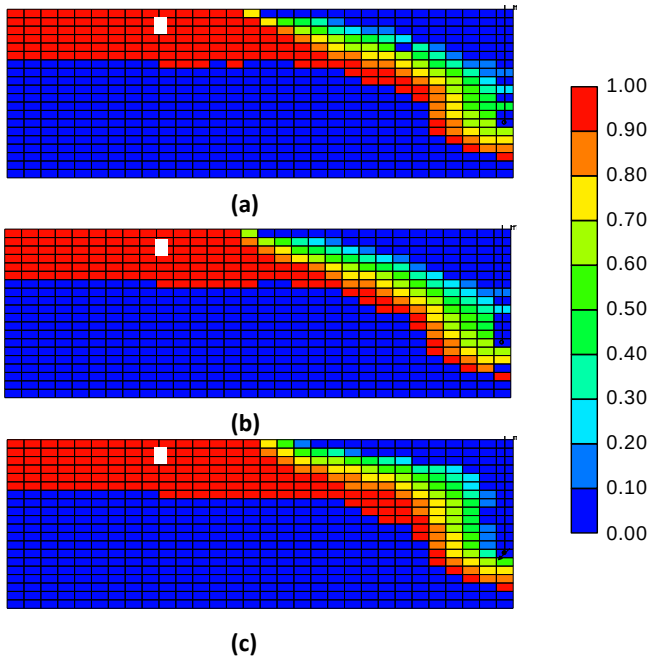

Figure 4-17 C_6H_{14} gas mole fraction in oil phase at the end of simulation of 520 days in cases with different soaking times (a) 10:5:85; (b) 10:10:80; (c) 10:20:70

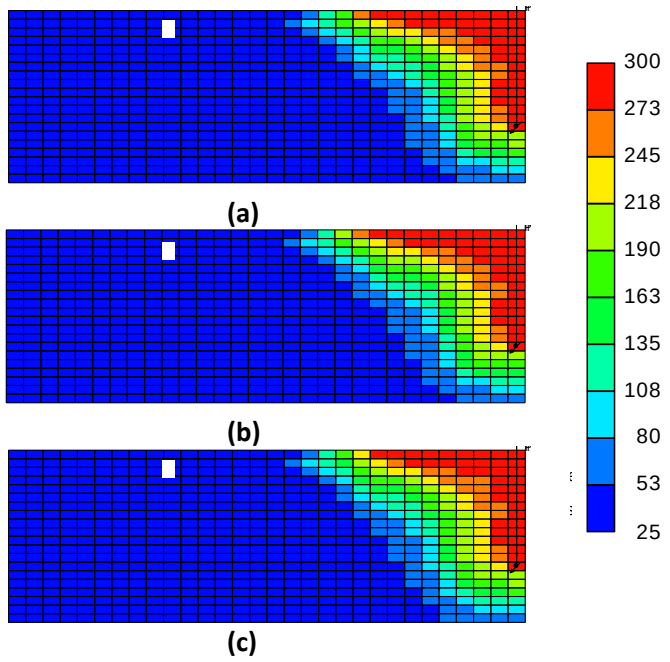

Figure 4-18 Temperature distribution at the end of simulation of 520 days in cases with different soaking times (a) 10:5:85; (b) 10:10:80; (c) 10:20:70

CHAPTER 5

CONCLUSIONS AND RECOMMENDATIONS

5.1 CONCLUSIONS

The conclusions drawn from this thesis research and recommendations for future research are given below:

- In ERH-S processes, the injector acts as an electrode and has higher cumulative oil recovery than that of a producer acting as electrode. However, the producer-as-electrode cases have a rapid oil recovery at the early time.
- ERH-S shows better oil recovery performance than the VAPEX process. In the ERH-S, there are three stages: First, mainly the electrical resistive heating increase reduces the viscosity. Second, the electrical resistive heating, accompanied with NC_4 dissolution, lessens the viscosity. In the last stage, when the electrical resistive heating terminates, the NC_4 dissolution plays the leading role in reducing the oil viscosity.
- In the ERH-S process, the distance between the injector and producer has an important effect on the cumulative oil recovery and oil rate when the solvent ratio of C1 to NC_4 is optimal.
- The lower injector pressure can lead to very satisfactory cumulative oil recovery of ERH-S; however, the higher injector pressure can have a fast starting oil rate.
- The lower the water saturation in ERH-S, the greater the effect will be obtained when comparing ERH-S with VAPEX.

- The lateral pattern of ERH-S shows very prosperous results. In this pattern, the electrical resistive heating and solvent injection develop their own influencing areas, which cover almost all the upper and the diagonal areas.
- With assistance of electrical heating, the effect of reservoir heterogeneity on the heavy oil recovery can be reduced.
- Compared with greater well spacing in SAGD, higher oil rate and cumulative oil production are yielded with smaller wall spacing in the ERH-S process.
- C_6H_{14} is more favourable to SAGD-S than C_4H_{10} in the reservoir and operating conditions because the vapourization temperature of C_6H_{14} is close to the steam injection temperature and pressure. Solvent injection can help to reduce the CSOR of SAGD in this model; however, it cannot increase the CDOR of SAGD.
- For CSS-S process, C_6H_{14} can effectively reduce CSOR and increase CDOR with given operating conditions and reservoir conditions.

5.2 RECOMMENDATIONS

- The simulation results should be verified by conducting physical modeling.
- Harris is conducting some pilot tests on hybrid process of electrical heating with solvent injection. It is recommended to track their pilot test data.
- New simulation models should be developed for other electrical heating processes, such as induction heating and electromagnetic heating.

REFERENCES

Ardali M., Mamora D., Barrufet M.A. (2011) Experimental Study of Co-injection of Potential Solvents with Steam to Enhance SAGD Process, *SPE Western North American Region Meeting*, Society of Petroleum Engineers, Anchorage, Alaska, USA.

Bagci A., Sotuminu O., Mackay E. (2008) Performance analysis of SAGD wind-down process with CO2 injection.

Batycky J.P., Leaute R.P., Dawe B.A. (1997) A Mechanistic Model of Cyclic Steam Stimulation, *International Thermal Operations and Heavy Oil Symposium*, Society of Petroleum Engineers, Inc., Bakersfield, California.

Beattie C.I., Boberg T.C., McNab G.S. (1991) Reservoir Simulation of Cyclic Steam Stimulation in the Cold Lake Oil Sands. *SPE Reservoir Engineering* 6:200-206. DOI: 10.2118/18752-pa.

Butler A.M., Jiang Q. (1997) Improved Vapex Performance Using Widely Spaced Horizontal Injectors And Producers, *Technical Meeting / Petroleum Conference Of The South Saskatchewan Section*, Petroleum Society of Canada, Regina.

Butler R.M. (1994) Steam-assisted Gravity Drainage: Concept, Development, Performance And Future. *Journal of Canadian Petroleum Technology* 33. DOI: 10.2118/94-02-05.

Chang J., Ivory J.J. (2012) Field Scale Simulation of Cyclic Solvent Injection (CSI), *SPE Heavy Oil Conference Canada*, Society of Petroleum Engineers, Calgary, Alberta, Canada.

Chang J., Ivory J., Rajan R.S.V. (2009) Cyclic Steam-Solvent Stimulation Using Horizontal Wells, *Canadian International Petroleum Conference*, Petroleum Society of Canada, Calgary, Alberta.

Cristofari J., Castanier L.M., Kovscek A.R. (2006) Laboratory Investigation of the Effect of Solvent Injection on In-Situ Combustion, *SPE/DOE Symposium on Improved Oil Recovery*, Society of Petroleum Engineers, Tulsa, Oklahoma, USA.

Das S.K. (1998) Vapex: An Efficient Process for the Recovery of Heavy Oil and Bitumen. *SPE Journal* 3:232-237. DOI: 10.2118/50941-pa.

Das S.K., Butler R.M. (1995) Extraction Of Heavy Oil And Bitumen Using Solvents At Reservoir Pressure, *Technical Meeting / Petroleum Conference Of The South Saskatchewan Section*, Petroleum Society of Canada, Regina.

Das S.K., Butler R.M. (1998) Mechanism of the vapor extraction process for heavy oil and bitumen. *Journal of Petroleum Science and Engineering* 21:43-59.

Deng X. (2005) Recovery Performance and Economics of Steam/Propane Hybrid Process, *SPE/PS-CIM/CHOA International Thermal Operations and Heavy Oil Symposium*, Calgary, Alberta, Canada.

Edmunds N., Chhina H. (2001) Economic Optimum Operating Pressure for SAGD Projects in Alberta. *Journal of Canadian Petroleum Technology* 40. DOI: 10.2118/01-12-das.

Edmunds N.R. (1998) Investigation of SAGD Steam Trap Control in Two and Three Dimensions, *SPE International Conference on Horizontal Well Technology*, Society of Petroleum Engineers, Calgary, Alberta, Canada.

Egermann P., Renard G., Delamaide E. (2001) SAGD Performance Optimization Through Numerical Simulations: Methodology and Field Case Example, *SPE International Thermal Operations and Heavy Oil Symposium*, Society of Petroleum Engineers, Porlamar, Margarita Island, Venezuela.

Farouq Ali S.M. (1982) Steam Injection Theories - A Unified Approach, *SPE California Regional Meeting*, Society of Petroleum Engineers of AIME, San Francisco, California.

Gates I.D., Chakrabarty N. (2005) Optimization of Steam-Assisted Gravity Drainage in McMurray Reservoir, *Canadian International Petroleum Conference*, Petroleum Society of Canada, Calgary, Alberta.

Ivory J., Chang J., Coates R., Forshner K. (2009) Investigation of Cyclic Solvent Injection Process for Heavy Oil Recovery, *Canadian International Petroleum Conference*, Petroleum Society of Canada, Calgary, Alberta.

Jiang Q., Thornton B., Russel-Houston J., Spence S. (2010) Review of Thermal Recovery Technologies for the Clearwater and Lower Grand Rapids Formations in the Cold Lake Area in Alberta. *Journal of Canadian Petroleum Technology* 49:2-13.

Jiang Q., Yuan J., Russel-Houston J., Thornton B., Squires A. (2009) Evaluation of Recovery Technologies for the Grosmont Carbonate Reservoirs, *Canadian International Petroleum Conference*, Petroleum Society of Canada, Calgary, Alberta.

King R.W., Zhao L., Huang H., McFarlane R., Gao J. (2005) Steam and Solvent Coinjection Test: Fluid Property Characterization, *SPE/PS-CIM/CHOA*

International Thermal Operations and Heavy Oil Symposium, Calgary, Alberta, Canada.

Koolman M., Huber N., Diehl D., Wacker B. (2008) Electromagnetic Heating Method To Improve Steam Assisted Gravity Drainage, *International Thermal Operations and Heavy Oil Symposium*, Calgary, Alberta, Canada.

Leaute R. (2002a) Liquid addition to steam for enhancing recovery (LASER) of bitumen with CSS: Evolution of technology from research concept to a field pilot at Cold Lake.

Leaute R., Carey B. (2005) Liquid addition to steam for enhancing recovery (LASER) of bitumen with CSS: Results from the first pilot cycle.

Leaute R.P. (2002b) Liquid Addition to Steam for Enhancing Recovery (LASER) of Bitumen with CSS: Evolution of Technology from Research Concept to a Field Pilot at Cold Lake, *SPE International Thermal Operations and Heavy Oil Symposium and International Horizontal Well Technology Conference*, Calgary, Alberta, Canada.

Leshchyshyn T., Ali S.M.F., Settari A., Chan M.Y. (1994) Estimation of Dilation From Fall-off Data In a Hydraulically Fractured McMurray Oil Sands Well, *Annual Technical Meeting*, Petroleum Society of Canada, Calgary, Alberta.

Lim G.B., Kry R.P., Harker B.C., Jha K.N. (1995) Cyclic Stimulation of Cold Lake Oil Sand With Supercritical Ethane, *SPE International Heavy Oil Symposium*, Society of Petroleum Engineers, Calgary, Alberta, Canada.

McCormack M. (2001) Mapping of the McMurray Formation for SAGD. *Journal of Canadian Petroleum Technology* 40. DOI: 10.2118/01-08-01.

McGee B.C.W., Arthur J.E., Best D.A. (1987) Analytical Analysis Of Cyclic Steam Stimulation Through Vertical Fractures, *Annual Technical Meeting*, Petroleum Society of Canada, Calgary, Alberta.

Mossop G.D. (1980) Facies control on bitumen saturation in the Athabasca oil sands.

Nasr T.N., Beaulieu G., Golbeck H., Heck G. (2003) Novel Expanding Solvent-SAGD Process "ES-SAGD". *Journal of Canadian Petroleum Technology* 42. DOI: 10.2118/03-01-tn.

Orr B. (2009) ES-SAGD; Past, Present and Future.

Pizarro J.O.S., Trevisan O.V. (1990) Electrical Heating of Oil Reservoirs: Numerical Simulation and Field Test Results. *SPE Journal of Petroleum Technology* 42:1320-1326. DOI: 10.2118/19685-pa.

Redford D.A., Hanna M.R. (1981) Gaseous and solvent additives for steam injection for thermal recovery of bitumen from tar sands, *Google Patents*.

Rice S.A., Kok A.L., Neate C.J. (1992) A Test Of The Electric Heating Process As A Means Of Stimulating The Productivity Of An Oil Well In The Schoonebeek Field, *Annual Technical Meeting*, Petroleum Society of Canada, Calgary, Alberta.

Richardson W.C., Mims D.S., Kimber K.D., Deemer A.R. (1997) Hydrocarbon-assisted thermal recovery method, *Google Patents*.

Rollenfusser B.A., Hunt P.L., Edmunds R. (1991) Applicability Of UTF Technology To The Athabasca Oil Sands Deposit, *Annual Technical Meeting*, Petroleum Society of Canada, Banff.

Scott G.R. (2002) Comparison of CSS and SAGD Performance in the Clearwater Formation at Cold Lake, *SPE/PS-CIM/CHOA International Thermal Operations*

and Heavy Oil Symposium and International Horizontal Well Technology Conference, Calgary, Alberta, Canada.

Sierra R., Tripathy B., Bridges J.E., Ali S.M.F. (2001) Promising Progress in Field Application of Reservoir Electrical Heating Methods, *SPE International Thermal Operations and Heavy Oil Symposium*, Society of Petroleum Engineers , Porlamar, Margarita Island, Venezuela.

Simangunsong R.A., Mamora D.D. (2006) Experimental and Analytical Modeling Studies of Steam Injection with Hydrocarbon Additives to Enhance Recovery of San Ardo Heavy Oil, *Canadian International Petroleum Conference*, Petroleum Society of Canada, Calgary, Alberta.

Stone T., Ivory J. (1987) An Examination Of Steam-CO2 Processes. *Journal of Canadian Petroleum Technology* 26. DOI: 10.2118/87-03-08.

Strom N., Dunbar A.B., Mink F.J. (1980) Bitumen Resources Of Alberta: Recovery And Conversion To Synthetic Oil Supply.

Vermeulen F., McGee B. (2000) In-Situ Electromagnetic Heating for Hydrocarbon Recovery and Environmental Remediation. *Journal of Canadian Petroleum Technology* 39. DOI: 10.2118/00-08-das.

Wan R.G., Gittins S., Picherack P. (2004) Insights Into Some Key Issues With Solvent Aided Process. *Journal of Canadian Petroleum Technology* 43. DOI: 10.2118/04-02-05.

Wang J., McGee B.C.W., Kantzas A. (2008) In-situ Water Vaporization Improves Bitumen Production During Electrothermal Processes, *SPE/PS/CHOA*

International Thermal Operations and Heavy Oil Symposium, Calgary, Alberta, Canada.

Yuan J.Y., Huang H., Mintz R., Wang X., Jossy C., Tunney C. (2004) Wet Electric Heating for Starting Up SAGD/VAPEX, *Canadian International Petroleum Conference*, Petroleum Society of Canada, Calgary, Alberta.

Zeng F., Knorr K.D., Wilton R.R. (2008) Enhancing Oil Rate in Solvent Vapour Extraction Processes Through Tee-Well Pattern, *SPE/PS/CHOA International Thermal Operations and Heavy Oil Symposium*, Calgary, Alberta, Canada.